ABSTRACT

Title of Dissertation: SYNTHESIS OF NOVEL CO-POLYMERS USING IONIZING RADIATION GRAFTING METHODS FOR THE EXTRACTION OF URANIUM FROM SEAWATER

Travis Cameron Dietz, Doctor of Philosophy, 2017

Dissertation directed by: Professor Mohamad Al-Sheikhly, Department of Materials Science and Engineering

The world's oceans contain a relatively uniform uranium concentration of 3 μg/L. While this is an exceedingly small concentration, the quantity of uranium throughout the oceans is about 1000 times higher than the quantity in known terrestrial deposits. To take advantage of this immense resource, radiation grafting techniques were used to attach uranium-chelating monomers to durable polymer substrates. Three novel, uranium extracting co-polymer systems have been fabricated through this process and characterized.

Three different compound classes were explored for their ability to extract uranium, specifically phosphates, oxalates, and azos. These classes displayed characteristics that provide advantages to the technology over state-of-the-art systems. For the phosphates and oxalates, monomers of these classes containing allyl groups were radiation grafted onto a polymer in a single step. For the azos, a chemical precursor containing a vinyl group was initially radiation grafted to a polymer. The azo compound was then chemically attached to the functionalized polymer surface.

For effective seawater deployment, a polymer substrate was chosen as an inexpensive, reusable platform for extraction. While different fabric substrates were tested, high surface area (14 m^2/g) nylon 6 fabric was chosen for its durability and its capacity for radiation grafting. Direct and indirect radiation induced graft polymerization methods were used in this work. For direct grafting, the nylon 6 fabric was immersed in the monomer solution and irradiated. However, for indirect grafting, only the fabric was irradiated followed by the immediate introduction of the monomer solution. All of these experiments were conducted under anaerobic conditions to prevent the reaction of oxygen with the radiolytically-produced, carbon-centered free radicals.

The grafted fabrics were characterized for attachment of the monomer and their ability to extract uranium. The degree of surface grafting was determined through attenuated total reflectance Fourier transform infrared spectroscopy, scanning electron microscopy, and energy dispersive X-ray spectroscopy, among other techniques. Electron paramagnetic resonance spectroscopy was used to determine radical decay kinetics in the polymer substrate. Pulse radiolysis was used to elucidate the polymerization reaction kinetics of certain monomers. These fabrics were then exposed to uranium-doped seawater solutions and the extraction capacities of the grafted materials were determined.

SYNTHESIS OF NOVEL CO-POLYMERS USING IONIZING RADIATION GRAFTING METHODS FOR THE EXTRACTION OF URANIUM FROM SEAWATER

by

Travis Cameron Dietz

Dissertation submitted to the Faculty of the Graduate School of the
University of Maryland, College Park, in partial fulfillment
of the requirements for the degree of
Doctor of Philosophy
2017

Advisory Committee:
Professor Mohamad Al-Sheikhly, Chair
Professor Raymond Phaneuf
Professor William McDonough
Professor Lourdes Salamanca-Riba
Associate Professor Liangbing Hu
Dr. Dianne Poster

Acknowledgements

This dissertation represents the accumulation of a four year scientific endeavor whose individual parts would not have been possible to complete without the help of a large number of people. However, there is one person who was fundamental to every step, my advisor, **Professor Mohamad Al-Sheikhly**. His guidance and belief in my abilities as a student and researcher allowed me to complete this body of work and to become the researcher I am today.

The work performed for this dissertation and the time I spent at the University of Maryland would not have been financially possible without the assistance of two funding sources. My support was provided by the Nuclear Regulatory Commission through their NRC Nuclear Education Grant Program under the federal grant number NRC-HQ-12-G-38-0023. This work was supported by the U.S. Department of Energy Office of Nuclear Energy under Contract No. DE-NE0000723.

There are a large number of colleagues I would also like to thank for their assistance throughout the project. **Professor Aaron Barkatt** for his work on the discovery and testing of the ligands used throughout this work as well as for his advice and discussion. **Dr. Mohamad Adel-Hadadi** for his work on the development and implementation of the spectrophotometric method for the determination of uranium in seawater along with his help in testing fabrics. **Drs. Lisa Karam, Fred Bateman, Lonnie Cumberland, and Marc Desrosiers** of the Radiation Physics Department at the National Institute of Standards and Technology for the use of the linear accelerator, Co-60 irradiator, and electron paramagnetic resonance facilities. **Dr. William Li** for his work on the attachment

of azo compounds to substrate fabrics. The Maryland NanoCenter and more specifically, **Jonathan Hummel** for his training on the scanning electron microscope in the aforementioned facility. **Tim Maugel** with the Laboratory for Biological Ultrastructure at the University of Maryland for the use of the scanning electron microscope in this facility. **Dr. Karen Gaskell** with the Materials Research Science and Engineering Center at the University of Maryland for her work with the X-ray photoelectron spectroscopy of samples and our discussions of said experiments. **Dr. Gary Gill** at Pacific Northwest National Laboratory for sending the flow columns used in the flow test apparatus. **Dr. Kim Morehouse** at the Food and Drug Administration for his assistance with taking electron paramagnetic resonance measurements of irradiated fabrics. **Dr. Richard Ash** for his help with obtain inductively coupled plasma-mass spectrometry measurements. Also, the facilities at Brookhaven National Laboratory and specifically **Dr. James Wishart, Dr. David Grills, and Bobby Lane** for their help with pulse radiolysis measurements of the polymerization reactions of the various monomer compounds used in this work.

Members of the Al-Sheikhly lab group throughout my tenure have also been instrumental in the completion of this work. I need to thank **Dr. Zois Tsinas** for his assistance with the synthesis of the polymer nanoparticles as well as for his instruction and guidance with the use of scanning electron microscopy, Fourier transform infrared spectroscopy, and numerous other characterization techniques. **Dr. Ileana Pazos** for her assistance with irradiations of fabric samples and for her help with the electron paramagnetic spectroscopy work. **Dr. Chanel Tissot** for her guidance and work with radiation grafting methods and the phosphate-functionalized fabrics. **Matt LeBlanc** for his construction of the flow system used for testing fabrics for uranium extraction. **Kevin**

Mecadon for his assistance with irradiations throughout the years. **Gang Li, Claire Tomaszewski, Eli Fastow, and Olga Nigliazzo** for their assistance with sample preparation and useful discussions concerning experiment development. My fellow group members including **Jaclyn Cua, Najlaa Hassan, and Azadeh Farzaneh** for their valuable scientific discussion in our office.

I would also like to thank the staff of the University of Maryland Materials Science and Engineering Department, including **Michael McNicholas, Olivia Noble, Ginette Villeneuve, Jenna Bishop, Kay Morris, and Novy Choi** for their assistance with some of the most important but often overlooked aspects of obtaining a PhD. I must also thank **Dr. Kathleen Hart** for her guidance and friendship while navigating my way towards my degree.

Last but certainly not least, I would like to express my appreciation for my family, **Ann, Garrett, and Kelsey Dietz** for their continued love and support throughout my entire tenure here at the University of Maryland. I also could not have made it through the process of completing this work without the friendship, support, and love from **Beth Tennyson**.

Table of Contents

List of Figures

List of Tables

List of Abbreviations

β	Stability Constant
DMSO	Dimethyl Sulfoxide
VBC	4-Vinylbenzyl Chloride
Kg-ad	Kilograms of adsorbent
DAOx	Diallyl Oxalate
DEAP	Diethyl Allyl Phosphate
B2MP	(bis[2-methacryloxy)ethyl] phosphate
PAR	4-(2-pyridylazo) resorcinol
DoG	Degree of Grafting
EPR	Electron paramagnetic resonance
ICP-AES	Inductively coupled plasma atomic emission spectroscopy
XPS	X-ray photoelectron spectroscopy
SEM	Scanning electron microscopy
EDS	Energy dispersive X-ray spectroscopy
ATR-FTIR	Attenuated total reflectance Fourier transform infrared spectroscopy
PUREX	Plutonium uranium redox extraction
MAA	Methacrylic acid
TAR	4-(2-thiazolylazo) resorcinol
pK_a	Logarithm of the acid dissociation constant
PET	Polyethylene terephthalate
MIRF	Medical, Industrial Radiation Facility

LINAC	Linear Accelerator
BNL	Brookhaven National Laboratory
LEAF	Linear Electron Accelerator Facility
NIST	National Institute of Standards and Technology
TTHA	Triethylenetetraminehexacetic acid
ICP-MS	Inductively coupled plasma mass spectrometry
e_{aq}^-	Aqueous electron
DCM	Dichloromethane
Br-PADAP	2-(5-Bromo-2-pyridylazo)-5-(diethylamino)phenol
PAN	1-(2-Pyridylazo)-2-naphthol
ISOPAN	2-(2-Pyridylazo)-1-naphthol

1. Introduction

1.1 The Extraction of Uranium from Seawater

1.1.1 Commercial Uranium Use

In the United States as of 2016, 20% of all power is produced through the fission of uranium in nuclear power plants across the country[1]. The entire fleet of nuclear reactors which supply this power are fueled solely by uranium, thereby producing a demand on the order of 23,000 tonnes of uranium annually as of January 2013[2].

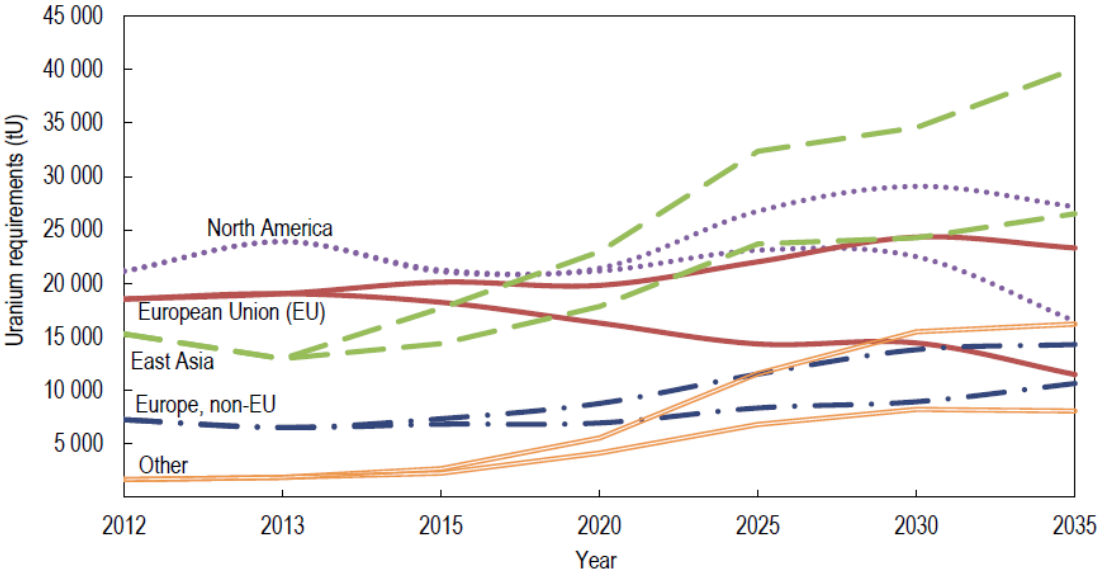

Figure 1.1 – The predicted change in uranium requirements in different regions from around the world. The two trends show for each region represent the upper and lower bounds to the predicted change in uranium requirements over this time period.[2]

Currently, this demand is being supplied by mining that takes place in the United States as well as from other countries around the world including Canada, Kazakhstan, and Australia[3], however demand is expected to increase for a number of regions throughout the world even for conservative estimates represented by the lower of the two lines for each region shown in Fig. 1. While terrestrial mining could support this growth for now, uranium mining can lead to significant environmental impacts as a result of the methods used to extract uranium from the ground[4–6]. The impact on the environment is not only due to the chemical processing required to convert uranium ore into usable uranium oxide, but also from the mining operations themselves. Further details on the environmental dangers of these mining methods will be discussed in section 1.1.5. While certain regions are predicted to diminish their use, globally the demand for nuclear power and therefore uranium has been predicted to increase over time, especially due to countries like China, where more than 40% of new nuclear power plant construction is occurring (as of 2013)[2]. Based on present day uranium demands and currently known quantities of uranium ore (which contain varying weight fractions of uranium), this increase in amount of uranium utilization will only be sustainable for a few hundred years into the future[2]. Consequentially, new technologies to obtain uranium ore need to be developed to extend the lifetime of uranium-based nuclear power as a significant and global provider of electricity.

1.1.2 Elements in Seawater and the History of Usage

Throughout all of history, man has used the oceans as a source for acquiring materials and other commodities. While fishing might be the most obvious resource from the oceans, man has also used the oceans for the production of power through the tides, harvesting of

seaweed as a crop, and the production of table salt. In fact, the extraction of salt from the seas is a practice that has been in existence at least since the mid-5th century BCE[7]. Extraction of elements from the oceans is therefore not an unfamiliar practice. Through the course of modern research and the development of techniques such as inductively coupled plasma mass spectrometry (ICP-MS), the concentration of other elements in the ocean has been made known[8]. This knowledge now allows for the proper evaluation of whether or not the extraction of the many elements found in seawater would be an economically viable prospect by comparing the quantity of the element in the ocean and the cost of its extraction with cost of production from traditional methods. While the overall concentrations of many elements are far below that of sodium chloride, the sheer size of the ocean at about 1.33×10^9 km^3 means that there are huge quantities of even trace constituents[9]. A number of different elements other than sodium chloride, such as magnesium and bromine, have been extracted from seawater at an industrial scale to supplement other forms of production [10].

More recent research efforts have focused on other elements that can be extracted from seawater. In particular, lithium has held significant focus for its use in modern battery technology and aircraft alloys. The estimated 250 billion tons present in the ocean represent a significant, global source of the element[11]. Previously, the extraction of this element was performed using a solid oxide adsorbent, which is similar to methods used for uranium[11,12]. In more recent times, lithium extraction has been explored using polymer adsorbents as well[13]. Concerns over concentration in regards to extraction of various elements from seawater have been voiced by scientists, such as Bardi, et al., based on the high efficiency required for commercial extraction and the quantity of seawater that would need to be processed for a viable technology to exist when competing against terrestrial mining in

today's markets[14]. Some of these concerns have been assuaged by the suggestion of the use of desalination waste water as a possible source for water with higher concentrations of the salts present in the ocean[10]. However, the increased concentration of the elements in the waste water in many cases would not make up for the decreased quantity of brine that the polymeric fabric would be exposed to[10].

The biggest issue with the extracting elements from seawater has been their concentration, or, extraction efficiency. As extraction technologies have advanced, direct extraction from seawater rather than extraction from the salt produced following evaporation, has helped reduce barriers to economical production. However even as extraction technologies have improved, the concentration of elements has still remained an issue. There have been proposals for the use of more concentrated brine than natural seawater, in locations such as the exit ports of desalination plants, as the energy use in the collection of an element has been shown to be inversely correlated to their concentration in the extraction medium[10,14,15].

1.1.3 Uranium in Seawater

One of the elements with the greatest potential for energy advantageous extraction from seawater is uranium, which is the focus of this work. The amount and the chemical form of uranium in seawater are both extremely important aspects to its ability to be extracted effectively.

1.1.3.1 Concentration

The world's oceans are a surprising reservoir for uranium. While only exhibiting concentrations at a relatively consistent 3 ppb, the ocean and its ~1.37 x 10^9 km^3 account

for roughly 4.5 billion tons of uranium worldwide, more than 1000 times the amount of uranium currently known in terrestrial deposits[16]. Accessing this uranium, however, is a challenge. Not only because of the extremely low concentration of this element, but also the large quantities of competing elements (see Table 1.1), the strength of the uranyl carbonate complex in the seawater environment, and the threat of biofouling[11,17–20].

Table 1.1 – Various concentrations of elements in the ocean. These elements will exist in various ionic forms in the seawater environment.

Ions of Following Elements	Concentration (ppb)[11,19,20]
Cl	**1.91×10^7**
Na	**1.08×10^7**
Mg	**1.33×10^6**
Ca	**4.22×10^5**
Li	**170**
U	**3 - 3.3**
Fe	**1 - 2**
V	**1.5**
Pb	**0.03**

1.1.3.2 Complexation

Uranium exists amidst the presence of a large number of other solutes in various oxidations states that exist at comparable (vanadium or iron) or much higher concentrations (calcium and magnesium). All of these metal ions can serve as competitors for any binding site present on an extraction technology and thereby either slow down or permanently reduce the uranium extraction capacity of the technology. Uranium is also found

predominantly as the extremely stable uranyl carbonate complex, $M_2(UO_2)(CO_3)_3$, where M is either magnesium or calcium, as shown in Fig. 1.2.

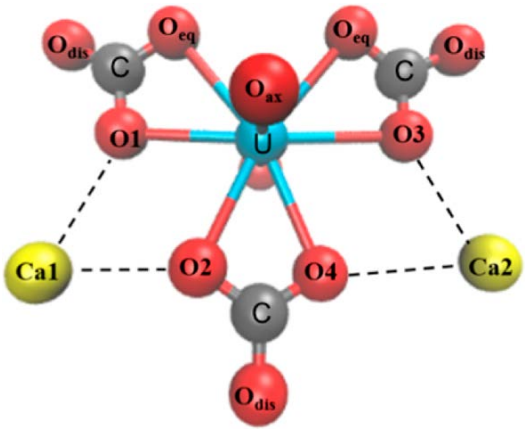

Figure 1.2 – One of the proposed sterochemistries for the uranyl carbonato complex present in seawater.[21]

The stability of this complex from a thermodynamic perspective, in order to allow it to be compared with the stability of the uranyl ion with uranium extraction monomers, can be described through the logarithm of its stability constant, β. The stability constant of the uranyl carbonato complex in seawater is a ratio of the concentration of the bound complex in seawater with the concentrations of the free ions of the components of the complex. Per this definition, the uranyl complex has a Logβ of 31 as per equation 1.1[22].

$$Log\beta = Log\ \frac{[M_2UO_2(CO_3)_3]}{[Ca^{2+}]^2[UO_2^{2+}][CO_3^{2-}]^3} \cong 31 \qquad (1.1)$$

In order for a uranium extracting fabric to be able to effectively extract the uranyl ion, the stability of the uranyl complex with the uranium extracting monomer must have a higher stability complex or must be at a concentration in the local environment that it can compete for the uranyl ion. This is fundamental to the viability of a technology for extracting uranium from seawater.

1.1.4 Geochemistry of Uranium in Seawater

One of the unique aspects of the extraction of uranium from seawater is that the geochemistry of the uranyl in seawater system indicates that the concentration of uranium in the ocean is in a steady-state. The geochemistry of uranium in ocean water can be simplified to a material balance between the uranium deposited in the ocean and the uranium leaving the aqueous state from the oceans. The majority of uranium is deposited in the ocean from rivers. Rivers which are especially high in phosphate concentration from fertilizer used during farming can have higher concentrations than uranium naturally drawn from surface and groundwater sediment. The largest sinks for uranium in the ocean are suboxic and anoxic sediments (sediments located in the ocean where oxygen levels are very low or negligible, respectively) as well as biogenic carbonate (formed by marine life such as corals and plankton). Fig. 1.3 shows a number of other contributions to the flux of uranium in seawater.

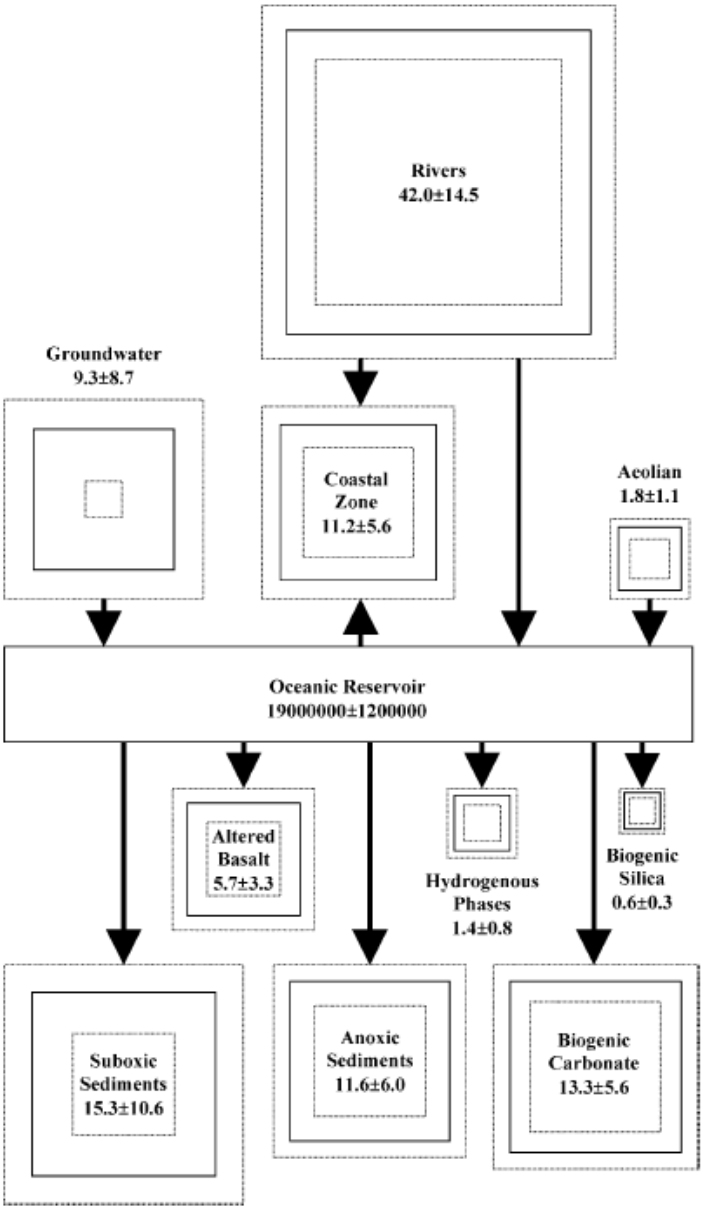

Figure 1.3 – Sources (above oceanic reservoir) and sinks (below oceanic reservoir) of uranium to and from the ocean. The area of each box is proportional to the magnitude of the source and the units are Mmol/year. The dashed lines indicate the uncertainty in the measurement. The oceanic reservoir is given in Mmol.[23]

Considering the massive reservoir of uranium dissolved in the ocean and the flux between sources and sinks of uranium, it is believed that uranium is at steady-state in the modern ocean[24]. As a result of this steady state, it is hypothesized that even with a massive uranium extraction endeavor, the flux of uranium sinks would adjust so the concentration of uranium in the ocean, and thus, would remain roughly the same. Based on this, some would even classify this source of uranium as renewable since the massive quantity of uranium in the ocean would support the growth of the nuclear industry for centuries or more[25].

1.1.5 Environmental Damage from Terrestrial Mining of Uranium

Developing technology for the extraction of uranium is not only advantageous for its use in providing access to an enormous reservoir of uranium, a reduction in the reliance on terrestrial mining for uranium could have extremely beneficial environmental effects. In situ leach uranium mining, which is well established in the United States and in various other countries throughout the world, can have significant impacts on groundwater quality and also requires the use of various hazardous chemicals, like sulfuric acid, and in the processing of the uranium ore to achieve the final usable product, uranium oxide. Uranium mill tailings can often contain highly toxic heavy metals, like arsenic and radium, and their high sulfide content may acidify groundwater which could lead to an acceleration of the release of radioactive and hazardous solutions[5]. While there have been concerns over what an industrial scale operation of uranium extracting fabric or braid could have on the oceanic environment, a progression of the technology towards the use of stable or more natural fibers could assuage these concerns.

1.2 Effects of Radiation on Materials

Radiation is used in a number of ways to functionalize and alter materials and their properties. Examples of these uses include the induction of cross-linking in polymers, coating and ink curing, sterilization, and radiation grafting[26]. This dissertation will focus on the radiation grafting technique for the production of novel materials for the extraction of uranium from seawater.

1.2.1 History of the Study of the Effect of Radiation on Materials

Radiation chemistry is the primary field exploring the effect of all types of radiation on materials. The history of radiation chemistry begins with the discovery of both X-rays by Roentgen in 1895 and radioactivity by Becquerel in the subsequent year[27]. The independent discoveries of these natural phenomena followed an observation of a change in a material following exposure to a radioactive element. Specifically, both forms of radiation discovered by Becquerel and Roentgen were found to render air electrically conductive and were able to activate photographic emulsions (the foundation of X-ray imaging today). Over the course of the next half-century, different researchers were able to explore the effects of radiation on various materials. In particular, Pierre and Marie Curie's discovery and isolation of the element radium and polonium in 1898 provided researchers access to a stable source of radiation. Although α particles produced by these elements were not capable of penetrating deeply into materials, they were still able to produce marked effects. For example Curie and Debierne in 1901 found that a hydrated radium salt in water causes

gas to be produced from the water. The exploration of the fundamental science behind this phenomena led to further developments in the theory that eventually led to a greater understanding of ionizing radiation's effect on molecules and atoms[27]. The field of radiation chemistry itself broke off as an independent field from other nuclear research around the time of the Manhattan Project in the 1940s to separate the study of radiation effects on materials from the use of radiation to generate new elements, a science known as radiochemistry.

1.2.1.1 Radiation Grafting

Radiation grafting is the process by which ionizing radiation is used to generate active sites on a substrate material that can interact with and bind to a monomer, as compared with other forms of grafting such as chemical grafting, which utilize chemically produced active sites[28,29]. A representation of a radiation grafted polymer is shown in Fig. 1.4.

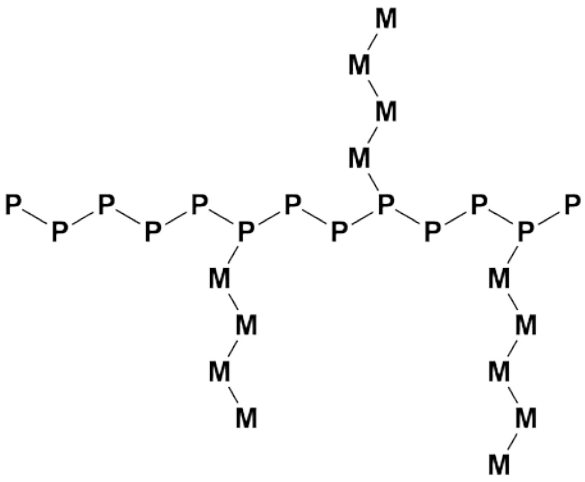

Figure 1.4 – A representation of a radiation grafted polymer, where chains of polymerized monomer, M, are growing off of the polymer substrate, P, backbone.

The radiation produced-active sites, often in the form of free radicals, are sufficiently reactive to interact with a monomer solution which subsequently induces the production of polymerized chains of the monomer on the surface of the irradiated substrate. This grafting technique has been used in a number of industries to improve various characteristics of the substrate material, including hydrophilicity, biocompatibility, and electrical conductivity[26,30]. The technology has been used for a number of different applications including the fabrication of fuel cell membranes, fire-retardant materials, ion exchange membranes, and hydrophilic or hydrophobic materials[31–33].

A large amount of control over the quantity, form, and density of a grafted copolymer can be exerted through the use of varying types of radiation, see Section 1.2.2, and the method of irradiation to produce a radiation grafted substrate, described in Section 1.2.3.

1.2.2 Types of Radiation

There are a number of different types of radiation: alpha, beta, X-ray, gamma, proton, neutron particles however the two types of radiation focused on and used most heavily in this thesis are beta and gamma ray irradiation. Each type of radiation describes the particle by which a target is irradiated. Depending on the charge and mass of the particle as well as the state of matter, density, temperature and other factors of the target material, the interaction with said target can vary wildly. A brief overview of different types of radiation will be given here.

Alpha (α) radiation is a flux of highly energetic nuclei of a helium atom. This particle has an atomic mass of four and a charge of 2+. Due to its large mass and high charge, α particles have extremely short ranges in materials even at high energies, penetrating only

about 3 cm in air and 30 μm in water for a 4.795 MeV alpha particle[27]. α particles can be produced as products of radioactive decay or through interactions between nuclear particles and atoms, such as when a neutron strikes a boron-10 atom to produce a lithium-6 atom and an α particle.

Beta (β) radiation is a flux of highly energetic electrons. This particle has the mass of an electron and a charge of 1-. The small mass allows the electron to penetrate further into a material than an α particle, however the 1- charge still causes significant interactions to occur in the material upon penetration of the radiation. As a result, the range of a β particle in air is measured is on the order of magnitude of meters at moderate energies, such as the 10.4 MeV electrons used in this dissertation. However, materials of higher density have the ability to stop β particles at very low penetration depths. This dependence of penetration depth on the density of a material is based on the Bethe equation for the rate of energy loss by an electron as it travels through a medium, eq. 1.2:

$$-\left(\frac{dE}{dx}\right) = \frac{2\pi N e^4 Z}{m_e v^2}\left[ln\frac{m_e v^2 E}{2I^2(1-\beta^2)} - \left(2\sqrt{1-\beta^2} - 1 + \beta^2\right)ln2 + 1 - \beta^2 + \frac{1}{8}\left(1-\sqrt{1-\beta^2}\right)^2\right] \qquad (1.2)$$

where v is the velocity of the electrons, c is the velocity of light, β is v/c, I is the mean excitation potential for the atoms of the stopping material, N is the number of atoms per unit volume, e is the charge on the electron, m_e is the rest mass of the electron, and Z is the atomic number of the stopping material[27]. The term used for this rate of energy loss is *stopping power* and its units are given in J m^{-1}, or energy per unit length. An aluminum foil of only a few millimeters in thickness for example can stop a beam of β particles at energies of about 1.71 MeV[27]. β radiation can be generated through a number of different means,

for example it is produced naturally through the decay of isotopes such as P-32. β radiation can also be generated through electrical means through the use of such devices as a Van de Graaff generator or linear accelerator (LINAC), both of which use electrical potentials to collect and accelerate packets of electrons at a target. The operation of these devices will be explored in more detail in sections 3.4 and 3.6 of this dissertation. Within this work, a LINAC is used to generate the β rays for radiation grafting of the uranium extracting material. At the 10.4 MeV electron energies used for irradiating the polymer material,

Another type of radiation are photons. Photons are massless particles of varying energies that are related to their wavelengths through the Planck-Einstein relation, eq. 1.3:

$$E = h\nu \tag{1.3}$$

where E is the energy of the photon, h is Plank's constant (4.14×10^{-15} eV · s), and ν is the photon frequency. A photon's frequency is related to its wavelength through the following equation, eq. 1.4:

$$\lambda = \frac{c}{\nu} \tag{1.4}$$

where λ is the wavelength of the photon and c is the speed of light in a vacuum (3.00×10^{8} m · s^{-1}). Of particular importance to this dissertation are high energy photons, such as X-rays and gamma rays, for their ability to ionize target atoms. X-rays and gamma rays are generated when an excited electron in the valence shell of an element drops to a much lower energy level or by the radioactive decay of the nucleus of an atom, respectively. X-rays can also be produced as Bremsstrahlung, wherein the X-ray is generated when high energy electrons are scattered by nuclei with a high-Z value, or through the use of high-energy protons. Gamma rays can also be produced by terrestrial atmospheric phenomena

like thunderstorms and a number of astronomical phenomena such as pulsars[34–36]. In terms of energies, X-rays are usually produced at energies from 100 eV to 100 keV whereas gamma rays are produced at energies above 100 keV. Within this work, gamma rays produced from the radioactive decay of Co-60 are used to graft uranium extracting chemicals to the surface of a polymer substrate.

Finally, proton and neutron radiation are energetic fluxes of the respective nucleons. Both types of radiation are generated through radioactive decay, though these processes are much rarer than radioactive decay by alpha, beta, or gamma particle emission. Proton and neutron radiation can also be produced through the use of particle accelerators or, specifically for neutrons, through nuclear fission or fusion.

1.2.3 Irradiation in Aqueous Solution

In an aqueous solution under irradiation, the majority of the radiation will interact with the water molecules to produce various radical species. The radical species produced upon water irradiation are shown in the reaction below, eq. 1.5:

$$\mathbf{H_2O} \xrightarrow{\sim\sim\sim} \mathbf{{}^{\bullet}OH,\ e_{aq}^{-},\ H^{\bullet},\ H^{+},\ H_2,\ H_2O_2} \qquad (1.5)$$

In order, the most important products of water radiolysis include the hydroxyl radical, the aqueous electron, the hydrogen radical, the hydrogen atom, hydrogen molecules, and hydrogen peroxide. The ratio of production of these different reactive species is heavily dependent on the energy and type of radiation inherent upon the water. Generally speaking, radiation involving heavier particles, particles with more charge, and particles of lower energy produce greater quantities of the molecular products H_2 and H_2O_2, and vice versa for the radical species. With respect to the work performed in this dissertation, the gamma

and high-energy electron beam irradiations performed can be considered to favor the production of the radical species. In order to quantify the amount of radical species produced in solution during an irradiation, the term dose is used, which equates to the amount of energy deposited per unit of mass in a material. The SI standard unit for dose is the gray which is equivalent to a J/kg. The quantity of radical species produced during an irradiation is known as a molecule's G value, which has units of μmol/J. For liquid water irradiated with gamma rays or fast electron irradiation (0.1-20 MeV electron energies), the G values of the radical species produced by the irradiation of water are as follows:

$$g(H_2) = 0.077\ \mu mol/J$$

$$g(H_2O_2) = 0.073\ \mu mol/J$$

$$g(e_{aq}^-) = 0.28\ \mu mol/J$$

$$g(H^\bullet) = 0.047\ \mu mol/J$$

$$g(^\bullet OH) = 0.28\ \mu mol/J$$

$$g(HO_2^\bullet) = 0.0027\ \mu mol/J$$

where, $HO_2^\bullet$ is known as the hydroperoxyl radical[37,38].

In the context of radiation grafting, the higher production of radical species in solution is extremely beneficial as it allows for the radical species to react with the monomer and substrate to induce grafting instead of the radical species quenching themselves to form the molecular species. Out of the radical species produced during the irradiation of an aqueous solution, the most important species is the hydroxyl radical, $^\bullet OH$. This species will readily attach carbon-carbon double bonds or abstract hydrogen from a polymer substrate backbone to promote the initiation of polymerization.

1.2.4 Irradiation in Organic Solution

Similar principles from the irradiation of aqueous solutions can be applied to the irradiation of organic solutions. Within this dissertation, three different organic solvents were used for various grafting experiments in an attempt to improve the grafting density of the uranium extracting monomer to the surface of the polymer substrate: methanol, ethanol, and dimethyl sulfoxide (DMSO). Due to the presence of minor components such as impurities or radiolysis products as well as the larger variety of radiolysis products produced, the radiation-chemical yields of many organic compounds are not as well established as those obtained for water[27].

Methanol under gamma irradiation produces a number of radical and molecular products with the G values shown in Table 1.2.

Table 1.2. Radical and Molecular Product Yields for Methanol (liquid) under γ Irradiation[39,40]

Product	G(Product) (μmol/J)
e_{aq}^-	0.21
$H^\bullet$	0.11
$^\bullet OH$	0.02
$^\bullet CH_3$	0.02
$^\bullet CH_2OH$	0.28
H_2	0.20
CO	0.008
CH_4	0.02
HCHO	0.23

Ethanol under gramma irradiation, in conjunction with the larger number of atoms that compose it, produces a larger amount of molecular byproducts than methanol but the radical yield products are relatively similar[41]. On top of the radical products for methanol, ethanol can also produce a radical ethanol, $CH_3C^\bullet HOH$, when one of its α-hydrogens is

kicked off. These radical species will act as initiators for the graft polymerization by abstracting hydrogen from the substrate to form free radicals on its surface.

The radiolysis of DMSO yields in the production of solvated electrons and positive ions, eq. 1.6:

$$DMSO \xrightarrow{\sim\sim\sim} DMSO^{\bullet +} + e^-_{sol} \qquad (1.6)$$

with a G value for the solvated electron of about 0.18 μmol/J[42,43]. Radicals such as $CH_3SOCH_2^{\bullet}$ and $CH_3SO^{\bullet}$ could also be produced through the irradiation of this solvent. These radicals can serve as the basis for the abstraction of hydrogen from the surface of the polymer substrate to allow grafting of the uranium extracting monomer.

1.2.5 Methods of Radiation Grafting

Within this work, two different methods for radiation grafting were used: direct and indirect. Both types of radiation grafting have their advantages and disadvantages in the course of the production of a material suitable for uranium extraction or other uses, which will be described in detail in this section.

1.2.5.1 Direct

Direct grafting is the method by which both the monomer and substrate are irradiated simultaneously. While advantageous in the fact that this allows for a single grafting step and can result in higher degree of grafting (DoG), this technique does produce larger amounts of homopolymerization and more chemical waste as was seen in the experiments conducted in this dissertation and following the theoretical basis for this technique[29,44,45]. Specifically, in a directly grafted system comparable to the fabric/monomer system used

in this here, the concentration of monomers, [M], will be much higher than the concentration of radicals on the substrate material [S]. As a result, the concentration in the solution of radicalized monomer [$M^{\bullet}$] will be orders of magnitude higher than [$S^{\bullet}$]. Therefore, based on the following reactions, shown in equations 1.7-1.9, the probability of a reaction between [$M^{\bullet}$] and [M] will be much greater than its reaction with any other species:

$$M^{\bullet} + M^{\bullet} \rightarrow M_2 \quad (1.7)$$

$$M^{\bullet} + M \rightarrow M_2^{\bullet} \quad (1.8)$$

$$M^{\bullet} + S^{\bullet} \rightarrow M\text{-}S \quad (1.9)$$

For this technique then, methods should be taken in order to increase the number of radicals formed on the substrate versus within the monomer solution. Further, higher temperatures should be used to allow for greater rates of diffusion of the radical monomers and growing monomer chains to react with radicals on the substrate surface, however too high of a temperature could result in a higher rate of termination reactions or degradation of the polymer substrate[29].

1.2.5.2 Indirect

Indirect grafting is the method by which the substrate is irradiated by itself in an inert atmosphere and following the irradiation, the monomer solution is added to the substrate to allow the radicals formed on the surface of the substrate to react with the monomers. This technique is advantageous over the direct grafting method in that it significantly reduces the amount of homopolymerization. The only way that free monomer radicals could form would be through a chain transfer mechanism. This technique has also shown during the course of the experiments to produce less chemical waste than direct grafting

since less initial monomer is required. Moreover, washing of grafted substrates following irradiation to remove excess monomer is significantly easier without the buildup of homopolymer on the surface of the substrate or in solution.

Conversely, this indirect grafting technique does increase the complexity of the irradiation as the substrate needs to be irradiated at lower temperatures in order to preserve as many of the free radicals as possible prior to the introduction of the monomer solution. Following this, indirect grafting also requires the added step of introducing the monomer to the substrate system following irradiation which means that the concentrations of radicals in this monomer-substrate system will not be as high as the radical concentration experienced in direct grafting. This extra processing step has led to lower degrees of grafting, as observed with the 4-vinylbenzyl chloride (VBC) grafting performed in section 4.2.4.2 of this dissertation.

1.2.6 Science and Mechanisms of Radiation Grafting on Polymers in Different Atmospheres

Fundamental to the production of a uranium extracting material within the confines of this work is the science of radiation grafting. Various aspects of the radiation grafting system can be manipulated to allow for successful grafting to occur using different techniques and different monomer-substrate systems, which will be described in detail below.

1.2.6.1 Radiation under Atmosphere

Irradiating polymers in a system under natural atmospheric conditions will have notable impact on the radiation chemistry that occurs. While under ambient, atmospheric

conditions, the presence of oxygen either in solution or around the sample in the irradiated vial can disrupt the experiment. Oxygen is an extremely reactive molecule and upon interaction with the radicals formed on the surface of either a polymer or monomer, peroxide radicals will form. This process can eventually lead to the quenching of radicals that could be used for radiation grafting, ridding the sample of any regions where grafting would have been possible. In a system containing a polymer, R, and oxygen, the following reactions can occur which show the quenching of the polymer radicals that could have been used to continue the polymerization process. Initially the polymer is peroxidized, see eq. 1.10:

$$R^{\bullet} + O_2 \rightarrow RO_2^{\bullet} \quad (1.10)$$

This peroxidic radical may disappear through either hydrogen abstraction of another polymer molecule, R`, or through the combination of two peroxidic radicals resulting in a loss of oxygen, see eq. 1.11 and 1.12:

$$RO_2^{\bullet} + R`H \rightarrow RO_2H + R`^{\bullet} \quad (1.11)$$

$$RO_2^{\bullet} + RO_2^{\bullet} \rightarrow ROOR + O_2 \quad (1.12)$$

The peroxide, ROOR, and hydroperoxides, RO_2H, formed remove the polymer molecule from further polymerizing until the molecule dissociates into two oxyl radicals or an oxyl and a hydroxyl radical respectively.

1.2.6.2 Radiation under Nitrous Oxide

During the irradiation of an aqueous system, both aqueous electrons and hydroxyl radicals are produced in solution. The hydroxyl radical in particular plays an important role in generating radical sites on the polymer backbone of a substrate for radiation-induced graft polymerization to begin to occur by abstracting hydrogen from the polymer substrate

backbone or by reacting with the carbon-carbon double bonds in the monomer to begin radical polymerization. As a result, it can be to the benefit of the final DoG of the system to have a high hydroxyl concentration in solution during the irradiation in order to induce as many sites for polymerization as possible. The introduction of a nitrous oxide, N_2O, atmosphere to the sample vial prior to irradiation will allow aqueous electrons to be converted into nitrogen gas and hydroxyl radicals through the following reaction, eq. 1.13:

$$e_{aq}^- + N_2O \longrightarrow N_2 + O^- \xrightarrow{H_2O} N_2 + {}^{\bullet}OH + {}^{-}OH \quad (1.13)$$

The reaction between aqueous electrons and nitrous oxide is extremely fast, $k = 9.1 \times 10^9\ M^{-1}s^{-1}$, thereby allowing the majority of aqueous electrons to be converted to hydroxyl radicals before they have a chance to react with other molecules in the aqueous system[27].

1.2.6.3 Radiation Under Inert Atmosphere

When irradiating under an inert atmosphere, the presence of oxygen can be ignored within the context of species interacting with the materials undergoing irradiation. As such, irradiating under an inert atmosphere is very useful for both direct and indirect grafting when using a non-aqueous solution. The elimination of oxygen from an indirectly grafted system allows the radicals generated on the surface of the fabric to remain on the fabric until the monomer solution is introduced to the vial. This allows for a greater percentage of the generated radicals to form grafted co-polymers on the surface of the fabric, increasing the final DoG of the system in theory. For a directly grafted system using a non-aqueous solution, the presence of an inert atmosphere will limit the interaction of monomer radicals with species other than the fabric substrate.

1.2.7 Copolymerization

Copolymerization is a method by which different monomers can be simultaneously grafted onto the same substrate during irradiation. This can be extremely useful when imparting different properties to a material without having to perform successive irradiation steps. While successive irradiation steps can be used to generate block co-polymers, it is beyond the scope of this work, where only combined solutions of different monomers were used to generate random copolymers.

1.3 History of the Extraction of Uranium from Seawater

While the concept of extracting elements from the ocean has existed since man began to mine the seas for salt, uranium specifically began to be considered as an element that could be extracted from seawater shortly after World War II by Dr. F. H. Burstall at the Chemical Research Laboratory, in Teddington through the use of ion-exchange resins[46]. Since this initial study, other techniques have been developed including the use of coagulation, coprecipitation, and membrane filtration[47–49].

1.3.1 Earliest/Foundational Work

The earliest attempts at developing a suitable adsorbent or sorber for uranium started in the middle of the 1950s[46]. Over the following decade, numerous sorbent systems were tested including titanium hydroxide, mono and di-basic phosphoric and phosphonic acids, salicylic acid, amino-carboxylic acid, and amino-phosphoric acid functional groups. Actual seawater testing was performed by Davies, et al. in 1964 using a zinc carbonate-

impregnated zinc carbonate cloth. While the loading capacity of this seawater system could not be calculated, the system managed to extract 0.25 g of uranium[46].

1.3.1.1 Systematic Screening Test of Available Adsorbents

One of the fundamental advances in the extraction of uranium from seawater was carried out by Schenk, et al. in 1982[18]. Within this work, about 200 different sorber materials were tested for their ability to extract uranium from seawater under the same conditions. The sorber materials were loaded onto organic ion-exchange resins and exposed to un-doped seawater.

This work also has a foundational impact on the field by outlining the requirements for a successful adsorbent for uranium. In particular, the adsorbent had to be available in large quantities and at low cost, and it should be practically be insoluble in seawater and eluents while being resistant to physical degradation and damage in order to prolong its service life. This would be especially important for recycling fabric. The performance of the adsorbent material would also be of extreme importance such that the uranium capacity of an adsorbent should be as high as possible to limit the amount of deployments required to obtain the same amount of uranium, while the contact time of the adsorbent with the ocean until it reaches a suitable saturation level should be as low as possible.

Based on the criteria outlined by Schenk, et al. the poly(acrylamidoximes) were identified as the most promising candidate sorbers as their ability to absorb uranium from the ocean resulted in a material with a similar concentration of uranium as to that of uranium ores.

1.3.2 Fabric Extraction

The development of fabric absorbents for the extraction of uranium from seawater has been a fundamental development in the tenability of this technology. The use of polymer fabrics as substrates for uranium extraction were extremely important for a number of reasons. The polymer backbone of a various fabrics allowed for (i) easy functionalization using chemical or radiation grafting, and for (ii) enhanced durability of the material without compromising on the flexibility. Particularly useful for utilizing the natural ocean currents that are present when the material is exposed to seawater. On top of this, various polymer shapes can be used and tailored to this specific use and the density of polymers can be readily tuned to be optimized for seawater deployment[50–52].

1.3.2.1 Amidoxime and Polyethylene

Since the mid-eighties of the last century, a research group in Japan sought to develop a system to extract uranium from seawater. As an island nation, Japan has access to a limited amount terrestrial energy resources, therefore, a technology with the ability to efficiently extract uranium from seawater would allow them to maintain the roughly 10,000 tons of uranium required per year for their power plants[51]. Nobukawa et al. attempted to circumvent previous designs for a forced flow system for collecting uranium from seawater by developing a more passive system for the collection of uranium from seawater[53,54]. The focus of this work was on the development of fabrics and fibers modified with the amidoxime functional group through radiation grafting and chemical functionalization, as portrayed in Fig. 1.5. This includes the use of a base treatment, where the grafted fabric is exposed to a highly concentrated basic solution, to deprotonate and thereby activate the

amidoxime functional group, which could be placed in the ocean and would passively extract uranium[55].

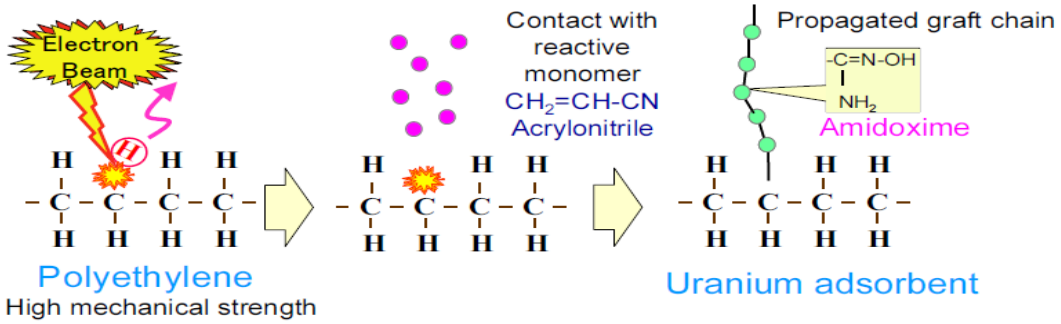

Figure 1.5 – This cartoon depicts the synthetic process for the creation of amidoxime-grafted polyethylene fabrics for fibers. Follow irradiation with electron beam, the radicals generated on the surface of the polyethylene react with acrylonitrile to form long polymer chains. These propagated graft chains are then amidoximated through treatment with hydroxylamine to produce the amidoxime molecules.[19]

The decision to use the chemical functional group amidoxime was influence by its declaration as the optimal chemical functional group for extracting uranium in 1982 by Schenk et al., previously mentioned in Section 1.3.1.1, who had tested hundreds of chemical compounds for this very purpose[18]. These fabrics could be picked up by boat after a certain length of time and brought back to shore where they could be chemically washed and processed in order to remove the uranium and prepare them for reuse in the ocean, as shown in Fig. 1.6.

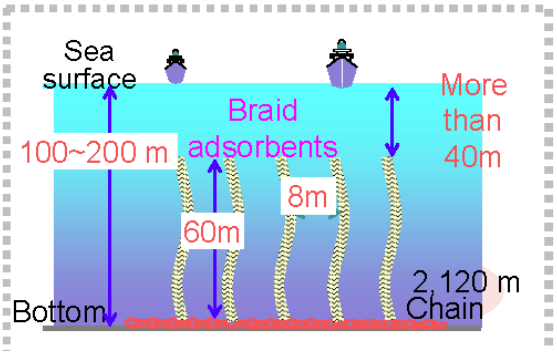

Figure 1.6 – A concept design for a mooring-based uranium extraction system. The long, amidoximated fabric braids would be moored to the bottom of the ocean. After a period of time they would be collected by ships to recover the collected uranium.[19]

Then, in 2003, Seko et al. produced large quantities of this functionalized fiber in the form of stacks and proceeded with *in situ* testing[51]. Over the course of three months, the fiber braids were able to extract >1 kg of uranium (in the form of the uranyl ion) total at a capacity of roughly 3 g-U/kg-ad[19]. In order to improve the economic viability of this passive method of extracting uranium from seawater, the grafted fabric was wound into braids which were left out in the ocean for 60 days and had a slight improvement in maximum capacity, up to 4 g-U/kg-ad[19]. An image of the braid in the ocean can be seen in Fig. 1.7. With the added benefit of reusing the fabric eight times before significant uranium uptake loss, the cost per kilogram of uranium was on the order of $96, which was still two to three higher than the spot price of uranium that year[19,56]. These amidoxime braids, though cheap to produce, ran into problems of reusability as the acid washing used to remove the uranyl ion from the fibers resulted in degradation of the polymer substrate as well as required a repeated base treatment in order functionalize them for uranium absorption[57].

Figure 1.7 – To-scale testing of a fabric adsorbent braid system performed in Japan. These fabric braids were composed of amidoxime grafted polyethylene. Over the course of a number of months this braid adsorbent obtained a loading capacity of 1.5 g U/kg adsorbent.[19]

1.3.3 Current Alternative Fabrics for Extracting Uranium

Following the successful seawater experiments performed, described in the previous Section, with large amounts of amidoxime grafted polyethylene, further efforts have been made with this material, among others, for the purpose of increasing the uranium extraction efficiency and capacity.

1.3.3.1 Amidoxime

Amidoxime remains a popular ligand for the purpose of extracting uranium from seawater[52,58–66]. While different substrates and different configurations have been used, the same basic chemical structure, see Fig. 1.8, has been used as an initial starting point for the fabric.

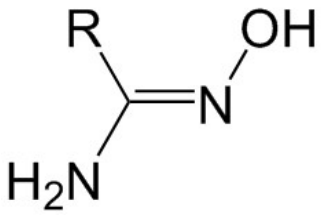

Figure 1.8 – The amidoxime unit molecule. R is a label that signifies the chemical substrate the amidoxime is bound to such as polyethylene.

The amidoxime molecule, through the use of different reflux temperatures and times, can result in an array of different amidoxime derivatives on the surface of the polymer substrate, see Fig. 1.9.

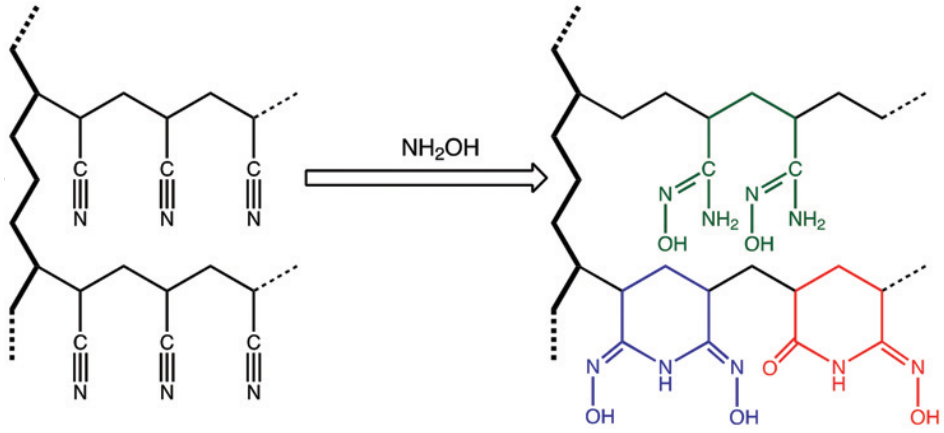

Figure 1.9 – Following the attachment of acrylonitrile to a polyethylene fiber, the cyano groups can be converted to amidoxime groups through treatment with hydroxylamine at elevated temperatures.[67]

The thermodynamic stability of each of these different forms of cyclic and acyclic amidoxime with uranium have been determined. The H_2L^I structure has been shown to have the lowest Logβ value when bound to uranyl when compared to other amidoxime-uranyl complexes, as illustrated in Fig. 1.10. Current research projects are aimed at increasing the concentration of the glutarimidedioxime group in the final fabric structure.

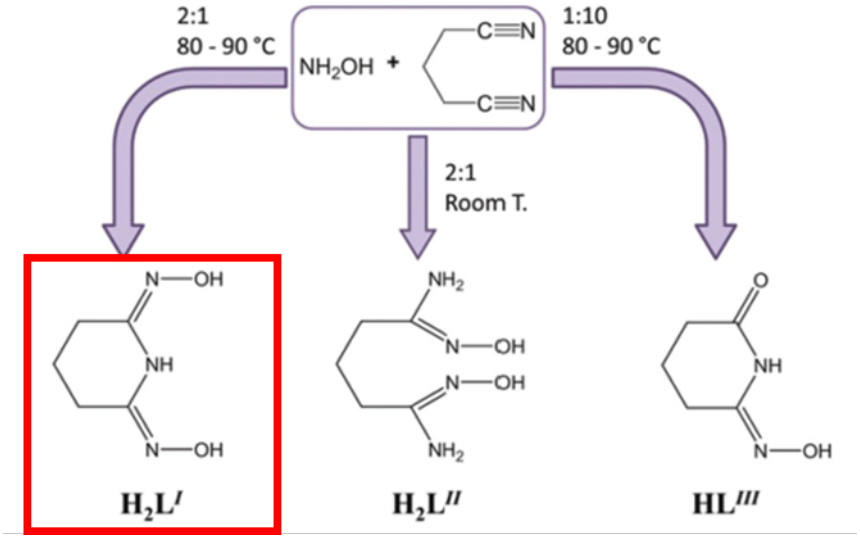

Figure 1.10 – The amidoximating conditions can cause a significant difference in the final chemical structure of the amidoxime molecules. The glutarimidedioxime compound shown framed in red is of particular interest as this compound has been shown to exhibit the highest stability constants when bound with the uranyl molecule.[67]

Amidoxime is believed to chelate to uranyl (the form of uranium in the ocean) through the binding mode shown in Fig. 1.11, however there has been significant scientific discussion and research regarding the actual method of binding to the uranyl ion[68]. Both experimental and computational studies have been performed in an attempt to understand the binding mode of this molecule to uranium[22,67,69–71].

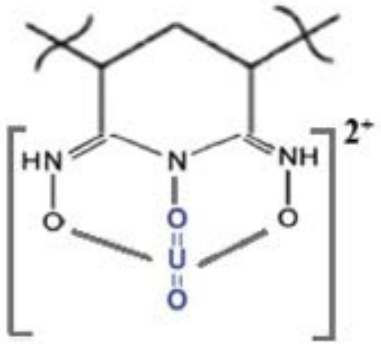

Figure 1.11 – This is the binding mode of the deprotonated glutarimidedioxime complex.[68]

1.3.3.1.1 Advantages

In current literature, amidoxime has shown the greatest potential for the extraction of uranium from seawater through experimental testing[63]. The high stability of the uranyl-amidoxime complex as compared to the carbonato complex along with its stability in an oceanic environment make it an extremely viable candidate for a uranium extraction technology. These reasons are the foundation for its widespread use in other research groups.

1.3.3.1.2 Disadvantages

There are several challenges facing the use of the amidoxime molecule. Most prominently is its reliance on a base treatment to deprotonate the molecule in order to allow it to extract uranium effectively. As a result of these base treatments, the underlying polymer substrate can begin to be chemically aged. While studies have shown that the amidoxime molecule is able to extract uranium without this base treatment, it does not attain nearly the same extraction capacities. Along with seawater exposure and the use of acid to elute off the uranyl following extraction, amidoxime-based technologies have shown significant decreases in extraction capacity following multiple, on the order of five, reuse cycles[72].

1.3.3.2 Natural compounds

A significant concern with any technology deployed in the ocean on an industrial scale is the possible impact it could have on the marine environment. Many groups have turned towards natural compounds as substrates for extracting uranium from seawater in order to reduce the possible environmental impact this technology could have over time from both a standpoint of ocean contamination and initial fabrication of the uranium extracting material.

1.3.3.2.1 Cellulose

While cellulose has not been shown to extract uranium from seawater to a significant degree on its own, there has been interest expressed in its use as a substrate material for the attachment of uranium extracting groups to its surface[73]. Cellulose is a major component of the structural make-up of plants and is usually found alongside

concentrations of hemicellulose and pectin, along with other biopolymers such as lignin, suberin or cutin.

1.3.3.2.1.1 Advantages

Cellulose is an abundant, naturally occurring compound found throughout the world in all plant-based life. As a result, the use of cellulose can be conducive to not only the promotion of green chemistry practices, it can also reduce the barriers to implementing this technology economically.

1.3.3.2.1.2 Disadvantages

Cellulose does not provide the same quantity of binding sites that many artificial polymers such as polyethylene and nylon can. As well, different plant sources for this material can be non-uniform in terms of the distribution of their chemical make-up, which can make obtaining a consistent final product difficult. While the use of the same plant source can lead to more consistent cellulose concentrations, the chemical impurities in the cellulose may not always be the same.

On top of this, as a naturally occurring molecule, organisms are more capable of possessing chemical mechanisms for breaking down this compound. As a result, cellulose-based extraction technologies have to be even more conscious of the effects of biofouling. While the use of co-polymers and molecules with the cellulose such as lignin can provide some protection against degradation from marine life, the material still has lower resistance to degradation.

1.3.3.2.2 Chitin

Chitin is another natural biopolymer that is found in numerous animals throughout the world. It is most commonly known as the material that makes up the majority of hair

and fingernails in various species, but within the context of uranium extraction from seawater the material has most often been extracted from shrimp shells.

1.3.3.2.2.1 Advantages

As a biopolymer, this material is extremely abundant. Particularly because the shrimp industry disposes of vast amounts of natural chitin in its disposal of used shells[74,75].

1.3.3.2.2.2 Disadvantages

In order to be turned into a usable, moldable form, current technology uses ionic liquids to dissolve and reform this biopolymer. Ionic liquids are very expensive per unit weight, and while some of the ionic liquid can be recuperated throughout the purification process, the efficiency is not 100%[74].

Similar to cellulose, chitin is also prone to faster degradation in a seawater environment versus artificial polymers due to the fact that chitin is considered biodegradable[76]. While technologies of incorporating degradation-resistant molecules like lignin into the chitin matrix have been developed, complete resistance to degradation is not afforded[76].

1.3.3.3 Designer Molecules

While many simple molecules possess the ability to bind to uranyl in seawater, their specificity for that particular ion can be lacking. As a result, many groups have looked into developing molecules that are able to bind to uranium more selectively in order to improve extraction capacities and decrease the amount of extraneous elements that are extracted with each exposure. The development of these molecules can take many forms, including the use of computational studies to compare different chemical structures[77]. Groups have also turned towards biology in order to improve their ability to find the highest extraction

capacities for uranium[78]. Using libraries of different initial molecules, these molecules can be synthesized into different combinations of resin beads and exposed to seawater solutions. The beads with the highest quantities of uranium bound to their surface contain the specific blend of molecules that lead to the highest extraction of uranium.

1.3.3.3.1 Advantages

These tailored molecules allow for greater binding efficiency to uranium in the seawater environment. Many other uranyl binding compounds have difficulties specifically binding to only uranyl and are hampered by high extraction efficiencies of vanadium, iron, and other elements.

1.3.3.3.2 Disadvantages

These designer molecules can have an extensive number of synthetic steps required for them to be attached to a substrate and functionalized correctly. This leads to high production costs of the final extraction technology.

1.3.3.4 Combination with Hydrophilic Monomers

The aqueous nature of the extraction environment has led many groups to improve the hydrophilicity of their uranium extracting fabrics in order to (i) improve the wetting of the fabrics and (ii) have seawater penetrate further into the grafted fabrics. Compounds like methacrylic and itaconic acid have been co-grafted with uranium extracting monomers to create grafted copolymers of the two chemicals[68]. Different configurations of these two types of monomers have been used in order to test which configuration of the two monomers on the grafted copolymer will lead to the highest uranium extraction capacities[68].

1.4 Synthesis of Novel Fabrics for Extraction Uranium from Seawater

The objective of this dissertation is to synthesize various novel fabrics using radiation-induced graft polymerization, as through a similar mechanism to the one shown in Fig. 1.12. This approach is described as follows:

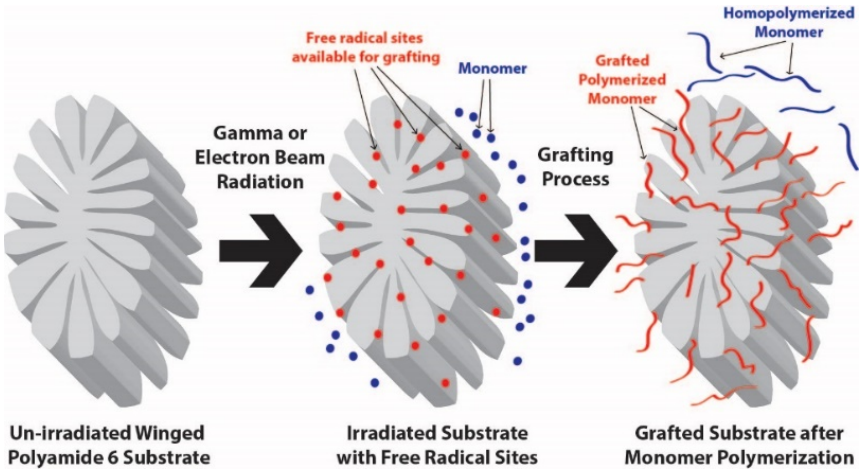

Figure 1.12 – An example of the direct grafting mechanism for radiation-induced graft polymerization.[79]

1. Enhance the loading capacity of uranium on the adsorbent fabric

2. Accelerate the kinetics of uptake of uranium on the adsorbent fabric

3. Improve the regeneration capacity of adsorbent fabric

4. Develop a reliable and reproducible procedure for grafting the adsorbing species on the polymer under “green chemistry” conditions

Each of these objectives will be met through the following means:

1.4.1 High-Capacity Ligands

Adsorbents used in a large majority of studies aimed at recovery of uranium from seawater are based on the use of radiation grafting and chemical processing to produce polymeric supports, in particular polyethylene, with attached amidoxime groups[18,55,57,65,66,80–82]. This functional group has been concluded to offer the best candidate for use in uranium recovery based on studies which were performed by Schenk et al. in the 1980's[18], as described above in Section 1.3.1.2. Substantial progress has been made in improving the characteristics of amidoxime-based adsorbents[65,66,81]. At the same time, a number of potential candidates were not included in the scoping studies of the 1980's or were developed since then. During earlier stages of the study, 18 such candidates had been explored including eight organic phosphorous compounds, three oxalates, three amines, two azo compounds, one oxime, and one ketone. The testing procedure consisted of two stages. During the first stage, the candidate ligands were sorbed on activated carbon and tested for their capability to remove uranium from seawater. Ligands that did not perform well were removed from consideration, but the results obtained for all ligands proved to be very useful in providing guidance for the search for additional candidate ligands. Three classes of ligands have been concluded so far to merit further study: (i) oxalates such as diallyl oxalate (DAOx), pyridylazo (ii) thiazolylazo compounds (azo compounds) such as 4-(2-pyridylazo) resorcinol (PAR), and (iii) phosphates such as (bis[2-(methacryloxy)ethyl] phosphate (B2MP). For their chemical structures see Table 2.1.

The selection of candidate ligands for testing in this dissertation has been based on a systematic approach of searching for trends. Initially, organic phosphorous compounds

were explored due to the existence of natural uranium-phosphate ores. Examples of existing uranium extraction techniques that implement phosphorus compounds include the Plutonium Uranium Redox Extraction (PUREX) process, and previous work that demonstrated successful extraction of heavy metals from aqueous solutions using organophosphorus compounds[2,83,84]. B2MP was specifically identified following an observation that among organic phosphate compounds screened in preliminary tests phosphates performed much more effectively than the corresponding phosphonates. DAOx was selected for testing following the identification of ammonium oxalate as an effective regenerant of B2MP-grafted nylon 6 which had adsorbed uranium from seawater. Ammonium oxalate has been used previously as an eluent for uranium from complex aqueous systems[85–87]. Azo compounds were selected for testing as a result of a survey of uranium complexants for use in the development of a rapid and sensitive spectrophotometric test for uranium. During this survey it was noted that azo compounds are particularly suitable for use at the pH range of seawater[88]. It is our intention to continue searching systematically for highly effective ligands while focusing on improving the performance of the compounds already identified as promising candidates by optimizing the grafting techniques for these compounds.

1.4.2 Improved Surface Grafting Techniques

The synthesis of the adsorbent fabrics is based on radiation-induced grafting, in which ionizing radiation is used to attach desirable functional groups onto a polymeric substrate. One of the most important factors controlling the capacity of the adsorbent for uranium is the DoG of the monomer onto the polymer (ultra-high surface area winged nylon 6, in this case). Two approaches to the grafting of the active monomer on the polymer were tested in

preliminary experiments. The first was *direct grafting*, described in Section 1.2.3.1, where the nylon is immersed and irradiated in the monomer solution under an inert atmosphere, as shown in Fig. 1.13.

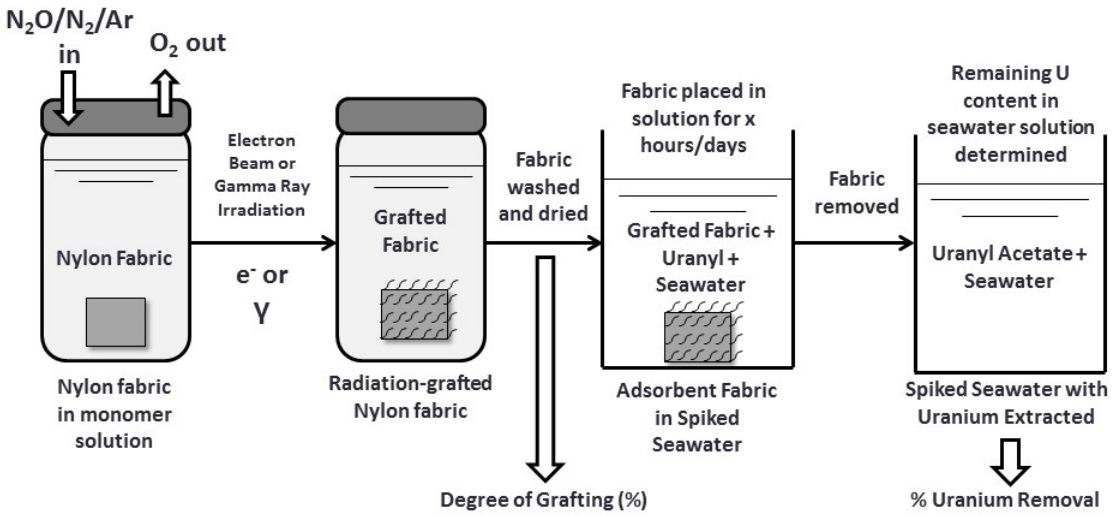

Figure 1.13 – In this diagram, the direct grafting process is illustrated. Following the simultaneous irradiation of the substrate fabric and the monomer or monomer solution under anaerobic conditions, the sample is washed, dried, and tested for uranium extraction.

The second was *indirect grafting*, see Section 1.2.3.2, which consisted of irradiating the nylon 6 polymer in the absence of oxygen and then placing it in an oxygen-free monomer solution in order to cause addition of the radiolytically produced carbon centered radicals to the double bonds of the monomers to initiate grafting, as shown in Fig. 1.14.

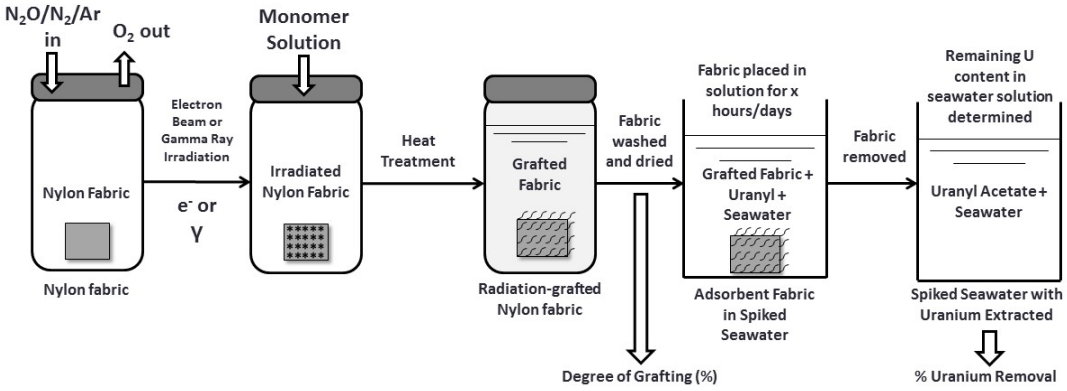

Figure 1.14 – In this diagram, the indirect grafting process is illustrated. Following the irradiation of the substrate fabric under anaerobic conditions, the monomer or monomer solution is added to the fabric under an inert atmosphere. The monomer is allowed to react with the fabric and then the sample is washed, dried, and tested for uranium extraction.

The extent of monomer grafting on the surface of the polymer substrate, also known as the DoG, is evaluated using the equation below, eq. 1.15:

$$Degree\ of\ Grafting\ (\%) = \frac{m_f - m_i}{m_i} * 100 \qquad (1.15)$$

Wherein m_f is the final mass of the fabric (after grafting) and m_i is the initial mass of the fabric.

While winged nylon 6 has shown to be the most effective polymeric substrate of all the fabrics tested, future work will involve the grafting of additional fabrics with selected monomers to investigate whether a new fabric may show greater radiation resistance,

improved mechanical properties, and a higher spin concentration than winged nylon. Proposed fabrics for testing include, but are not limited to, polyethylene and additional ultra-high surface area winged fibers. Electron paramagnetic resonance (EPR) spectroscopy will be used to study the structure and decay of radical species formed on the polymer substrate during irradiation. The various fabrics will also be tested in grafting experiments to compare their grafting densities.

While the optimization of grafting conditions for the selected monomers onto winged nylon 6 has made significant progress, the grafting procedure for all promising ligands will continue to be varied and adjusted to maximize adsorbent efficiency and to reduce processing complexity and cost. Emphasis will be placed on maintaining the standards of "green chemistry", including the elimination of organic solvents and minimizing the formation of waste.

1.4.3 Testing in Lightly Spiked and Non-spiked Seawater

In order to evaluate the uranium extraction capacity of the fabricated adsorbents, grafted fabric samples are placed in seawater solutions containing a known initial concentration of uranium on the order of 0.2-20 mg-U/L. Following the extraction period, the fabric is removed from solution and the seawater is tested for the percentage of uranium remaining in solution. From these measurements, the % uranium that is extracted can be calculated using the following equation, eq. 1.16:

$$\%\ Uranium\ Extraction = \frac{m_{U,i} - m_{U,f}}{m_{U,i}} * 100 \qquad (1.16)$$

Wherein $m_{U,f}$ is the final mass of uranium in solution and $m_{U,i}$ is the initial mass of uranium in solution. Initial tests of the adsorbents were performed with seawater spiked with 1-20mg/L U due to the use of an inductively coupled plasma atomic emission spectrometer (ICP-AES) in the analysis with a detection limit of 1 ppm. This method was supplanted by a spectrophotometric method, which determines the uranium concentration derived from the initial works of S.B. Savvin[89,90]. Through the use of the Arsenazo III compound with this new spectrophotometric technique, uranium concentrations in water could be determined down to 0.2 ppm.

1.4.4 Improvements in the Characterization of Adsorbents

Little information has been reported so far regarding the characteristics of the adsorbent fabrics and of their changes resulting from the contact with seawater and the uptake of uranium. However, such information can be very valuable in gaining better insight into the adsorption process, thus, laying the ground for further optimization of the adsorbent. This information is also essential for assessing the effects of the exposure to seawater on the structure of the adsorbent and the implications of such effects on the durability of the adsorbent and the potential for regeneration. Accordingly, we performed a series of measurements aimed at determining and characterizing experimental adsorbents developed for enhanced extraction of uranium before *and* after contacting them with seawater.

X-ray photoelectron spectroscopy (XPS) is a powerful tool that can provide critical information about bonding between the polymeric adsorbent and adsorbed species such as uranyl and vanadyl. Until now, the amount of information available regarding the nature of this bonding has been limited. XPS measurements will provide data that will describe

the elemental concentrations, speciation, and bonding of the monomer, uranyl, among other adsorbed species.

Energy-dispersive X-ray spectroscopy (EDS) in combination with scanning electron microscopy (SEM) can be used to establish the chemical distribution of competing ions on the adsorbent. Furthermore, EDS can provide direct qualitative information regarding the relative amounts of various adsorbed ions on the adsorbent.

Attenuated total reflectance Fourier transform infrared spectroscopy (FTIR-ATR) will also be implemented to confirm the presence of grafted monomer on the surface of the polymer substrates. This method can also be used to identify the total conversion of the chlorine groups present after grafting with VBC chloride group converted to azo group.

1.4.5 Optimization of Elution/Regeneration Processes

Economically viable recovery of uranium from seawater requires the development of a recyclable/reusable polymeric adsorbent technology for the of uranium adsorption followed by elution/regeneration without a significant deterioration in performance. In the case of amidoxime-polyethylene fabrics, strong acids have been used to elute the bound ions from the surface of the fabrics[57]. The fabrics are then activated again for uranium adsorption with a base treatment and reused. This process was only repeated less than ten times due to the degradation of the amidoxime functional group with repeated acid treatment[57]. Likewise with our grafted fabrics, the objective is to avoid any possible degradation of grafted fabric by using alternative elution processes involving eluants that do not result in significant degradation of the adsorbents over as many regeneration cycles as possible.

1.4.6 Investigation of the Adsorption/Desorption Thermodynamics and Kinetics

The thermodynamics of the adsorption and elution processes must be studied to determine whether or not the selected monomers will be able to remove the uranyl ion from the carbonate complex that it is mostly bound to in seawater. The thermodynamic stability of the uranyl carbonate complex is very high, with a logβ of the $Ca_2UO_2(CO_3)_3$ complex of about 30 in a seawater environment[22]. The stability of the monomer-bound uranyl complex in the extraction system produced in this work must exceed this "holy grail" value in order to successfully act as an adsorbent for uranium in a natural seawater environment.

The kinetics of the adsorption and elution processes is of great scientific interest as well as of critical economic importance. The time required for the adsorption process to take place is a combination of (i) the time needed to dissolve uranium where then it must reach the adsorption sites at the adsorbent surface and (ii) the time required for the adsorption to take place. The relatively long times required for approaching full loading of uranyl shown in literature may be due to a more complex adsorption mechanism operating. In the case of removal of uranyl from seawater, where only very small concentrations of UO_2^{2+} ions exist at equilibrium with much higher concentrations of $UO_2(CO_3)^{4-}$ ions[71,91]. Here, longer time is necessary for a substantial fraction of uranyl ions to be released from the carbonate complexes so that they can attach to the adsorbent. Another reason for the relatively slow adsorption is that it is likely that other cations, which have lower distribution coefficients but are present in seawater at higher concentrations than uranyl may become attached to the adsorption sites on the surface of the polymeric adsorbent when the adsorbent is first contacted with seawater. Subsequently, these are slowly replaced by uranyl due to a high

distribution coefficient with respect to the uranyl ion, but this replacement may be a much slower process than the initial uptake of various cations.

Detailed studies of the adsorption kinetics are planned for adsorbents based on the highest performing of the currently selected ligands. These experiments will be used to elucidate the adsorption mechanism and to obtain important information for the eventual upscaling and commercialization of the process.

The uptake of potentially competing cations, e.g. vanadyl, on the adsorbents can also be measured. The critical question is, "Do vanadyl or other competing cations compete for the same sites as the uranyl compound?" This can be answered by adding controlled concentrations of the metal ions to the uranyl-containing solution used in the adsorption experiments and determining the effects of such additions on the uranyl uptake.

Experiments are also planned to study the elution kinetics of uranyl from the polymeric adsorbent using selected regenerant solutions. A mathematical model describing the kinetics of adsorption and desorption will be developed and the rate constants of these two processes will be developed based on the experimental results of the kinetic studies on these two processes. For instance, if adsorption is the rate-determining step and it is first order with respect to the concentration of uranyl, the overall rate of uranium recovery from seawater, R, will described by the following equation, eq. 1.17:

$$R = \frac{Q}{T} = \frac{C_0[1-e^{-k_a t_a}]V}{t_a} \tag{1.17}$$

where Q is the total amount of uranium removed from the water, T is the total time of one cycle, V is the volume of the seawater contacted with the adsorbent, C_0 is the initial

concentration of uranium in the seawater, t_a is the time allowed for the adsorption process, and k_a is the rate constant of the adsorption process. The expression may need to be modified if the adsorption and desorption are not simple first order processes. This mathematical model will be applied to interpreting experimental data that is obtained during the multi-cycle semi-continuous adsorption/desorption tests.

2. Ligand Selection

The fundamental unit for the extraction from uranium from seawater is the uranium chelating ligand. Above all else, if this ligand does not extract uranium from a seawater environment then the technology developed cannot be considered a reasonable avenue for expansion of the technology as an alternative source of uranium in the centuries to come. In their foundational paper, Schenk, et al. described a number of characteristics of a sorber that would allow for the effective extraction of uranium from seawater, which included the use of a sorber that was low cost and available in large quantities, negligible amounts of degradation with reuse, resistance to chemical, biological, and physical damage during use, excellent loading kinetics observed through a rapid rate of uranium uptake, and high loading capacities to allow for the greatest amount of uranium to bind to the smallest amount of sorber.

Speaking to each of these characteristics, the sorber must first be available in large quantities and at low cost. Due to the low concentrations of uranium in seawater combined with the other difficulties of ionic species in competition with uranium, even with a well-designed sorbent, the quantity of said sorbent required to remove significant amounts of uranium is massive. During the late 1990's and early 2000's, Tamada, et al. fabricated hundreds of kilograms of amidoxime grafted sorbent, but after months of extraction this only resulted in a kilogram of processed uranium in the form of yellow cake. Even with order of magnitude increases to extraction capacity of a sorber compared to the aforementioned work, the sheer amount of material in terms of substrate material and uranium-chelating sorbent to attach to the substrate would have to be significant for. The viability of this technology is therefore partially reliant on the chemicals and components

that were used to synthesize the sorber must be available in large quantities and preferably at low cost.

Second, the sorber must experience negligible amounts of degradation during reuse. With the large quantity of sorber already required in order to extract a usable and measurable amount of uranium from seawater with one use, any fabricated sorber must also be able to be reused multiple times for extraction. Following the elution of the uranium from the sorber, the sorber must be able to be placed back in the ocean and extract similar amounts of uranium from the ocean. The quantity of reuse cycles has been shown to be a significant factor in the final cost of any uranium extraction technology[92]. This will also reduce the total amount of material used, reducing any environmental impact from sorbent fabrication. Significant challenges face any sorber technology considering the most commonly used method for eluting extracted uranium from a sorber has been the use of a strong acid. Combined with the activation step of amidoxime using a strong base, this has led to significant chemical and physical degradation of sorbers produced by other groups, reducing the loading capacities of sorbers by more than 20% after only five reuse cycles.

Next, the sorber must be resistance to chemical, biological, and physical damage during use. Current uranium sorber technologies still require a length of time close to a month for the sorber to reach a sufficient loading capacity. If during this time, the chemical, biological, and physical conditions experienced by the sorber cause it to degrade, a significant portion of uranium or uranium extraction capacity could be lost not only for the current loading cycle, but for the following loading cycles during reuse of the sorber. The basic conditions of the ocean, the acidic uranium elution step, and the base treatment of current amidoxime extraction technologies, among others, contribute to chemical damage

of the fiber resulting in a loss or conversion of uranium chelating functional groups on sorbents. Biofouling caused by microorganisms present throughout the world's oceans are a significant concern. Biofouling can limit the amount of seawater accessible to the entirety of the fabric and it can also induce chemical degradation in the fabric through the consumption of sorber material or the production of chemicals that would cause the sorber to degrade. Finally, the physical conditions of the ocean including currents and waves can cause a significant amount of physical stress of any sorber produced. Fabrics and fibers were chosen as substrates for uranium sorber technology in a number of groups for their ability to resist physical degradation in a seawater environment, but loss of material is still a present problem. This is especially important when considering any technology that does not use a biodegradable polymer wherein some small amount of material displaced from original sorber is equivalent to free-floating pollution in the ocean.

The loading kinetics of the sorber must also be as fast as possible. Factors such as biofouling, chemical degradation, and all together the feasibility of a uranium sorber technology are heavily reliant on the amount of time the sorber spends in a seawater environment. The extremely small concentration of uranium in the ocean couple with the extremely stable carbonato complex of the uranyl ion in seawater predicates a challenge to the kinetics of adsorption onto any sorber technology. While previous technologies have relied on currents to increase the amount of seawater exposed to a sorber technology present in the ocean (as any forced flow system, as used by a technology like a resin, would add a significant energy cost to the technology), the most significant impacts to a sorber's loading kinetics will be the kinetics of the sorber extraction uranyl from the carbonato

complex in seawater. This is a chemical feature of the sorbent molecule that relies on the sterics and electronics of the chelate.

Finally, the loading capacity of the sorber must be as high as possible. Due to the limited use of a forced flow system for extracting uranium from seawater, a uranium extraction technology will have to be placed in seawater in areas of high current and locations where it will not impacted by sea traffic and other factors. This has usually meant that the sorbent material will have to be placed a significant distance off shore. Deploying and retrieving the sorber material therefore becomes a significant portion of its viability as a technology, of which the total amount of uranium retrieved with each deployment plays a part. The ability for a sorber technology to concentrate uranyl to a significant degree higher than its ppb concentration in seawater requires a high loading capacity. The foundation for a high loading capacity for a chemical chelator is the thermodynamics of uranyl binding to the monomer. The greater stability of the chelate to uranyl as compared to the uranyl-carbonato complex will play a significant role in the final loading capacity of a fabric. However, the ability of a chelator to also bind to other elements unfavorably also plays a role in the final loading capacity of the fabric. This has been seen as a source of difficulty with amidoxime-based adsorbents where vanadyl has been shown to compete with uranyl for the same sites on sorbent material[20,69,93].

2.1 Choice of Absorbent Monomer

With the prior components of a suitable sorber for uranium from seawater considered, monomers need to be chosen that could meet these criteria. There are a number of initial

requirements for a uranyl chelating functional group or chemical that can be inferred from the criteria.

The low cost and high availability of the sorber as well as its resistance to degradation during deployment and after reuse suggest the use of a polymer backbone grafted with a uranyl chelating monomer. A grafted polymer of this type could maintain the durability of the substrate while allowing uranyl to bind selectively to the polymer through the grafted monomer. The massive quantity of fabric required for deployment and the uniformity of grafting required suggest the use of radiation grafting for the fabrication of the uranium extracting sorber. The penetration depth of various forms of radiation, such as electron beam and gamma, provide a platform for the generation of a high quantity of binding sites for a suitably designed monomer.

To fit into this fabrication model, the monomer itself has to express certain qualities. First and foremost, the foundation of the molecule must be its ability to bind to uranium. A number of different chemical groups, phosphates, oxalates, azos, among others, were chosen as candidates for uranium extraction. In order to graft these compounds to a polymer substrate through radiation grafting, the final monomer would have to contain at least one carbon-carbon double bond, such as in the form of a vinyl or allyl group, to allow it to graft to the surface of the polymer through the process known as radiation induced graft polymerization. Some examples of the molecules chosen from the listed monomer classes are shown in Table 2.1.

Table 2.1 – Chemical structures for some of the compounds used in this work.

Monomers	Structure
Bis[2-(methacryloyloxy)ethyl] phosphate (B2MP)	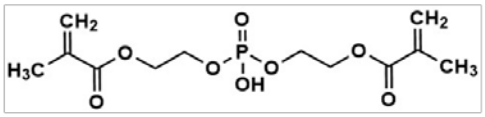
Diallyl Oxalate (DAOx)	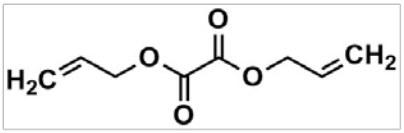
4-(2-Pyridylazo)resorcinol (PAR) And other azo compounds	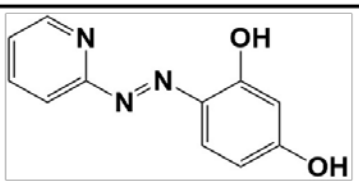

2.2 Phosphates

Phosphates have been historically known to bind to uranium in a number of contexts. Most directly, significant deposits of uranium have been found in phosphate deposits throughout the world and have actually been considered as possible sources for commercial uranium mining should the need arise[2,94]. Under certain aqueous conditions, especially around neutral pH and at higher phosphate concentration, the uranyl phosphate complex dominates the uranyl carbonate complex as seen in Fig. 2.1.

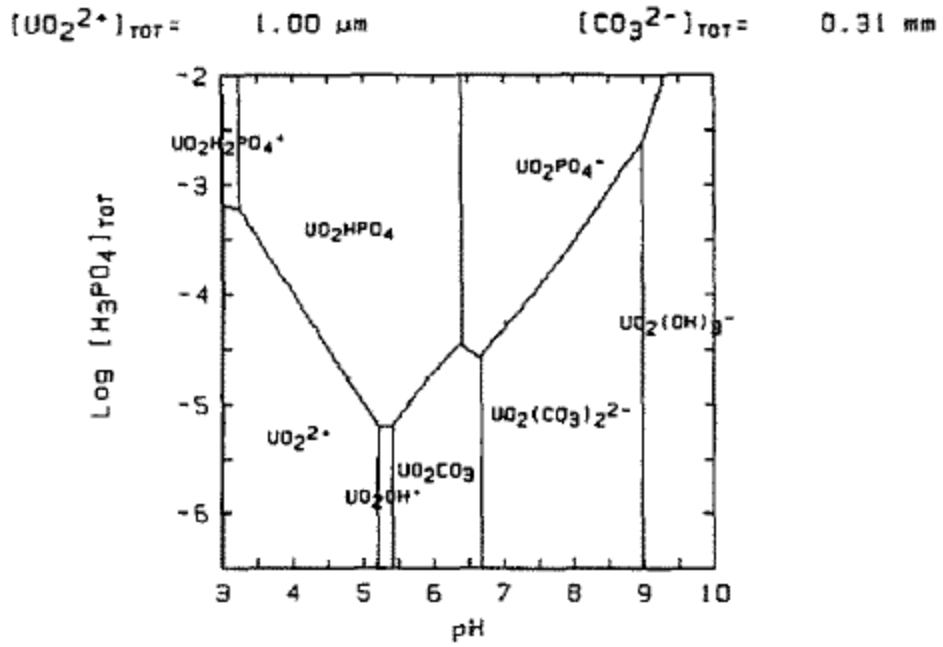

Figure 2.1 – Predominance-area diagram for the system U(VI)-CO2-H3PO4-H2O in aqueous phase at 25°C. [95]

At a temperature of 25 °C and an ionic strength of 0.5 M, the logβ of the $UO_2PO_4^-$ complex was found to be 11.28. Phosphate complexation is shown to be a predominant process when the ratio $[HPO_4^{2-}]/[HCO_3^-]$ is greater than 1 x 10^{-3} however this is only considered for a freshwater system[96].

Phosphates have also been known to extract uranium effectively from various complex ionic systems. The PUREX process, for example, makes use of tributyl phosphate to separate uranium from [84]. It was based on these considerations that phosphates, and closely related molecular analogues such as phosphonates, were tested for their ability to extract uranium from seawater. A number of these compounds were tested in initial screening, all of which contained a phosphate or similar phosphorous-based compound along with an

allyl or vinyl group. Diethyl allyl phosphate (DEAP) and B2MP were chosen following this initial screening for grafting and uranium extraction testing.

2.3 Oxalate

The oxalate ion forms a variety of complexes with the uranyl ion[97,98]. Early studies of the complexation constants showed that logarithm of the stability constant of $[(UO_2)(C_2O_4)]^0$ ($\log\beta_{11}$) is approximately 6.3[99]. This value significantly increases with increasing ionic strength but is only slightly affected by the pH[98]. Values of 6.77 and 12.00 were reported for the logarithms of the stability constants (β) in mildly acidic solutions for $[(UO_2)(C_2O_4)]^0$ and $[(UO_2)(C_2O_4)_2]^{2-}$, respectively[100]. At a temperature of 25 ºC and ionic strength of 3.0 M, the logβ values of the complexes $[(UO_2)(C_2O_4)]^0$, $[(UO_2)(C_2O_4)_2]^{2-}$, $[(UO_2)(C_2O_4)_3]^{4-}$, $[(UO_2)_2(C_2O_4)_3]^{2-}$ and $^-$, $[(UO_2)_2(C_2O_4)_5]^{6-}$ were found to be 6.31, 11.21, 13.8, 18.5, and 28.5, respectively[101]. At an ionic strength of 0.05 M, the logβ value of $[(UO_2)(C_2O_4)]^0$ was reported to be 5.71[102]. An extensive study including both uranyl oxalate and uranyl oxalate hydroxide complexes at 25 ºC and an ionic strength of 1.0 M, yielded, for the complexes $[(UO_2)(C_2O_4)]^0$, $[(UO_2)(C_2O_4)_2]^{2-}$ and $[(UO_2)(C_2O_4)_3]^{4-}$, logβ values of 5.87, 190.484 and 12.61, respectively, and for the complexes $[(UO_2)(C_2O_4)OH]^-$, $[(UO_2)(C_2O_4)_2(OH)_2]^{2-}$, $[(UO_2)(C_2O_4)_2OH]^{3-}$ and $[(UO_2)(C_2O_4)_3OH]^{5-}$, logβ values of 0.62, -6.25, 3.93 and 5.32, respectively[103]. Based on these values, at pH 8, an ionic strength of 1.0 M, a temperature of 25 ºC, a uranyl ion concentration of $5x10^{-4}$ M, and a much higher oxalate concentration of 0.1 M, the majority species is $UO_2(C_2O_4)(OH)_2^{2-}$ (about 65%), followed by $(UO_2)_3(OH)_7^-$ (about 20%), $UO_2(C_2O_4)_2OH^{3-}$ (about 10%) and $UO_2(C_2O_4)OH^-$ (about 5%). A roughly similar distribution is obtained under these conditions when the

concentration of uranyl ion is lowered to $1x10^{-4}$ M and the concentration of oxalate to $3x10^{-4}$ M[103].

Crystallographic measurements on $UO_2(C_2O_4)(H_2O)_3$ have shown that each uranium atom exists as a linear $(O\text{-}U\text{-}O)^{2+}$ ion with five secondary oxygen atoms coordinated to it in a perpendicular plane[104]. According to this study, the oxalate groups have a tetradentate nature, with each oxalate group acting as a bridge between two uranyl ions using all four oxygen atoms for coordination. The oxalate groups occupy centrosymmetric positions and are planar. Further studies confirmed that the uranium atom has pentagonal bipyramidal coordination[105]. The water molecules are hydrogen-bonded into zigzag chains. The resulting structure consists of $[UO_2(C_2O_4)(H_2O)]$ chains[105,106] with each third oxygen atom of the chain formed of water molecules coordinated to the uranium atom, with the uranyl oxalate chains linked into $[UO_2(C_2O_4)(H_2O)]\cdot 2H_2O$ layers[106]. The structural reported by the aforementioned papers, including the existence of hydrogen-bonded chains, have been supported by XRD and IR studies[107].

Furthermore, according to molecular dynamics simulations, the most stable form of the $UO_2(C_2O_4)(H_2O)_3$ complex is a five-coordinate chelate[108]. It is reasonable to expect that the complex $UO_2(C_2O_4)(OH)_2^{2-}$, which is probably the dominant form of uranyl under the conditions prevailing near the surface of an oxalate-grafted polymeric surface at pH 8 (see above) may have a similar structure to the five-coordinated $UO_2(C_2O_4)(H_2O)_3$ with two of the water molecules replaced by hydroxide groups. This is compatible with the structural models described above, which represent the $UO_2(C_2O_4)(H_2O)_3$ complex in the form of $[UO_2(C_2O_4)(H_2O)]\cdot 2H_2O$, where two of the three water molecules being more amenable to change. Another finding that is compatible with this model is the observation

that upon heating $UO_2(C_2O_4)(H_2O)_3$ two of the three water molecules are lost at a much lower temperature than the third one[99].

The present study was aimed at studying the effectiveness of polymer-grafted DAOx in removing uranium from seawater environments. Initial measurements performed with ammonium oxalate and dimethyl oxalate absorbed on active carbon showed these compounds to be largely ineffective in adsorbing uranium. However, DAOx was observed to have significant activity. In addition, the presence of double bonds in DAOx makes it possible to graft it onto polymeric substrates exposed to ionizing radiation. Accordingly, the study focused on measuring the uptake of uranium from seawater by polymeric fabrics grafted with DAOx under various conditions. A key objective of the study was to investigate the effects of grafting (direct or indirect), the medium (an aqueous or organic solution of DAOx or pure liquid DAOx), the radiation parameters (dose and dose rate), the dissolved gases present, etc., on the DoG of the fabrics and on the effectiveness of these fabrics in removing uranium from seawater. Following the grafting process, the study was aimed at investigating the relationship between the DoG and uranium uptake from seawater, as well as at characterization of the changes in chemical composition and morphology that take place during the grafting and the subsequent contact with seawater.

2.4 Azo

Compounds with an azo group have been previously used as spectrophotometric agents for the determination of uranium concentration in complex aqueous solutions[88,109–113]. The use of azo groups for the determination of the concentration of rare earths, including uranium, in aqueous solutions was first proposed by Kuznetsov in 1941, but was experimentally explored by Fritz, et al. in 1958 through the use of the trisodium salt of 3-

(2-arsonophenylazo)-4,5-dihydroxy-2,7-naphthalenedisulfonic acid[89,114,115]. The arsenazo series of compounds was improved upon in later work by Savvin through the use of Arsenazo III, which was found to be especially suitable for the determination of uranyl concentration, among other ions and elements[89,90,116]. The library of azo compounds shown to chelate to uranyl ions was expanded in the following years to include PAR and 4-(2-thiazolylazo) resorcinol (TAR)[109,110,117].

Based on these compounds' previous success in binding to uranium at low concentrations in order to produce a spectrometric change in the absorbance of the compound, it was believed that if bound to a suitable substrate azo groups could also successfully extract uranium from seawater. The stability constant of the PAR complex with uranyl at the pH of seawater was found to be These compounds were especially promising in the face of the drawbacks of amidoxime compound as the pK_a values of many of the azo compounds were lower than the pH of seawater, meaning the compound would be deprotonated naturally upon exposure[118,119].

A number of commercially available azo compounds are available, and PAR was chosen for its performance in preliminary testing of different azo compounds. While this compound contains a number of carbon-carbon double bonds, none of them are suitable for radiation grafting to a polymeric fabric, which has been explored as a suitable method for the extraction of uranium from seawater. Instead, a chemical precursor, VBC can be radiation grafted to the surface of a suitable substrate and then the azo compound can be reacted chemically to attach it to the VBC grafted surface. VBC was co-grafted to the polymer substrate with methacrylic acid (MAA), which has been previously explored as a hydrophilic co-monomer, in order to improve the extraction of uranium by the grafted

substrate[120,121].

In order for the PAR compound to successfully extract uranium from the seawater medium, it must replace the carbonate molecules that normally chelate to the uranyl ion. The following reaction can serve as a chemical depiction of the removal of uranium by the grafted azo compound, see Fig. 2.2.

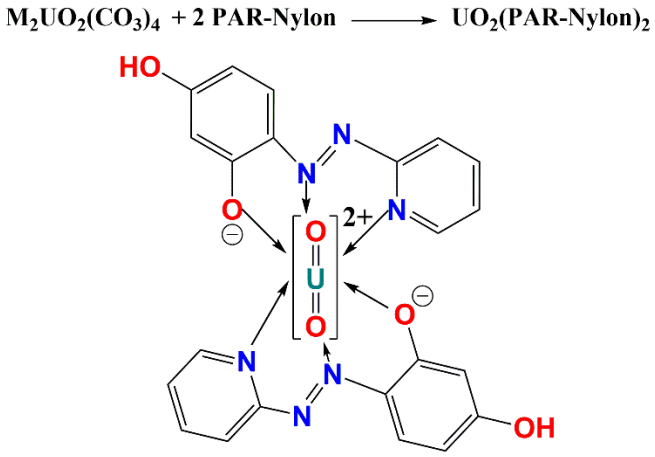

Figure 2.2 - Suggested PAR binding mechanism to extracted uranyl ion from metal carbonate complex. (M= Mg^{2+} or Ca^{2+})

One of the key difficulties in the use of azo-based chemicals such as PAR is the fact that these monomers do not have the previously mentioned carbon-carbon double bonds. In order to attach these compounds to a desired polymer substrate, a two-step process of attachment will have to be used. The para-hydroxyl group on PAR and related chemical functional groups on other azo compounds can react with a chloride group on a compound such as VBC. Two options are then available for the attachment of the azo group to the surface of the substrate, as shown in Fig. 2.3.

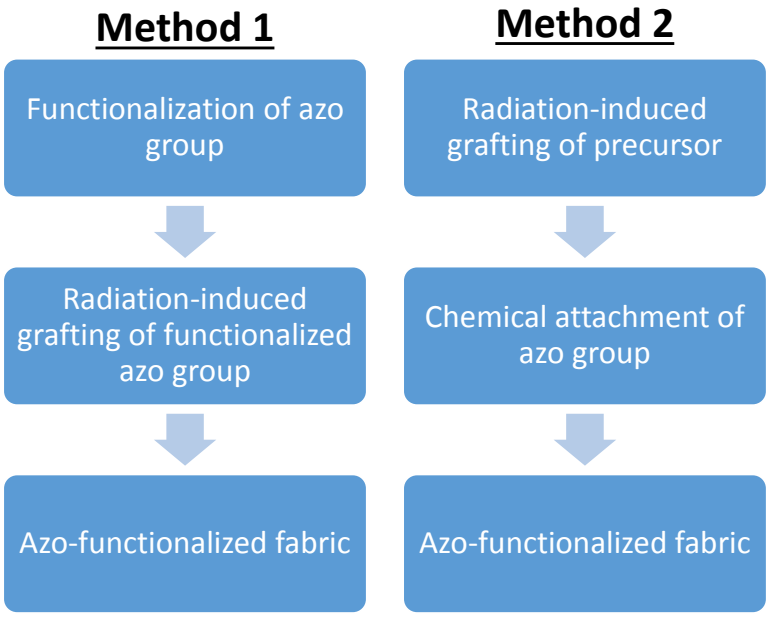

Figure 2.3 – Description of two separate azo attachment methods to the polymer substrate.

Using the two compounds listed as examples, first the PAR can be attached to the VBC and then crystallized into a powder. The equivalent to this process using the TAR compound is shown in Fig. 2.4. The new PAR-based compound with a carbon-carbon double bond can then be grafted to the substrate through similar methods as other monomers to produce an azo-grafted substrate.

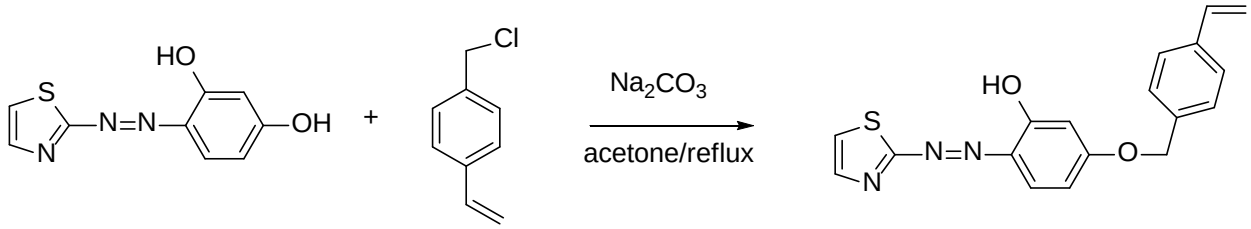

Figure 2.4 – Attachment reaction of TAR to VBC as an example of the first step of the first method.

Second, the VBC can be grafted to the substrate and then the grafted substrate can be reacted with the azo compound to produce an azo-functionalized substrate.

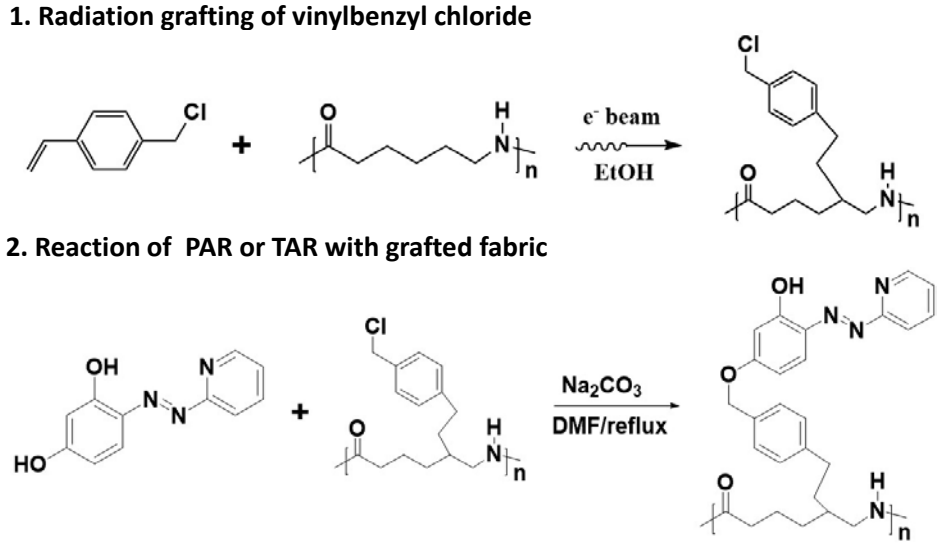

Figure 2.5 – The two steps of the second method for attaching PAR to the surface of nylon 6.

While the requirement of two steps, shown in Figure 2.5, to attach the azo compound to the surface of a substrate material reduces the simplicity of deployment in seawater as compared to amidoxime-based approaches, the fact that the azo compounds have decreased pK_a values for their hydroxyl groups means they should not require a base treatment prior to deployment. This should improve the durability and reusability of azo-based uranium extraction sorbents.

3. Experimental Methods and Materials

At its core, the fundamental experimental process within this dissertation is the fabrication and characterization of radiation grafted substrates. The following two images provide pictorial representations for the two different methods used in this work, direct grafting, see Fig. 3.1, and indirect grafting, see Fig. 3.2. Each element of the images will be discussed in further detail in the following sections.

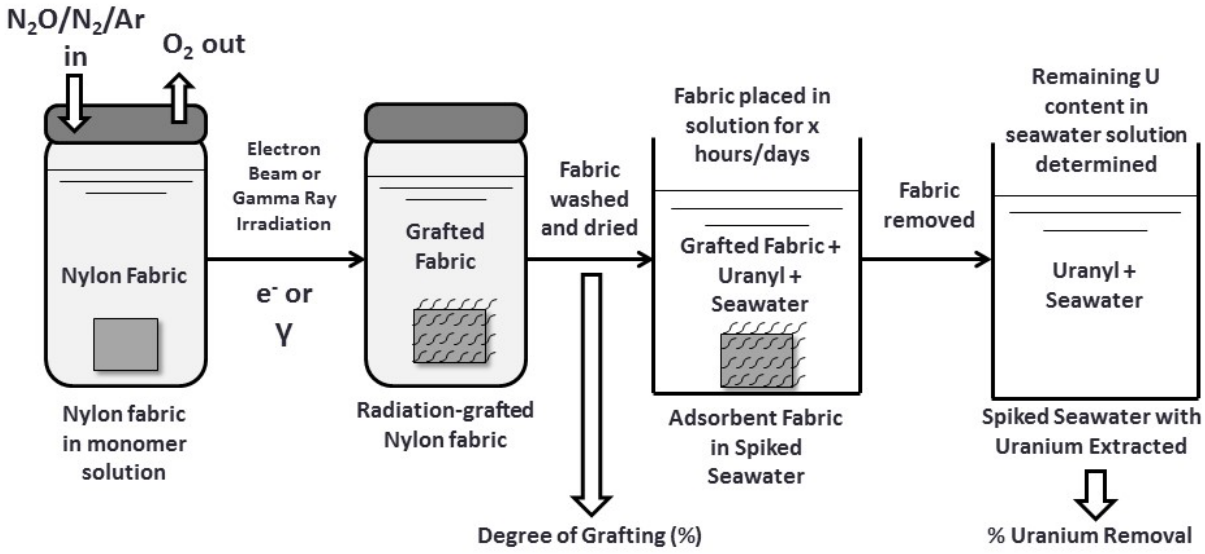

Figure 3.1 – A schematic of the processing steps required for direct grafting of a uranium extracting monomer to the surface of a substrate and the subsequent testing procedure.

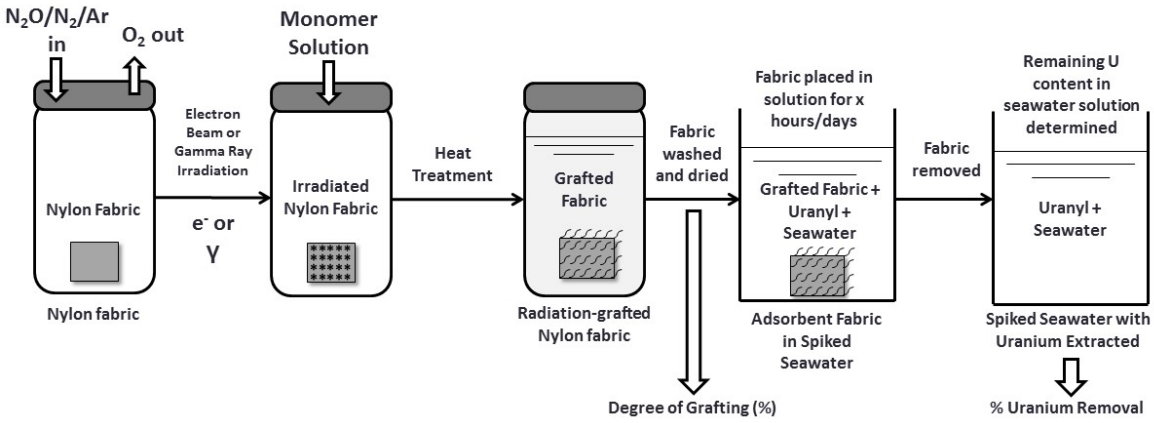

Figure 3.2 - A schematic of the processing steps required for indirect grafting of a uranium extracting monomer to the surface of a substrate and the subsequent testing procedure.

3.1 Substrate Selection

3.1.1 Activated carbon

Candidate monomers for uranium extraction needed to be tested prior to radiation grafting in order to ascertain their ability to extract uranium successfully in a seawater environment. By using activated carbon powder doped with the candidate monomer, the difference in adsorption capacity of the doped versus undoped activated carbon is used as an estimate for the ligand's performance once grafted to a fabric substrate. In order to dope the activated carbon with the candidate monomer, the monomer was first dissolved in methanol or another suitable solvent which already contained a specific mass of activated carbon powder. This solution was stirred overnight on a stirrer plate and during the following day the solvent was able to evaporate leaving behind doped carbon. This doped

carbon was collected and massed in order to obtain an estimate for the DoG of the monomer to the activated carbon. DoG does not accurately describe how the monomer was loaded onto the activated carbon, as the monomer would more likely merely be chelated to the various carboxyl and other carbon-oxygen groups on the surface. DoG is used in this instance alongside actual chemical grafting due to radiation as the calculation to determine the value of the DoG is the same.

3.1.2 Nylon 6

While many previous and current studies on the extraction of uranium from seawater have focused on the use of polyethylene fibers as the substrate for radiation grafting, my work has mainly relied on the use of nylon 6[19,64–66,122]. The chemical structure of this compound is shown in Fig. 3.3 and an SEM image of the polymer as a fiber is shown in Fig. 3.4. Throughout the radiation grafting experiments and chemical treatments performed on this substrate material during the course of my graduate studies, nylon 6 has shown resistance to degradation which is supported by the material's resistance to many types of chemical attack, not including strong acids[123].

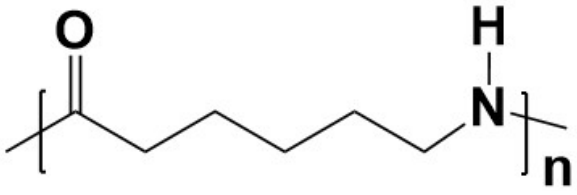

Figure 3.3 – The chemical structure of nylon 6.

Figure 3.4 – An SEM micrograph of a nylon 6 fabric produced by the 3M Company.

3.1.3 Polypropylene

Polypropylene has been used to a certain degree in grafting experiments, however this material does not possess the same amount of chemical resistances as nylon 6 nor has it provided any similar level of grafting to that level achieved with nylon 6 under the same radiation conditions[123]. The chemical structure of this material is shown in Fig. 3.5. The polypropylene used in this work is of the winged variety that will be discussed in Section 3.1.5.

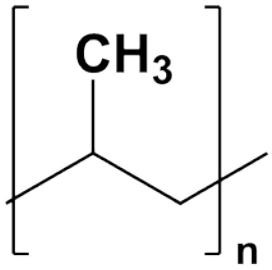

Figure 3.5 – The chemical structure of polypropylene.

3.1.4 Other polymers

Other polymers were used as substrates in an attempt to improve grafting. For example, polyethylene terephthalate (PET) was used for this purpose. PET was available as a winged fiber as described in Section 3.1.5, the chemical structure for which is shown in Fig. 3.6.

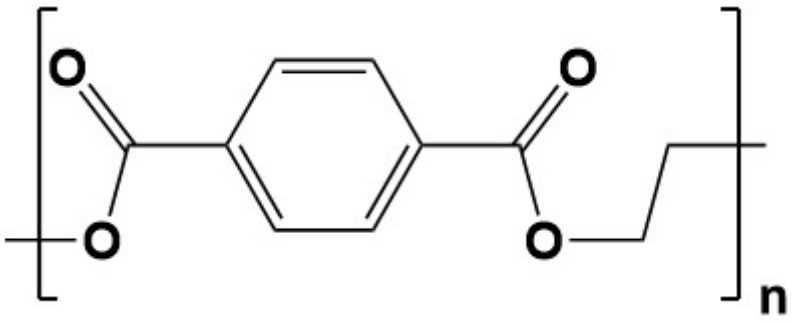

Figure 3.6 – The chemical structure of PET.

Unfortunately, the DoGs obtained with this substrate and the compounds tested were negligible so their use was discontinued within the bounds of this dissertation.

3.1.5. Winged Polymers

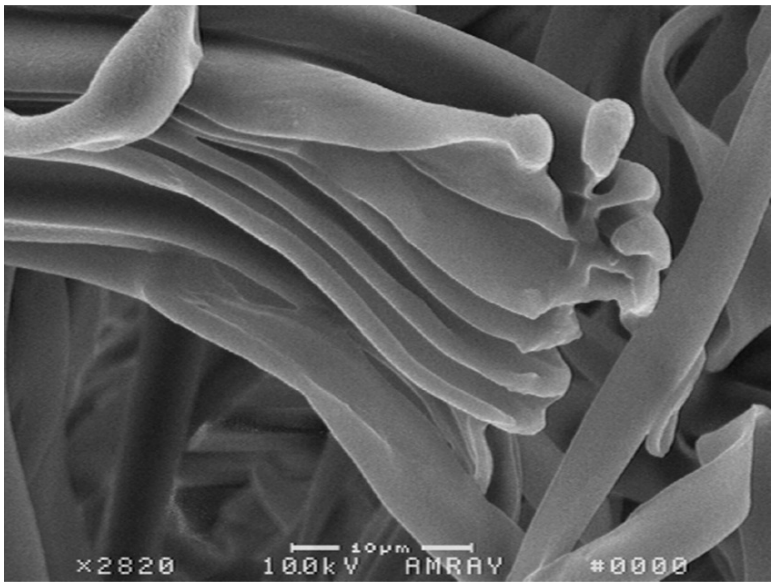

Figure 3.7 – An SEM micrograph of winged nylon 6 fabric. This view shows the end of one of the "winged" fibers.

Winged fibers were obtained from Allasso Industries and are preferred, as they provide (i) higher surface areas upon which to graft both uranium extracting monomer and (ii) a greater surface area upon which uranium extraction could occur. The channels seen in Fig. 3.7, of width one micron or less, are possible locations for the growth of grafted monomer chains. This patented fiber design has already been suggested for use in purification/separation systems with an average specific surface area of about 140,000 cm^2/g[124].

3.2 Sample Preparation

The general procedure for fabric sample preparation prior to irradiation grafting can be described as follows. Square pieces of fabric were cut from larger swathes of sample nylon-6 or polypropylene obtained from Allasso Industries through the use of clean fabric scissors. Note, these fabrics had previously been stored in plastic bags to reduce contamination from dust. The cut pieces of fabric were trimmed until their mass fell within a specified range, 0.020 – 0.021 g or 0.045 – 0.046 g. Mass ranges were selected to reduce any impact that sample size might have on the total grafting of the final sample. The magnitude of the mass range (1 mg) was selected based on the accuracy of the scale used to physically weigh each fabric. These numbers were also chosen as they would allow for the highest accuracy of the ranged balanced combined with the ease of cutting the samples, such that their masses would fall in aforementioned specified range. The former mass range of 20-21 mg was initially chosen based on previous work performed in the group on this project. The estimated final mass of the fabric after grafting, based on an optimal DoG of about 100% as found by the same previous work, meant the fabrics would have final masses in the range of 40-42 mg. This mass range would allow for about three separate cuts of the same grafted sample, all with masses close to 15 mg, therefore, leaving triplets of the same sample for precaution. The ~15 mg samples would then be tested for their ability to extract uranium from seawater. Having at least 3-4 samples for uranium extraction testing in this mass range allowed for statistically significant results to be generated for reach grafted sample. The mass range of the initial, cut fabric was increased to 45-46 mg in later experiments to allow for more samples to be generated for testing in 0.2 and 1 ppm uranyl

doped seawater solutions, among other testing solutions, as well as to compensate for the reduced DoG seen with indirect grafting.

Once samples had been cut and massed, they were placed in labeled sample vials, the majority of which were capped with silicone septa. In both direct and indirect grafting this allowed for the subsequent purging of the atmosphere and/or the solution inside the vial with inert gas. In some cases, prior to the purging step, cut fabrics were washed with acetone and dried in their vials for at least one hour at 60°C in an oven with the goal of removing any residual contamination (note, this was only performed on the nylon-6 fabric). Grafting results revealed that this extra washing step did not result in an experimentally significant increase in the grafting density of the fabrics or an increase in their uranium extraction capacity.

Following the preparation of the fabric samples, the monomer solutions were prepared per the concentrations of different monomers and solvents described for each independent experiment.

All monomer solutions were prepared in ambient air. In all cases, complete mixing was insured through stirring and/or sonication. Following solution preparation in the case of direct grafting, 10 mL of monomer solution was transferred to each sample vial. These vials were then purged with an inert gas, either nitrogen or argon, or with nitrous oxide in the case of some aqueous monomer solutions. In order to ensure that the atmosphere of the sample vial was excluded of oxygen, the purging needles were removed to prevent any back flow of atmosphere into the vials, i.e. the outlet needle was removed prior to the purging needle. This most likely resulted in a slight over pressure of the sample vial, but

this should only have had the effect of prolonging the maintenance of an inert vial atmosphere.

3.3 Co-60 Irradiation for Sample Fabrication

3.3.1 National Institute of Standards and Technology Co-60 Irradiator Set-up

Fabrics have been irradiated using two Co-60 irradiators located at the National Institute of Standards and Technology (NIST), each of which can provide a different dose rate, specifically 5 kGy per hour and 1 kGy per hour. Samples in vials were placed inside a metal canister, which was then lowered into the gamma field inside of the standalone irradiator. An example of the type of irradiator used for these experiments is shown in Fig. 3.8 and the geometry of the Co-60 pencils within the irradiator is shown in Fig. 3.9. This facility provided low to intermediate dose rates that were separate from the much higher dose rates (>100 kGy/hr) used with the LINAC facilities.

Figure 3.8 – A Co-60 irradiator of similar design to those housed at NIST. The pencils of Co-60 are located within the body of the irradiator.[125]

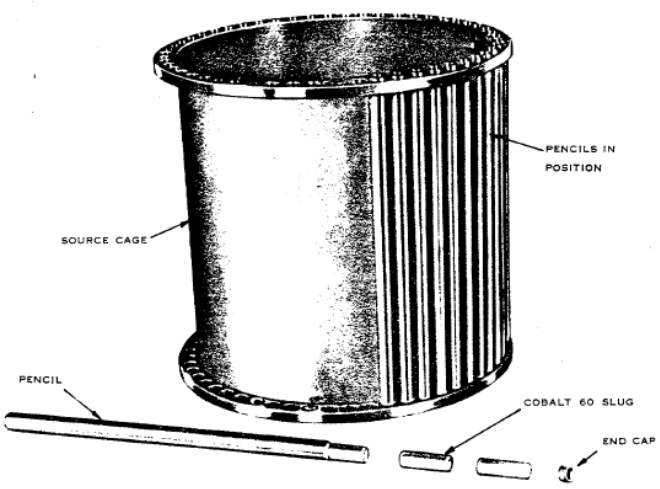

Figure 3.9 – Within the Co-60 irradiator, an array of metal tubes filled with Co-60 slugs surrounds the sample chamber. This pencil configuration allows for a more even irradiation of samples.[126]

3.3.2 Dosimetry

Dosimetry for the NIST Co-60 irradiators was carried out using pellets of alanine. These pellets are composed of alanine and a binder and are roughly half a centimeter in diameter. The alanine pellets are irradiated to a number of different doses. Subsequently, the pellets are analyzed in an EPR spectrometer, which is able to measure the change in the absorbance of a microwave in the sample which is absorbed by the splitting of the unpaired electrons generated in alanine during their irradiation. The specific relationship between dose and the area of the peaks generated in the EPR is dependent on a number of factors, including the geometry of the pellet in the EPR. The determination of the radical concentration-peak area relationship using a ruby standard, and knowledge of the amount of energy required to produce an unpaired electron in alanine. Based on the alanine dosimetry and the assumption that the gamma rays completely penetrate through both the container inside the irradiator (assuming negligible attenuation) and the glass vials in which the fabric samples sit, the dose and dose rate of a Co-60 irradiation can be determined for all samples. The assumption that there is negligible attenuation of the gamma rays due to the glass vials is founded on the significant penetration power exhibited by this neutrally charged, highly energetic particle.

3.4 Linear Accelerator – Radiation Grafting & Medical, Industrial Radiation Facility (MIRF)

The majority of irradiations were performed at the MIRF facility using a pulsed electron beam LINAC with a fixed pulse repetition rate (100 Hz per 6 μs pulse) and electron energies from 7-32 MeV, however all irradiations were carried out at about 10 MeV. The layout of this facility is shown in Fig. 3.10. This energy was chosen for a number of reasons. For example, the accelerator has difficulties operating at energies below this value and any energy values greater than 10 MeV have a greatly increased probability of activating the samples. Due to the high energy of the electrons and variable current that it can operate at, in comparison to the fixed rate of the Co-60 irradiatior, this facility is ideal for polymer modification at intermediate to very high dose rates.

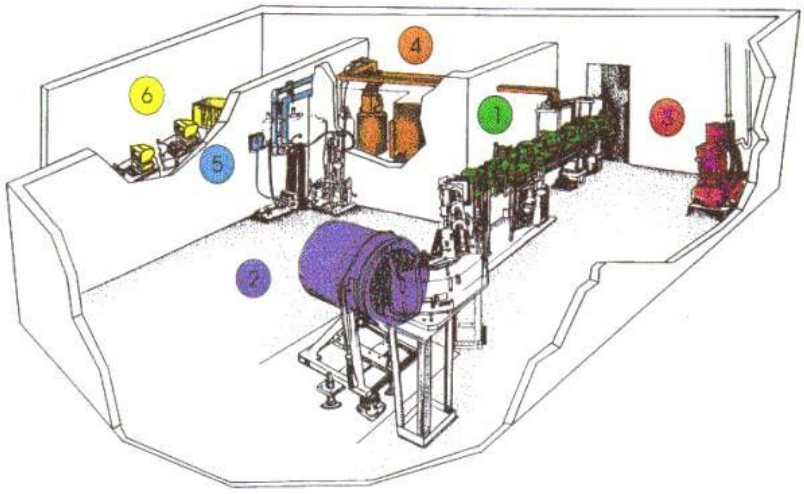

Figure 3.10 – The schematic of the MIRF LINAC facility. The components of the facility are labeled as follows: (1) Two-stage traveling-wave radiofrequency LINAC, (2) collimator head for medical treatment beam, (3) 380 V motor generator to convert to 50 Hz, (4) 8 MW Klystron and waveguide for 3000 MHz rf, (5) water cooling system, and (6) operator's console and data acquisition system.[127]

A number of different sample irradiation configurations were used with the MIRF LINAC, one of which is shown in Fig. 3.11. These different configurations can be separated into two qualities: (i) the ability to irradiation samples at a desire temperature and (ii) the ability to irradiate multiple samples at one time using a rotating table. Contrary to latter, one or two samples could be placed at the front of the rotating sample table to allow for higher dose rates.

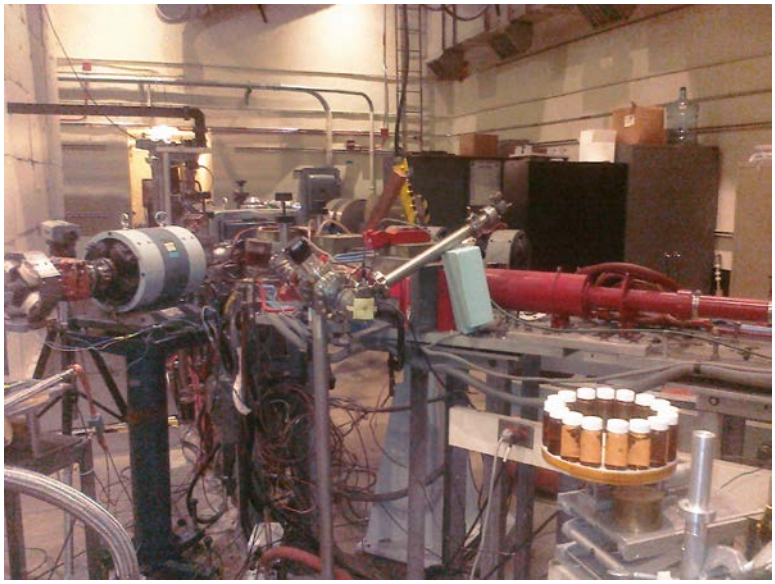

Figure 3.11 – The sample stage on which the sample vials are irradiated can be seen in the bottom right of this image. The exit port of the electron beam can be seen at the center of the image.

Figure 3.11 is of the initial irradiation set-up, where the vials were not irradiated in a temperature controlled chamber. The circular stage with white-capped vials on top of it was used as a means to irradiate a larger number of samples with a relatively even dose without having to irradiate each sample individually. In this particular configuration, 16 (though depending on vial size, this number could change) 20 mL vials fit around the edge of the rotating platform. The platform performs a full rotation approximately twice every minute. The platform was operated through the mechanism of a mechanical motor beneath the platform and was powered by an external voltage supply present in the control room of the LINAC facility.

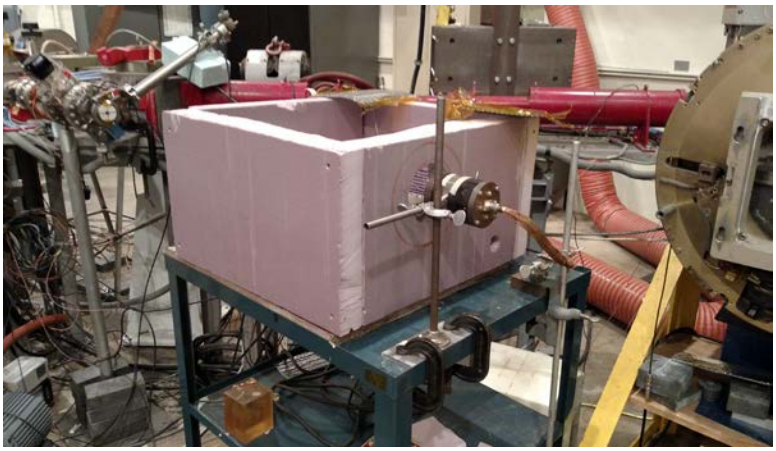

Figure 3.12 – The outside of the insulated irradiation chamber for controlling temperature during irradiations.

Figure 3.13 – The inside of the insulated irradiation chamber for controlling temperature during irradiations.

The two pictures above, Figs. 3.12 and 3.13, show the exterior and interior of an insulated box that was used for temperature control of the samples. Two holes were cut out

of the box in order to allow for the electron beam to enter and exit the box unimpeded by the foam walls. A Faraday cup was placed behind the sample stage to collect current from the electron beam. The reading received from this Faraday cup was measured on a current integrator, where 1×10^{-10} C of charge was integrated and counted as a single "count." The total number of counts collected over the course of an irradiation along with the total time of the irradiation were collected using a counter-timer linked to the current integrator. These counts could be equated to the dose inherent upon the sample when compared with the dosimetry discussed in section 3.4.1.

The method of heating the box (direct grafting), and cooling it (indirect grafting), varied slightly. Copper piping extended into the box (though this is not shown in the above photo). This copper piping was attached to a source of pressurized air. To cool the box, dry ice was placed in the bottom of the chamber and air was blown into the box. This allowed for irradiation temperatures of about -20 °C. Prior to an irradiation, the box was allowed to cool to a more stable temperature and also to let the sample vials reach temperature equilibrium with the surrounding box. During the irradiation, the sample vials would most likely begin to heat up due to the energy that is introduced by the electron beam, however the air flow in the chamber kept this from having a significant effect. For heating the chamber, a heating tape is wrapped around the outside of the copper tube, air inlet prior to entering the sample chamber. When turned on, the heated air passing through the tubing was able to heat the box to the desired temperature. In a similar fashion to the cooling process, the external temperature of the vials during the irradiation was higher than the temperature of the box, which was monitored through the use of two thermocouples at different locations in the box.

3.4.1 Dosimetry

The accurate determination of the dose reached by the irradiated samples was a fundamentally important aspect of the grafting experiments. Dose measurements are reliant on the geometry and physical state of the system being irradiated. Therefore, individual dosimetry measurements had to be performed for a number of different sample irradiation configurations, direct and indirect grafting, and for both the rotating platform and the higher dose rate direct irradiation configurations. In all cases, BioMax Alanine Dosimeter Films, shown in Fig. 3.14, were attached to calibration sample vials prior to the irradiation of any actual samples.

Figure 3.14 – BioMax Alanine Dosimeter Films

These reference vials would not contain sample fabric nor would they contain a monomer solution. For indirect grafting experiments, where the fabric is by itself in the sample vial, the calibration vials would be filled with air. For direct grafting experiments, the calibration vials would be filled with water to the same height as what would be characteristic of the monomer solution level in actual sample vials. During the rotating platform experiments, three to four sample vials would have alanine films stuck onto their outer surface, two per vial. The alanine strips would be oriented in such a way so that when the sample is in the direct path of the electron beam the alanine strip would be parallel to the electron beam. Alanine strips would be placed on vials around the platform at even intervals.

For the higher dose rate irradiations where either one or two vials would be placed directly in the beam path, one alanine strip would be placed on each side of the vial(s), parallel to the beam path. The alanine strips were both oriented vertically, so the alanine strip was running up and down the vial, or horizontally around the bottom of the vial. These two orientations were selected as a means of more accurately referencing the beam profile that would be observed by the sample for that particular dosimetry. Directly grafted samples, with vials full of monomer solution, and larger fabric samples standing up in the vial during indirect grafting would have beam profiles more similar to the vertically oriented alanine strips. However, indirectly grafted samples lying on the bottom of the vial would have a beam profile more similar to the horizontal orientation.
The BioMax alanine strips have a limited calibrated range and so the strips could not be irradiated to doses above roughly 80 kGy or below 3 kGy otherwise there could be significant deviations. Based on previously measured doses/dose rates and assuming an

increase or decrease in dose rate based on the configuration of the samples, a time was chosen for the irradiation of the samples (about five minutes in most cases). Following the irradiation of the calibration vials and the alanine strips, the strips were taken to a Bruker Alanine Dosimeter Reader, see Fig 3.15.

Figure 3.15 – The Bruker Alanine Dosimeter Reader

This alanine dosimeter reader is an EPR spectrometer capable of reading the unpaired electron signal generated in the alanine on the strip during the irradiation. By integrating the area under the peaks in the alanine spectra and comparing the values to an internal standard, the dose received by the strip can be determined. The doses received by the various strips during the irradiation are then averaged. This final dose was used for the determination of the counts/kGy of the sample configuration tested. It is assumed that the average of the dose received on the front and back side of the sample vial could be used to estimate the dose received inside the vial. Since the greatest attenuation of the electrons from the LINAC would be from the glass, especially for the indirect-grafted sample vials,

the dose inside the vial can be estimated to be the average of the dose entering and leaving the vial. The high energy electrons leaving the LINAC would have enough energy wherein there would not be a significant loss of electron energy through particle interactions. This was later verified by placing an alanine strip inside some vials during the irradiation by a 2 MeV Van da Graaff accelerator. The difference between the average value of the two exterior alanine strips and the one interior alanine strip was minimal. Using the calculated dose, the time of the irradiation, and the total counts received via the Faraday cup allowed for an accurate and rigorous prediction of time of irradiation to reach a desired dose for the actual fabric samples. While sample irradiations could not be stopped at a specific number of counts, the irradiations could be stopped well within 1% of the desired dose, especially for larger doses. Dosimetry was used as an initial calibration step; therefore, it was not performed every time a sample irradiation was carried out and was only performed if the sample configuration was changed. However, all evaluations of the standard error of the dose measurement (under the same irradiation conditions), $\sigma_{tot,}$ can be considered to have less than 4% error based on the individual contributions to the standard error from both the accuracy of the measurement from the dose reading off the alanine strips ($\leq 1\%$), $\sigma_{alanine}$, and the standard error value for the distribution of doses obtained from the placement of the alanine strips on the irradiation stage at different positions ($\leq 3\%$), $\sigma_{location}$, per equation 3.1[128]:

$$\sigma_{tot} = \sqrt{\sigma_{alanine}^2 + \sigma_{location}^2} \tag{3.1}$$

3.5 Post-radiation processing of samples

Following the irradiation of the sample vial, the fabric had to be processed through a number of extra experimental steps to prepare the samples for uranium extraction experiments, as described in this Section of the thesis.

3.5.1 Directly Grafted Samples

Following the irradiation of vials containing both the monomer and fabric solution, in some cases the vials were left overnight at about 60 °C. This heat treatment was shown to increase the DoG of the substrate in many cases. Once the heat treatment was completed, the grafted substrate would have to be cleaned of any excess monomer. This was often carried out through multiple washes with an appropriate solvent, such as methanol, water, dichloromethane (DCM), etc. Samples would be sonicated and rinse multiple times. Once the washing was completed, the sample would be dried in an oven at 60 °C. The final mass of the sample would then be obtained with the use of a mass balance once the sample had cooled back to room temperature.

3.5.2 Indirectly Grafted Samples

For samples grafted through the indirect process, the monomer solution needs to be added very quickly after the initial irradiation. This is to make sure that the decay of radicals is limited as much as possible following the irradiation. Immediately following the irradiation, sample vials containing only the substrate material are moved into a glove bag along with purged vials of monomer solution. This glove bag is sealed and purged with

argon gas to prevent any oxygen penetration into the sample vials as this would further decrease the radical concentration in the samples. The monomer solution is then transferred to the sample vials via syringe or pouring. Once the monomer solution has been transferred, the vials are shaken to ensure the complete penetration of solution into and around the substrate and they are moved into an oven at 60 °C where they remain at least overnight. This heat treatment is believed to allow for increased radical mobility inside the substrate material, thereby allowing the radicals to react more readily with the vinyl groups in the monomer solution. Following the heat treatment step, the indirectly grafted substrates are washed, dried, and massed in similar fashion to the directly grafted samples.

3.5.3 Azo group attachment

Once samples had been grafted with the VBC precursor, they subsequently had to have the selected azo compound chemically bound to their surface. The samples chosen for azo attachment were placed into polypropylene baskets and individually labeled. A mixture of sodium carbonate, dimethyl formamide, and the azo compound were mixed together in a flask under nitrogen. There were roughly 8 equivalents of azo compound to the estimated molar quantity of chlorine groups on the surface of the VBC grafted fabric. This mixture was stirred at 40-50 °C for 30 minutes. The fibers in their baskets were then added one by one. Once all the baskets had been added, the mixture was heated and stirred under nitrogen for 3-4 days.

Following this time period, the samples were removed from reflux, washed of excess reactant using methanol and water repeatedly, and then dried in an oven overnight at 60 °C. The dried fabrics cooled and their final masses were obtained.

3.6 Linear Accelerator – Pulse Radiolysis

Pulse radiolysis measurements were carried out at facilities at Brookhaven National Laboratory (BNL). Sample solutions were prepared in the laboratories at BNL. No pulse radiolysis experiments were performed with substrates, only solutions of monomer were irradiated.

3.6.1 Van de Graaff and FTIR

In order to study the decay of specific vibrational modes of monomer correlating to the polymerization of the monomer under ionizing radiation, a combination of a 2 MeV Van de Graaff accelerator and time resolved FTIR was used. Different concentrations of a specific monomer were prepared in solutions and placed in vials like the one in Fig. 3.16.

Figure 3.16 – The reservoir bottle from which monomer solution was drawn for Van de Graaff pulse radiolysis experiments. The cap of this bottle allows the solution to be sparged with a gas while sample is withdrawn using a syringe pump.

These vials allowed for the purging of the monomer solution with an inert or N_2O atmosphere (which in aqueous solution irradiations quenches the production of aqueous electrons in solution while doubling the amount of hydroxyl radicals), while also allowing for the solution to be pumped into a thin cell window, shown below.

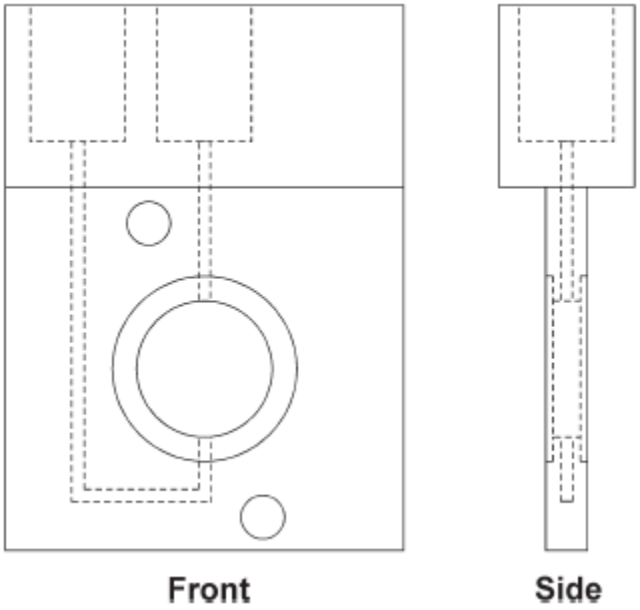

Figure 3.17 – This schematic illustrates the inlet and outlet of the IR window used during pulse radiolysis experiments. From the front, the electron beam is allowed to pass through the circular quartz window where it can interact with a thin film of monomer solution. From the side, the FTIR beam can pass through the irradiated sample for sample data collection.[129]

This thin cell window, shown in Fig. 3.17, allows for the electron beam generated by the Van de Graaff accelerator to pass through a window which is composed of a thin layer of monomer solution sandwiched between two quartz windows. The set-up as it was used during the experiments is shown in Fig. 3.18.

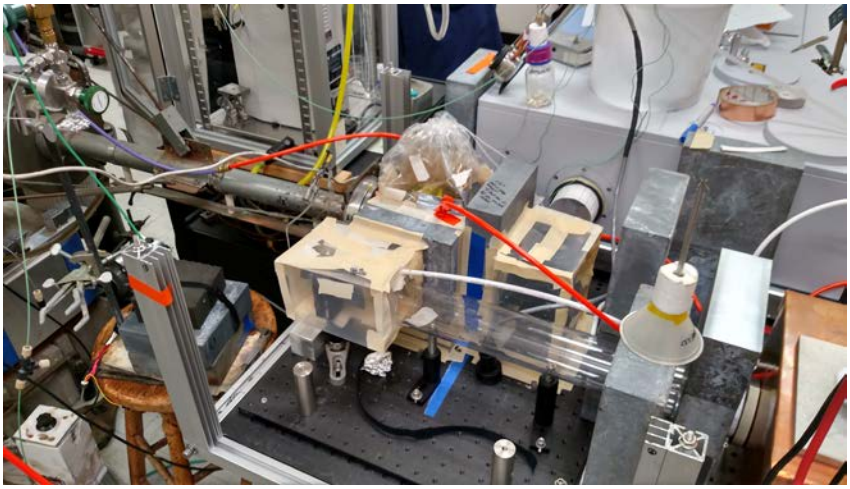

Figure 3.18 – This image illustrates the FTIR pulse radiolysis set-up. The beam tube and exit port of the Van de Graaff can be seen on the left side of this image. In the center of the image, within the plastic bag, is the FTIR cell window containing the monomer solution. In the back right of the image, the FTIR spectrometer can be seen.

During and following the irradiation of the monomer solution, the fluctuating chemistry inside the cell window is monitored through the use of real-time FTIR. Once FTIR measurements are completed, the cell is purged of the irradiated solution through the use of a syringe pump. Once a fresh solution is in the cell, a new irradiation run can be carried out.

3.6.2 Linear Electron Accelerator Facility (LEAF)

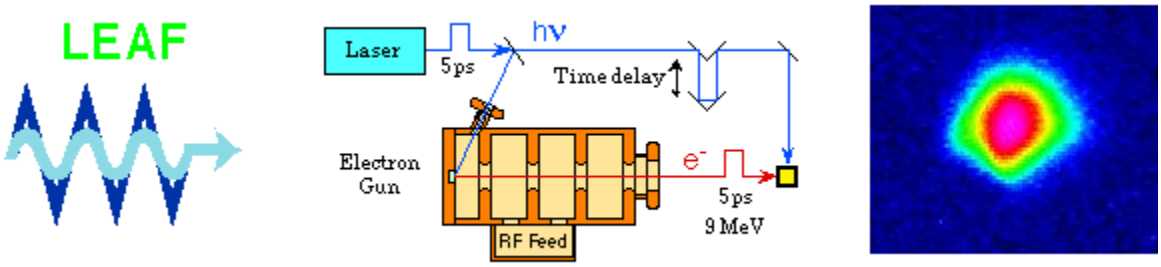

Figure 3.19 – The center image shows a drawing illustrating the mechanism of the LEAF facility. On the right, an image of the electron beam cross section is shown.[130]

The decay of a number of free radical species, such as the aqueous electron and the hydroxyl radical, can be studied through the use of ultrafast UV-Visible spectroscopy coupled with a pulsed electron beam. The decay of these free radical species provides valuable insight into the mechanism and rate of polymerization of a selected monomer species. The LEAF facility, see Fig. 3.19, is capable of nanosecond spectroscopy measurements, with absorbance measurements taken at intervals of 0.5 ns. For these experiments, a number of solutions are prepared depending on the desired dominant radical species.

For hydroxyl radical production, a solution of monomer in water in a quartz cuvette is purged with nitrous oxide before being placed in a sample holder. This sample holder, shown as a yellow square in the above image of the facility is incident both to the pulsed electron beam and a UV-Visible laser pulse. An initial electron pulse is produced when the high-energy laser pulse is directed towards a metal plate. Through the photoelectric effect, a packet of electrons is ejected from the plate and accelerated down a beam line using a

series of sequential, alternating electric fields. The laser pulse that past the beam splitter is time delayed before hitting the aqueous sample so that the absorption of the sample at the specific laser wavelength can be measured following the initial electron excitation, but still fast enough to monitor transient radical species.

For aqueous electron production, an aqueous solution of monomer with 20 wt. % tert-butyl alcohol is prepared. The procedure remains the same as that described for the N_2O purged solution.

3.6.3 Dosimetry

Dosimetry of the Van de Graaff accelerator was not specifically determined. The dose received by any sample was estimated based on previous knowledge by the facility of the dose received by aqueous solutions in the IR cell. The dose received by the aqueous solutions in the LEAF facility were obtained through the use of thiocyanate dosimetry.

3.6.3.1 Thiocyanate dosimetry

In order to determine the inherent dose upon the sample in the LEAF facility, a thiocyanate dosimeter was used. The thiocyanate dosimeter is a 10 mM solution of potassium thiocyante in water and purged with N_2O. This solution is irradiated with the pulsed beam and the absorbance of a 480 nm light pulse in the sample is recorded over time. An example of a trace of the absorption of a 10 mM thiocyanate solution is shown in Fig. 3.20.

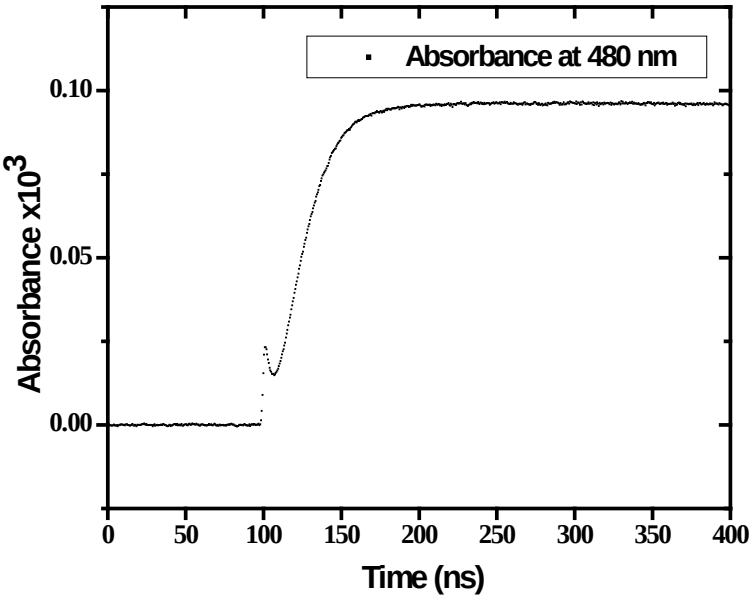

Figure 3.20 – A trace of the absorbance of the thiocyante solution at 480 nm after an electron pulse showing the production and quenching of the aqueous electron at about 100 ns and the continued production of the $(SCN)_2^{\bullet -}$ following.

The adsorption of thiocyante at 480 nm is due to the $(SCN)_2^{\bullet -}$ species which is formed via the following reaction pathway shown in equations 3.2 and 3.3 upon interaction of the thiocyante ion with the hydroxyl radical[131,132]:

$$^{\bullet}OH + SCN^- \rightarrow SCN^{\bullet} + OH^- \quad (3.2)$$

$$SCN^{\bullet} + SCN^- \rightarrow (SCN)_2^{\bullet -} \quad (3.3)$$

The dose per pulse of pulse radiolysis experiments is obtainable through the use of the following equation, eq. 3.4:

$$D_D = \frac{\Delta A}{\Delta \varepsilon l \rho G(P)} \quad (3.4)$$

where D_D is the dose (per pulse, in the case of pulse radiolysis), ΔA is the change in adsorption at 480 nm following the electron pulse (unitless), $\Delta\varepsilon$ is the difference in molar adsorption coefficient between the reactant and product at 480 nm ($m^2\,mol^{-1}$), l is the path length (m), ρ is the density of the solution ($kg\,m^{-3}$), and G(P) is the radiation yield of the product molecule ($mol\,J^{-1}$)[27]. If the units of the radiation yield of the product are in molecules/100 eV, then the numerator of the equation will be multiplied by 9.648×10^6, $\Delta\varepsilon$ will be in $M^{-1}cm^{-1}$, density will be in $g\,cm^{-3}$, and path length will be in centimeters to obtain the same units.

Within the thiocyanate system used in this dissertation, with $\Delta\varepsilon \times G(CNS)_2^{\bullet -} = 2.23 \times 10^{-4}\ m^2J^{-1}$, l = 0.010 m, and $\rho \cong 1000\ kg/m^3$, the dose per pulse can be calculated based on the average adsorption of initial pulse radiolysis adsorption measurements of a 10 mM solution of thiocyanate. With an average adsorption value of 0.095 ± 0.00049 of the different runs, the average dose per pulse of the LEAF facility during the pulse radiolysis experiments of DAOx was 42 ± 0.22 Gy/pulse.

3.6.4 Reaction Kinetics Analysis

The determination of the reaction kinetics of the aqueous-monomer systems through the data recorded from the pulse radiolysis experiments described throughout section 3.6 was carried out by fitting the data to the appropriate rate constants. In particular, the pulse radiolysis data obtained for the 1697 cm^{-1} and 1798 cm^{-1} B2MP peaks and the transient absorption of DAOx at 480 nm were fit to first order, second order, and pseudo-first order rate constants respectively.

In particular for the build-up of product at the 1798 cm^{-1} peak during and following the irradiation of B2MP solution in D_2O special consideration must be made for the evaluation

of the second order kinetics. As the product is adsorbing, i.e. the product of the second order reaction is what is being monitored, not the decay of the reactants, the reaction rate cannot simply be fit to a trend of the inverse of the absorbance versus time. In order to obtain a useful relationship, an equation relating the slope of the inverse of the change in absorbance versus time to the rate constant of the reaction if the adsorption coefficient, ε, and path length, l, are known for the investigated system[133]. For a system where the product adsorbs and the reaction is predicted as a reaction between two identical radical species as portrayed in the following reaction, eq. 3.5:

$$A + A \rightarrow M \tag{3.5}$$

where A is the radical species and M is the product of the reaction between the two radical species. In this case, if we let x = [M] and by stoichiometry [A] = $[A]_\circ$ – 2x, then we obtain the following, equations 3.6-3.8, if only M absorbs:

$$\frac{d[M]}{dt} = k[A]^2 \tag{3.6}$$

$$\int_0^{[M]_t} \frac{dx}{([A]_\circ - 2x)^2} = \int_0^t k dt \tag{3.7}$$

$$\frac{1}{2([A]_\circ - 2[M]_t)} - \frac{1}{2[A]_\circ} = kt \tag{3.8}$$

Assuming the reaction essentially goes to completion, then we will obtain equations 3.9 and 3.10

$$[A]_\circ \cong 2[M]_\infty \tag{3.9}$$

$$\frac{1}{4([M]_\infty - 2[M]_t)} - \frac{1}{4[M]_\infty} = kt \tag{3.10}$$

Assuming Beer's Law holds (A = [M]εl) then we obtain equation 3.11

$$\frac{1}{A_\infty - A_t} = \frac{4kt}{\varepsilon l} + \frac{1}{A_\infty} \tag{3.10}$$

Therefore plotting $[A_\infty - A_t]^{-1}$ vs. t should give a straight line with equation 3.12

$$Slope = \frac{4k}{\varepsilon l} \tag{3.12}$$

3.7 Sample Characterization

Following the grafting of uranium extraction monomer to the surface of various substrates, multiple characterization techniques were employed to (i) determine the attachment of the monomer (ii) examine the surface morphology of the substrate, and (iii) examine the concentrations of various elements on the surface.

3.7.1 Gravimetric analysis

Gravimetric analysis was performed on all fabrics following the cleaning and drying stage of the sample preparation. Samples were massed on a MS205DU Mettler-Toledo scale. These measurements were performed in order to obtain the mass difference of substrates following grafting to provide information on the total DoG of the monomer on the polymer backbone.

3.7.2 FTIR-ATR

All FTIR-ATR measurements were carried out using a Thermo Nicolet NEXUS 670 FTIR with a SMART Endurance ATR attachment in place. The ATR attachment was purged for at least 15 minutes before any samples were run. Samples were run from 4000 to 650 cm^{-1} with a resolution of 2 cm^{-1} with 48 scans per sample. Background spectra were obtained prior to each different sample number and the surface of the ATR module was

cleaned with organic solvent and dried prior to starting the next sample analysis. These measurements were carried out at random space intervals throughout the sample, with usually three measurements on one side of a fabric substrate and three more on the other side.

3.7.3 SEM-EDS

A scanning electron microscope (SEM) equipped with an energy dispersive spectroscopy (EDS) detector was used to characterize the morphology of the adsorbent fabric and to identify the chemical species extracted by it. Adsorbent samples that have been exposed to Atlantic Ocean Seawater seawater during the adsorption experiments were dried overnight in a vacuum dessicator and mounted on a SME aluminum stub for EDS analysis. The EDS detector was part of a Hitachi S-3400 variable pressure SEM.

3.7.4 XPS

XPS measurements were carried out using a Kratos Axis 165 spectrometer using monochromatic Al radiation (at a power of 280 W) with a vacuum level at or below 5×10^{-8} torr throughout the data collection process. Due to the insulating nature of the nylon 6 samples, charge neutralization was required to minimize sample charging. All survey spectra were collected with a pass energy of 160 eV and all high resolution spectra with a pass energy of 20 eV. All spectra were calibrated to C-C/C-H bonding at 284.8 eV. Samples were prepared by attaching the grafted fabric directly to the metal stage using copper tape.

3.7.4.1 Uranyl binding to azo compounds

Binding of uranyl to a number of azo compounds was carried out using XPS. Equivalent molar quantities of an azo compound and uranyl acetate were dissolved in separate solutions of methanol. Once dissolved, these solutions were mixed and stirred. The methanol was then allowed to evaporate off and the precipitate was collected for testing in the XPS.

3.7.5 Zeta Potential Measurements

Microparticle solutions were prepared using pieces of nylon 6 grafted fabric via the "solvent in water" precipitation method. Samples were first dissolved in acetic acid at 80℃, at a concentration of 20 mg/mL to form the diffusing phase (organic phase). This phase was then added drop by drop into filtered deionized water, which is the dispersing phase (aqueous phase), under moderate magnetic stirring. The formation of microparticles was instantaneous and the solution was kept under mild agitation for 4 h to allow for particle stabilization. Small aliquots from each microparticle solution were diluted in DI water and titrated to pH 8.3, pH 4.5, and pH 3 using sodium hydroxide and hydrochloric acid solutions prior to surface charge characterization. The zeta potential of nylon 6 microparticles was assessed by means of electrophoretic light scattering (Zetasizer nano-ZS90; Malvern instruments; Westborough, MA).

3.7.6 Electron Paramagnetic Resonance Spectroscopy

EPR spectroscopy is a powerful technique for detecting the spin of unpaired electrons, also known as free radicals, in a material. In a magnetic field, the magnetic fields of the

unpaired electrons will align parallel to the generated magnetic field. During a measurement, photons of a range of frequencies in the microwave region are supplied to the sample. These photons can be adsorbed by the aligned, unpaired electrons causing the alignment of the electron's magnetic field to become antiparallel to the generated magnetic field. The relationship between the microwave energy and the energy required to flip the spin of the electron is described by the following equation, eq. 3.13:

$$\Delta E = \hbar\nu = g\mu_{\circ}B \tag{3.13}$$

where ΔE is the energy required to flip the spin of the electron, ħ is the reduced Planck's constant, 1.055×10^{-34} J ● s, ν is the frequency of the microwave inherent upon the sample, g is the g-factor which is approximately 2, $\mu_{\circ}$ is the Bohr magneton, 9.264×10^{-24} J●T^{-1}, and B is the magnitude of the magnetic field in gauss[134].

When an EPR spectra is obtained, a constant microwave frequency is applied to the sample and the magnetic field is swept over a range of strengths. The intensity of the adsorption of the microwave is recorded by the EPR, however the first derivative of this adsorption spectrum is often what is reported. The generated spectrum contains many subtleties regarding its behavior and shape. For example, in many samples the free radical is located close enough to an unpaired nuclear spin, i.e. a hydrogen atom, which will apply a small but measureable magnetic field to the free radical along with the magnetic field from the EPR. Therefore the resulting magnetic field applied to the unpaired electron will actually be a sum of these two magnetic fields, shown in equation 3.14:

$$B = B_{\circ} \pm B_I \tag{3.14}$$

where B is the total field strength applied to the unpaired electron, $B_{\circ}$ is the field strength from the EPR magnet, and B_I is the magnetic field strength contribution from the local

unpaired nuclear spin. B_I can be positive or negative, similarly to the orientation of unpaired electron being antiparallel or parallel to the EPR magnetic field. Since there are now two different magnetic fields affecting the orientation of the unpaired electron spin, the adsorption peak will be split into two identical peaks. Known as the hyperfine interaction, the magnitude of this interaction follow's Pascal's triangle.

When interpreting an EPR spectrum (reported as the first derivative of the actual adsorption spectra), the number and splitting of the peaks present in the spectrum are directly related to the local chemical environment of the free radical. Nomenclature of EPR dictates that the atom that is bound to the free radical is the α atom, while the nearest neighbor atoms are the β atoms.

Figure 3.21 – An example image of a Bruker Elexsys Spectrometer.[135]

EPR spectroscopy was carried out at NIST on a Bruker Elexys, shown in Fig. 3.21, using an EPR spectrometer equipped with a Bruker 4119 cavity and operating in the X-band. The spectral recording parameters utilized for the measurements in this dissertation

were as follows: 12.7 mW microwave power; 10 mT field sweep; 0.4 mT modulation amplitude; 20 ms conversion time; 20 ms time constant; and a spectral resolution of 1024 data points. This instrument and these instrument parameters were used to study the behavior of radical decay in irradiated polymer substrates. The intensity of the peaks in the EPR spectrum will be directly correlated to the concentration of unpaired electrons in the measured material. Within the context of this dissertation, the main source of unpaired electrons within an irradiated substrate material, like nylon 6, would be the result of an irradiation. The experiments associated with this were aimed at determining the radical decay time inside nylon 6 to validate the indirect grafting method and to improve the understanding of the grafting mechanism.

Substrate samples were irradiated at MIRF under 10.5 MeV electrons to varying doses, particularly doses that would reflect normal grafting procedures, i.e. 150-250 kGy. These samples were irradiated in inert atmosphere conditions at dry ice temperatures. Following the irradiation, the vials containing the substrate samples were moved inside an argon purged glove bag while still in contact with dry ice, where the fabric was removed from the vial and transferred to quartz EPR tubes. These tubes were sealed with parafilm to limit the presence of oxygen in the tubes since oxygen would promote separate paths for radical decay separate from the monomer-substrate radical interactions that would be present during the indirect grafting process.

3.8 Uranium Extraction Testing

3.8.1 Rotator

Test solutions of uranium in seawater were prepared by dissolving a suitable quantity of uranyl acetate dihydrate in Atlantic Ocean Seawater. In each test, the adsorbent sample was added to a desired volume of a solution of uranium in seawater and the combination of test solution and solid adsorbent was rotated for a desired period of time, usually seven days, at 30 rpm in a rotating agitator. An image of the rotator is shown in Fig. 3.22. At the end of this period, the solution was separated from the adsorbent and analyzed to determine the amount of uranium remaining in the solution.

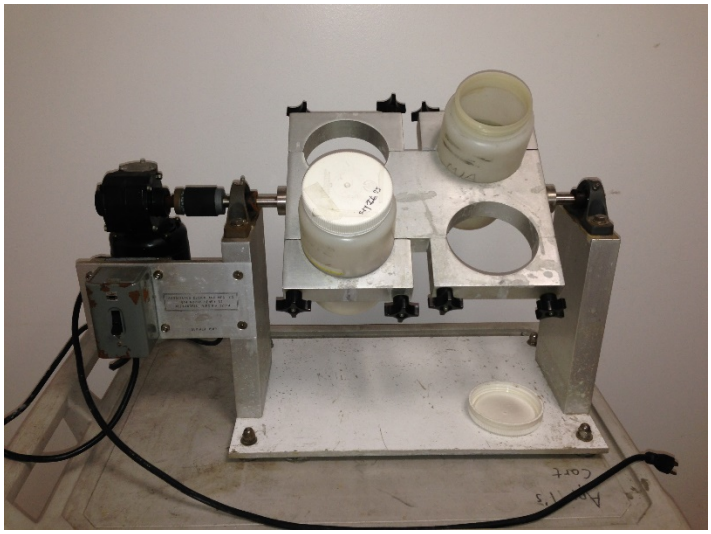

Figure 3.22 – The sample rotator used for agitating solutions of doped seawater in contact with grafted fabric samples.

3.8.2 Flow loop

In order to improve the testing conditions for the extraction samples, a separate testing system was manufactured to resemble the testing facilities at Pacific Northwest National Laboratory[136]. This flow loop design is shown in Figs. 3.23 and 3.24. Flow columns were obtained from PNNL which were then attached to a plastic tube via quick-connect fittings. A pump drives undoped seawater from a large reservoir through the four columns. Flow rate meter along with needle valves at the end of the columns allow for precise control over the flow rate in the columns. Samples are packed into glass wool and then placed among plastic beads inside the columns to make sure the uranium extraction sample remains in place throughout the entirety of the experiment. The flow loop reservoir was filled using Nutri-SeaWater saltwater, which is ocean water that has been filtered and replenished with certain trace elements, including uranium. Once samples were in place in the flow columns, the system was run for two weeks at ~0.4 gpm.

Figure 3.23 – The front view of the flow system designed to test fabrics under conditions similar to the testing performed at PNNL.

Figure 3.24 – A top down view of the flow system showing a clearer view of the seawater reservoir, the pump, and the pressure manifold.

3.8.3 Determination of Uranium Extraction

Fundamental to the development of materials capable of extracting uranium from seawater is the determination of their capacity for extraction. A number of different experimental methods were employed for the determination of a sample's extraction efficiency following exposure to uranium-doped seawater.

3.8.3.1 Inductively Coupled Plasma Atomic Emission Spectroscopy (ICP-AES)

Figure 3.25 – The Perkin Elmer Plasma 400 ICP-AES used for the uranium extraction testing experiments.[137]

ICP-AES was used for the determination of the concentration of uranium in the test solutions following the extraction period. This instrument, the Perkin Elmer Plasm 400 shown in Fig. 3.25, was capable of 1 ppm U resolution and, therefore, test solutions of less than 1 ppm were not analyzed with this technique. Prior to testing solutions, a series of

uranium standards were made at varying concentrations. These standards were evaluated using the standard addition method to extrapolate uranium adsorption signal back to 0 ppm concentration. The standard addition method was used due to the complexity of the seawater matrix present in the test solution. Solutions of uranium in seawater following the extraction period were run through the spectrometer. The fraction of the uranium taken up by the adsorbent was calculated from the difference in concentration of uranium in the test solution resulting from the contact with the adsorbent.

3.8.3.2 Spectrophotometric

Uranium detection sensitivity was improved for later experiments through the use of a spectrophotometric procedure for the determination of uranium in solution. This technique has a detection limit of 0.2 ppm U, one order of magnitude better than ICP-AES measurements, thus, enabling test solutions to be used which are closer to the natural concentration of seawater in the ocean. The fundamental chemical required for this procedure is Arsenazo III, the structure of which is shown in Fig. 3.26.

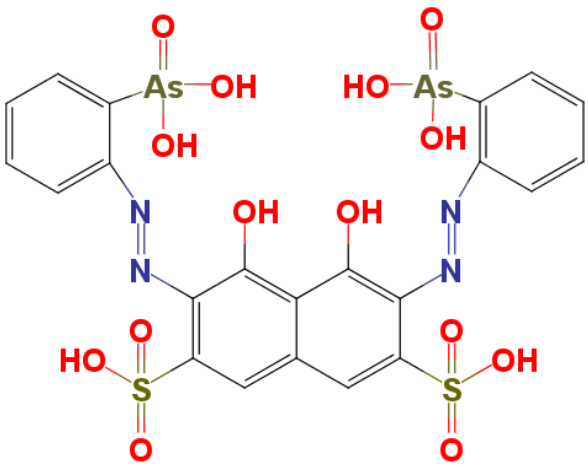

Figure 3.26 - The chemical structure of Arsenazo III.

Arsenazo III forms a complex with uranium with an absorption peak at 651 nm. An aqueous solution of this chemical along with a masking agent, triethylenetetraminehexa-acetic acid (TTHA), were combined with seawater samples and tested for their absorbance at 651 nm using a Cary 3 UV Spectrometer.

A 0.05 wt. % solution of Arsenazo III in ultra high purity, deionized H_2O and a 5 wt. % TTHA were created. 2 mL of each of these solutions were added to 1 mL of uranyl solution in seawater or simulated seawater. In order to improve the sensitivity of the Arsenazo III compound, the pH of the resulting solution was adjusted to 1 using different concentrations of hydrochloric acid. Once the appropriate amount of acid was determined in order to adjust the pH of this solution to 1, 2 mL of 0.05 wt. % Arsenazo III solution, 2 mL of 5 wt. % TTHA solution, and 1 mL of varying concentrations of uranium in a representative seawater solution were created. The seawater solutions containing specific concentrations of uranium were generated through the volumetric dilution of a standard stock solution of uranium. These solutions sat for at least one hour to allow the solutions to come to equilibrium. Afterwards, the solutions were tested for their absorbance at 651 nm in the UV-Vis spectrometer. The absorbances for the standard solutions were used as the standard reference for the test samples. Once the concentration of the uranium in the final solution was determined, the fraction of the uranium taken up by the adsorbent was calculated from the difference in concentration of uranium in the test solution resulting from the contact with the adsorbent.

3.8.3.3 Inductively Coupled Plasma Mass Spectrometry

While the prior characterization techniques provided reliable quantitative results for the concentration of uranium in extraction test solutions, they do not provide the required resolution of uranium concentration in seawater to match the concentration present in the actual ocean (3.3 ppb). In order to provide some insight into how the manufactured fabrics perform in lower concentrations of seawater, ICP-MS can be used.

3.8.4.3.1 Solution based

In order to process the fabric samples using ICP-MS that had been exposed to a solution of uranium in seawater, the uranium first had to be dissolved into an acidic solution. While an acidic solution would dissolve the Nylon 6, its complete dissolution would ensure that the entirety of the uranium present on its surface was in solution. While it was found that 2 % nitric acid could not dissolve the nylon fabrics by itself very quickly, a concentrated solution of nitric acid heated to 80 °C overnight was used to digest the fabric. Following this digestion, the concentrated nitric acid was boiled off and the remaining compound in the Teflon container which held the remaining fabric particles and metal ions was re-dissolved in 2 % nitric acid, which is the desired concentration for ICP-MS solution processing.

The uranyl test solution was processed using an ELEMENT 2 ICP-MS, shown in Fig. 3.27. After being loaded into a syringe pump, the sample solution was sent into an argon plasma where the elements in solution were ionized and accelerated through a series of cones to a bending magnet which separated the evaporated ions according to mass and charge. The concentration of uranium in the test solution was determined with the use of a standard solution of uranium. The counts per second read by the detector in the ICP-MS

was correlated to varying concentrations of uranium and other elements. This relationship was then used to determine the concentration of uranium in the test solution. Since the volume of the test solution was known, the mass of uranium in the solution could be determined which could then be used to calculate the mass of uranium present on the fabric prior dissolution.

Figure 3.27 – An image of the ELEMENT 2 ICP-MS instrument used in all ICP-MS experiments performed in this dissertation.

3.8.3.3.2 Laser Ablation

In order to look at uranium concentration at varying locations in the fabric, laser ablation ICP-MS can be performed. Instead of completely dissolving the uranium exposed fabric to obtain a bulk measurement, this experimental technique uses a laser to ablate a sample material. This ablated material is then blown into the ICP using a stream of helium

gas. Fig. 3.28 shows the New Wave Research UP-213 nanometer wavelength laser ablation unit.

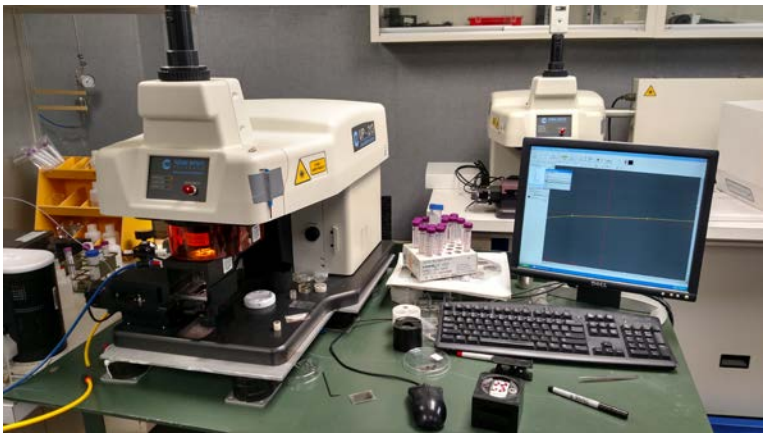

Figure 3.28 – An image of the New Wave Research UP-213 nanometer wavelength laser ablation unit used for laser ablation experiments on fabrics exposed to seawater.

Prior to the ablation of samples, a calibration standard was ablated to provide a reference for determining the concentration of uranium in ppm. Orchard leaves were doped with specific concentrations of uranium and vanadium. The orchard leaves acted as an analogue to the nylon 6 fabric as the carbon composition of both compounds were similar. These orchard leaves were then ablated and the carbon to uranium ratio was used to establish a calibration for the uranium in any samples where the carbon content is known, which is shown in Fig. 3.29.

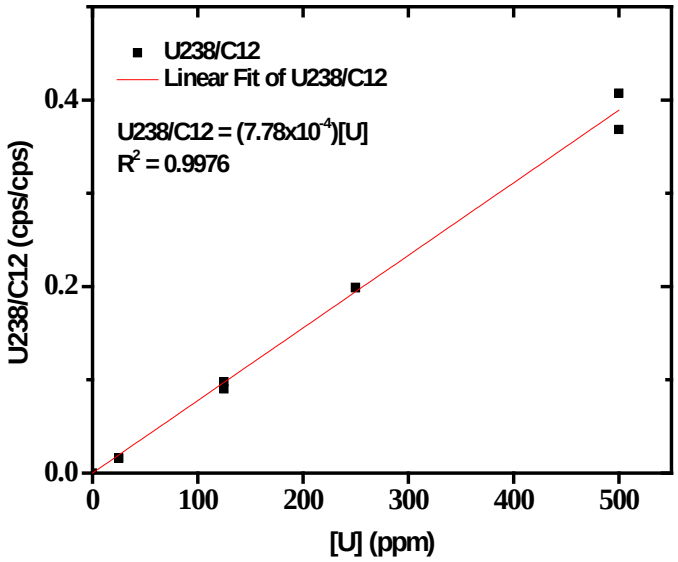

Figure 3.29 – The calibration curve for the ration between U-238 and C-12 counts from the mass spectrometer versus the concentration of uranium in the orchard leaf calibration standard.

For the polymer substrate samples, the carbon content is based on the knowledge of the chemical structure of the polymer samples and the mass of the initial fabric prior to uranium extraction testing.

Fig 3.30 shows the control and uranium exposed samples on the sample holder for the laser ablation unit. The samples were placed on double-sided sticky tape onto a glass slide. This sample compartment was then placed inside the laser ablation unit and left for at least 15 minutes to allow for the helium to purge the internal atmosphere of the compartment of air.

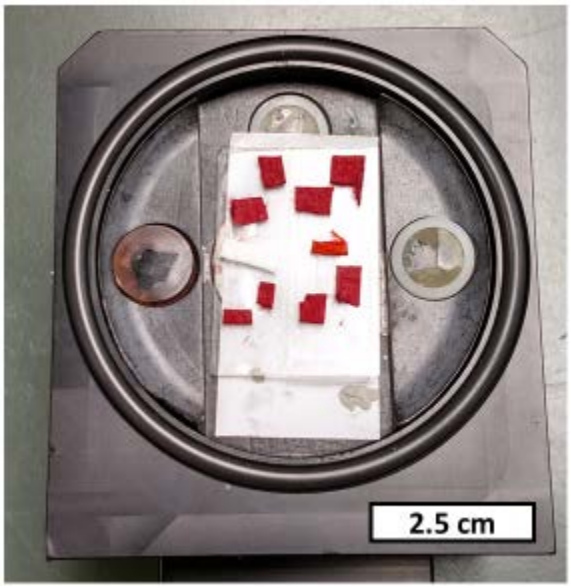

Figure 3.30 – Sample positioning on the laser ablation unit sample holder. A glass slide with double-sided sticky tape was used to hold the samples in place.

The fabric samples were then exposed to various beam conditions involving different beam diameters, dwell times, and laser shot frequency rates. Data collection for each run was started 20 seconds prior to the firing of the laser and was continued for about 30 seconds to one minute after the laser beam stop was removed.

4. Results and Discussion

Over the course of this project numerous monomers and radiation grafting techniques were utilized in an effort to fulfill the listed objectives for the project. Testing involved the evaluation of a monomer repertoire that included eight organophosphorus compounds (including phosphates, phosphonates, three oxalates, four amines, one ketone, and four azo compounds. The preliminary studies in order to determine whether or not these compounds could actually remove uranyl from seawater were performed by incorporating the compound onto the surface of activated carbon. These doped samples would then be exposed to a solution of uranyl in seawater under different concentrations and exposure times. The compounds which had the best extraction performance would then be used in grafting experiments as possible candidates for a successful uranium extraction monomer. Throughout this work, standard error is used for the values of the error bars unless otherwise noted.

4.1 Substrate Selection

Throughout this project, the substrate used for the majority of grafting experiments was a high surface area, nylon 6 fabric purchased under the name winged nylon 6. An SEM image of this material next to a macroscale image of a sample piece of fabric in Fig. 4.1. This fabric was chosen for its high surface area and its chemical resilience, which would assist with increasing grafting densities and regenerability following extraction respectively.

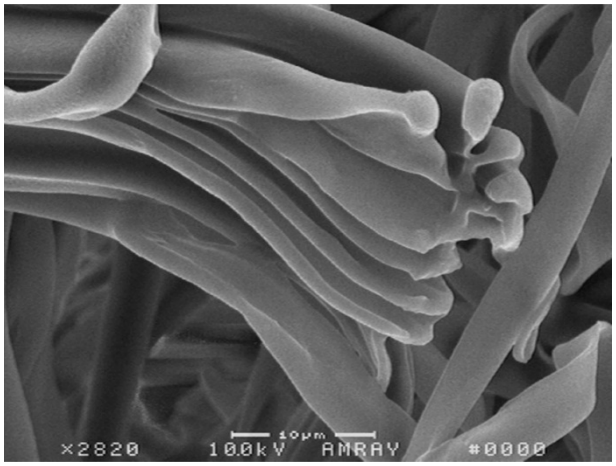

Figure 4.1– Pictures of the nylon 6 fabric prior to grafting (left) and an SEM image of the fibers that compose the fabric (right).

In order to better characterize the response of the fabric to irradiation, EPR spectroscopy was performed on the nylon fabric following irradiation. This technique can be used to elucidate the lifetime and location of the radicals on the polymer backbone. Fig. 4.2 provides an example of the decay of the nylon radicals over the course of 2.5 hours following an irradiation to 150 kGy.

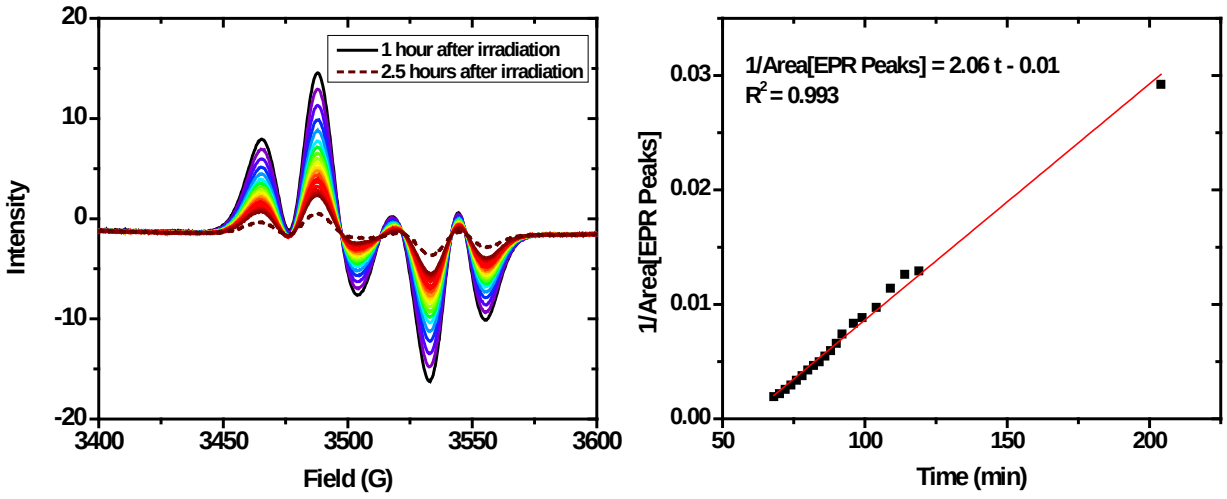

Figure 4.2 – **(a)** The EPR signal of winged nylon 6 irradiated to 150 kGy under electron beam. Time dependent spectra are shown from one hour after irradiation to 2.5 hours after irradiation. **(b)** The second order fit of the area of the EPR peaks for winged nylon 6 irradiated to 150 kGy.

Based on previous studies, the radical generated by irradiation of nylon 6 should be dominantly located on the carbon next to the amine that is not the carbonyl, see Fig. 4.3[138,139].

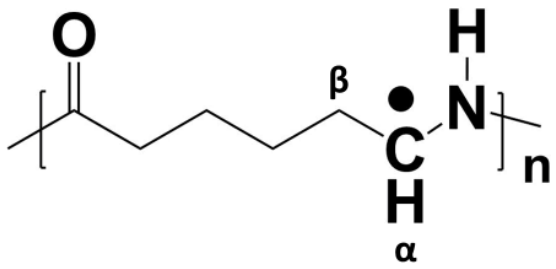

Figure 4.3 – The most likely position of the nylon 6 radical generated during irradiation. α and β signify the locations of the respective protons seen in the EPR spectrum.

The position of this radical matches the EPR spectra recorded. This free radical has two identical β protons, which create a triplet peak with intensity ratios 1:2:1. These peaks are further split by the single α proton, thereby forming a 1:3:3:1 intensity ratio of the peaks. The magnitude of the splitting should be 28 gauss for the β proton and 22 gauss for the α proton[139]. Fig. 4.4 shows the collected EPR spectra with the regions labeled with their respective intensity ratios.

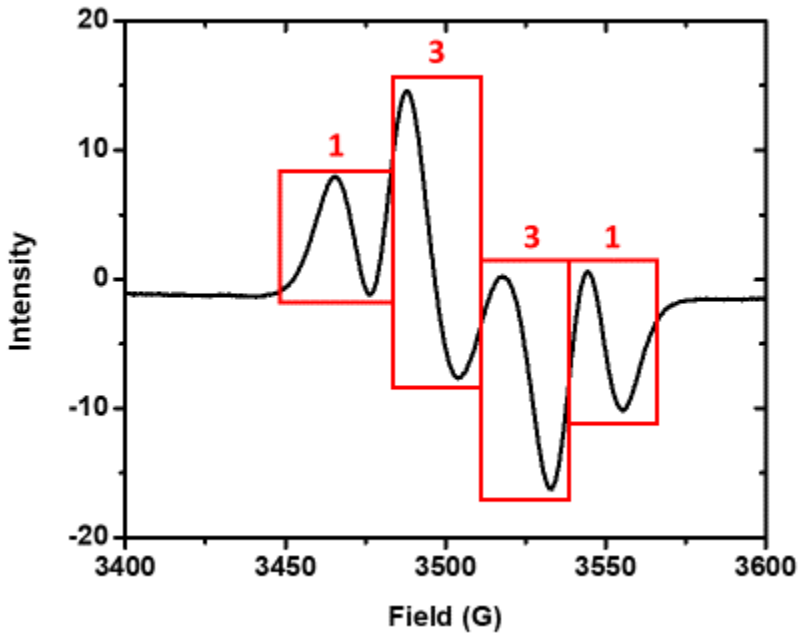

Figure 4.4 – The red boxes highlight the location of the 1:3:3:1 peaks associated with the overlap of the α and β proton splitting of the nylon 6 radical.

The decay of the nylon 6 radical most likely proceeds via a second order reaction through the following scheme:

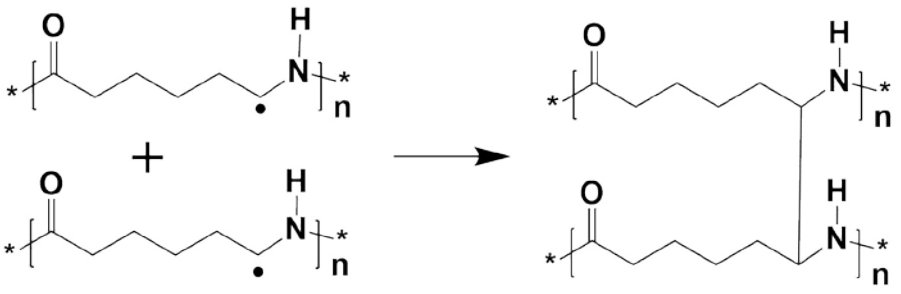

This conclusion is further corroborated by the kinetics of the decay of the radical, where the data is shown to have a significantly better fit to second order kinetics behavior in Fig. 4.5.

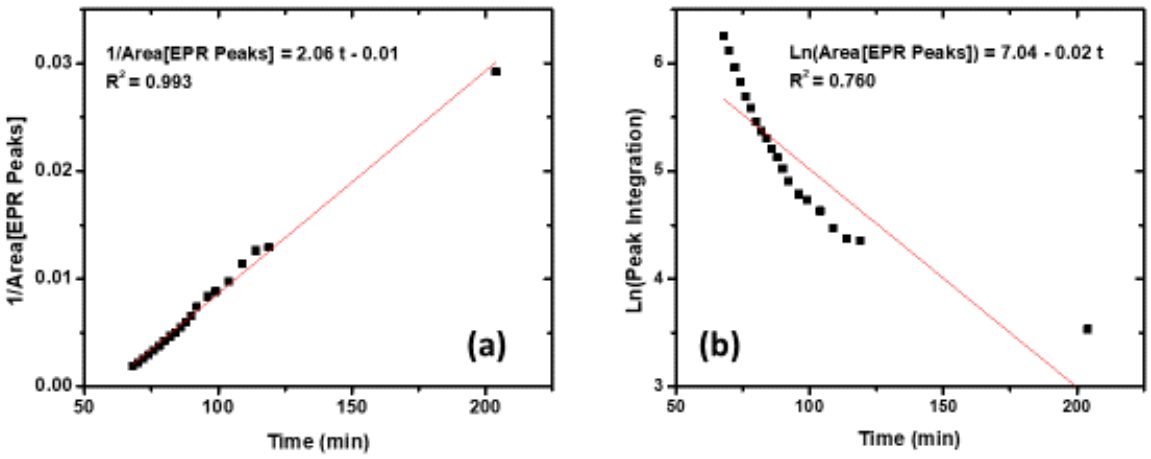

Figure 4.5 – The second order (a) and first order (b) fits for the nylon 6 radical decay.

4.2 Phosphate Compounds

The ubiquitous relationship between phosphates and uranyl ions has been well established, particularly in both geological deposits, with phosphate mine being a significant source of uranium, as well as in industrial separations of uranyl and other actinides from aqueous solutions, in the case of the PUREX process. Phosphates were initially explored as an option for the extraction of uranium from seawater based on this relationship.

4.2.1 Selection

Initial efforts to extract uranium from seawater were focused on obtaining allyl or vinyl functionalized phosphate derivatives. Phosphates have previously been used for the extraction of uranium from aqueous solutions and have been found complexed with uranium in natural ore deposits[140]. Commercially available ligands that matched these parameters were found and vetted using the activated carbon exposure method in order to determine which group was able to adsorb the most uranium from seawater in the shortest amount of time. The results of this initial experiment revealed bis-(2-methacryloxyethyl) phosphonate (B2MP) as the most successful candidate for extraction, see table 4.1.

Table 4.1 – All listed monomers were γ-irradiated at 5 kGy/hr for one hour onto winged nylon and tested for their ability to extract uranium which is exhibited by their K_D value (given in mL/g, K_D is equivalent to the mass of uranium adsorbed by the fabric per mass of the fabric given in g/g, divided by the concentration of uranium in the solution given in g/mL).

Monomer	Structure	k_D
Diethyl allyl phosphonate	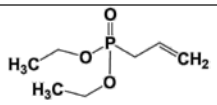	116.9
Vinylphosphonic acid	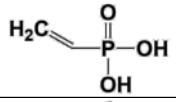	168.0
Diethylvinylphosphonate	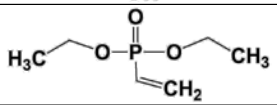	354.1
Dimethylvinylphosphonate	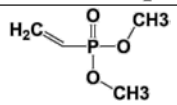	185.1
Bis(2-methacryloxyethyl) phosphonate	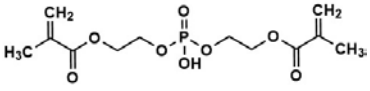	46980.1

4.2.2 Grafting

DEAP was also one of the initial compounds chosen for grafting and extraction testing following initial testing with B2MP. In an effort to promote green chemistry concepts, the solubility of DEAP in water was tested by attempting to dissolve 20 µL of the compound in various solvents including water. Unfortunately, there was no clear indication that DEAP was soluble, most likely due to the large organic chains outweighing any kind of hydrogen bonding experience by the hydroxyl group on the phosphate. Initial grafting experiments of this compound were conducted in ethanol at concentrations varying from 56 to 112 mM and the samples were irradiated to 12 kGy at a dose rate of 1.06 kGy/hr using Co-60 gamma irradiation. No noticeable grafting was observed in these initial experiments most likely due to the low total dose and the fact that the sample vials were not purged of oxygen.

The following grafting experiment used 0.23 M solutions of DEAP irradiated to doses from 10-40 kGy at 5.54 kGy/hr using Co-60 gamma irradiation at NIST. The resulting DoGs were measureable, but ranged from 3 to 7%. Previous work on phosphate compounds had found that DoGs obtained the highest uranium extraction capacities at around 100%, so these low DoGs in initial grafting experiments were not acceptable for uranium extraction testing. The low quantity of dissolved DEAP in solution was believed to be the cause of these low DoGs as the solutions were only sonicated for 30 minutes prior to irradiation.

The DoG of DEAP was further increased through the use of the MIRF facility's LINAC combined with more attention paid to the complete dissolution of the monomer prior to the irradiation treatment. Doses were increased to 60-120 kGy however the total DoG only increased to 8-13%.

Due to the limitations on this monomer's solubility in an aqueous system and the weak relationship between dose and DoG, an alternative means of improving monomer grafting was required. One method that was considered was the use of the compound Mohr's Salt, $(NH_4)_2Fe(SO_4)_2$, which has been shown in previous work to reduce homopolymerization[30,61,141,142]. Unfortunately, this compound did not produce significant increases to the DoG of the DEAP monomer. In lieu of these results, DEAP was not tested for its capacity to extract uranium following its grafting to a polymer substrate.

Another phosphate monomer was tested for grafting and uranium extraction, B2MP. Initial grafting experiments were focused on establishing a baseline of grafting parameters to use with the monomer. B2MP was irradiated to 20 and 30 kGy using Co-60 irradiation and 30, 50, 60, and 70 kGy using electron beam. When B2MP monomer by itself was used with no solvent, the monomer completely solidified at all doses. When solvated in aqueous solution to 1 wt. %, the B2MP achieved DoGs of about 10%. Finally when solutions of 100 mg B2MP mixed with 0.1 mg TWEEN20 surfactant in 10 mL of water was irradiated, DoGs of between 8 and 28 % were obtained. Both the aqueous and surfactant based solutions showed promise in terms of obtaining higher DoGs that would be more suitable for uranium extraction.

Further experimentation with B2MP in surfactant solution revealed that heat treatments for direct grafting at least post-irradiation hold promise for increasing the DoGs of the fabrics. Grafting with surfactant on the alternate polymer substrate, winged polypropylene, did not achieve the same DoGs seen by winged nylon 6. The much lower dose rates used for the surfactant experiments as compared to previous electron beam experiments may

have also contributed to the lower DoGs as was proven in later experiments when much higher dose rates were used to obtain DoGs orders of magnitude higher.

The kinetics of the radiation-induced polymerization reactions of B2MP in aqueous solutions were measured using a pulse radiolysis setup with an FTIR detection system at the BNL 2 MeV electron Van de Graaff.

Radiolysis of D_2O yields a mixture of oxidizing, reducing, and neutral species with the following radiation- chemical yields in μmole per joule[27]:

$$G(^{\bullet}OD) = 0.294$$

$$G(e_{aq}^{-}) = 0.307$$

$$G(D^{\bullet}) = 0.045$$

$$G(D_2) = 0.037$$

$$G(D_2O_2) = 0.068$$

D_2O solutions of 5 mM to 25 mM of B2MP were saturated with N_2O to convert the e_{aq}^{-} to $^{\bullet}OD$ as follows, eq. 4.1:

$$N_2O + e_{aq}^{-} + D_2O \rightarrow {}^{\bullet}OD + N_2 + OD^{-} \qquad (4.1)$$

Hence, the total G ($^{\bullet}OD$) is 0.603 μmole per joule. The solubility of N_2O in aqueous solutions is about 25 mM.

The polymerization reaction would be initiated by the addition of $^{\bullet}OD$ onto the carbon-carbon double of B2MP, giving rise to the formation of the OD-B2MP$^{\bullet}$ adducts, shown in equation 4.2:

$$^{\bullet}OD + B2MP \rightarrow OD\text{-}B2MP^{\bullet} \qquad (4.2)$$

The reaction rate constant of the addition of $^{\bullet}OD$ to the double bond of the B2MP is expected to be in the order of 1-5 x 10^8 $M^{-1}s^{-1}$. Taking into account that the [B2MP]

concentration is, for example, 20 mM, and a reaction rate constant of ~ 1 x 10^8 $M^{-1}s^{-1}$, one would expect the half-life of this reaction to be about 0.3 x 10^{-6} s. Therefore, this reaction cannot be detected when electron pulses of 4 μs pulse width are used.

It should also be mentioned that the D-atoms with G (D) = 0.045 add to the double bonds or abstract H atoms from the B2MP producing DB2MP$^{\bullet}$, and B2MP$^{\bullet}$(-H), respectively, equations 4.3 and 4.4:

$$D^{\bullet} + B2MP \rightarrow DB2MP^{\bullet} \quad (4.3)$$

$$D^{\bullet} + B2MP \rightarrow B2MP^{\bullet}(-H) + HD \quad (4.4)$$

The initiating C-centered free radicals, OD-B2MP$^{\bullet}$, DB2MP$^{\bullet}$ and B2MP$^{\bullet}$(-H), react relatively fast with the monomer, B2MP, via an addition reaction, triggering the propagation reaction.

As an example of the FTIR data, Figure 4.6 shows a series of FTIR difference spectra, recorded relative to the initial spectrum of 20 mM B2MP in N_2O-saturated D_2O, during and following irradiation of the solution with 4 ms electron pulses. Twelve consecutive pulses were used, separated by approx. 10-20 s, with each pulse depositing about 130 Gy/pulse for a total of 1.56 kGy. An FTIR spectrum was recorded immediately after each pulse, and then spectra were recorded at intervals as the polymerization reaction propagated. As shown in Figure 4.6, there is a decrease of the 1697 cm^{-1} n(C=O) and 1635 cm^{-1} n(C=C) absorption bands as a function of time. This is a strong indication that through the propagation reaction, the double bonds in the B2MP have reacted via the addition reactions of OD-B2MP$^{\bullet}$, DB2MP$^{\bullet}$ and B2MP$^{\bullet}$(-H) radicals, leading to the formation of more C-centered radicals. Figure 4.6 also shows the gradual increase of the peak at 1728

cm^{-1} as a function of time. This gradual increase may be related to the formation of the methyl 2-hydroxypropanoate structure within the dimerization of the B2MP radicals.

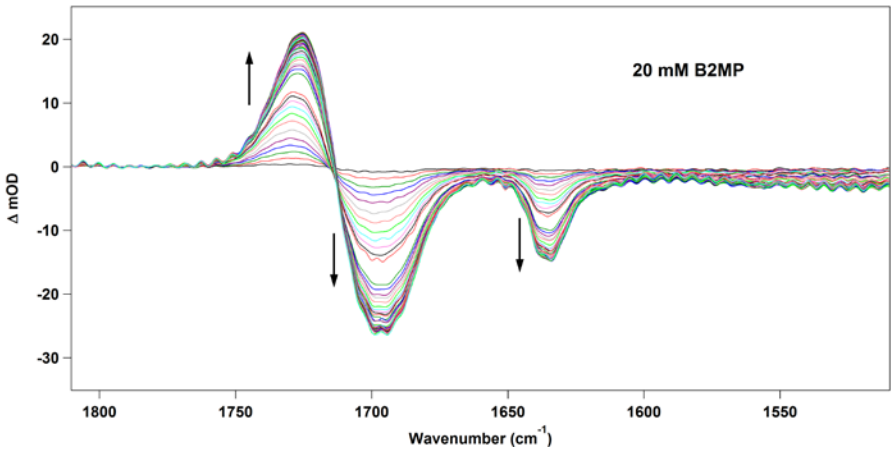

Figure 4.6 – The change in optical density of the 20 mM B2MP solution over the course of about seven hours. The new peak grew at 1728 cm^{-1} while the peaks at 1697 and 1635 cm^{-1} decayed following the irradiation.

Figure 4.7 illustrates some of the most significant radiation grafting reaction pathways that can occur during the radiation grafting of B2MP to nylon 6. Out of the five reactions illustrated, only one reaction is truly desirable: the grafting of monomer on the surface of the nylon 6 through the nylon 6 radical species. All the remaining reactions are undesired as they quench radicals produced by radiation without producing grafted material. There are tiers to desirability however. Monomer-substrate radical termination does produce a grafted material, however it does no produce high DoGs. Monomer dimerization and homopolymerization do produce polymers of the monomer that could still attach to the substrate if a substrate radical reacts with a carbon-carbon double bond in the homopolymer or dimer. Finally, substrate crosslinking is completely undesired as this

leads not only to the loss of radicals available for grafting, but it can also detrimentally alter the material properties of the substrate.

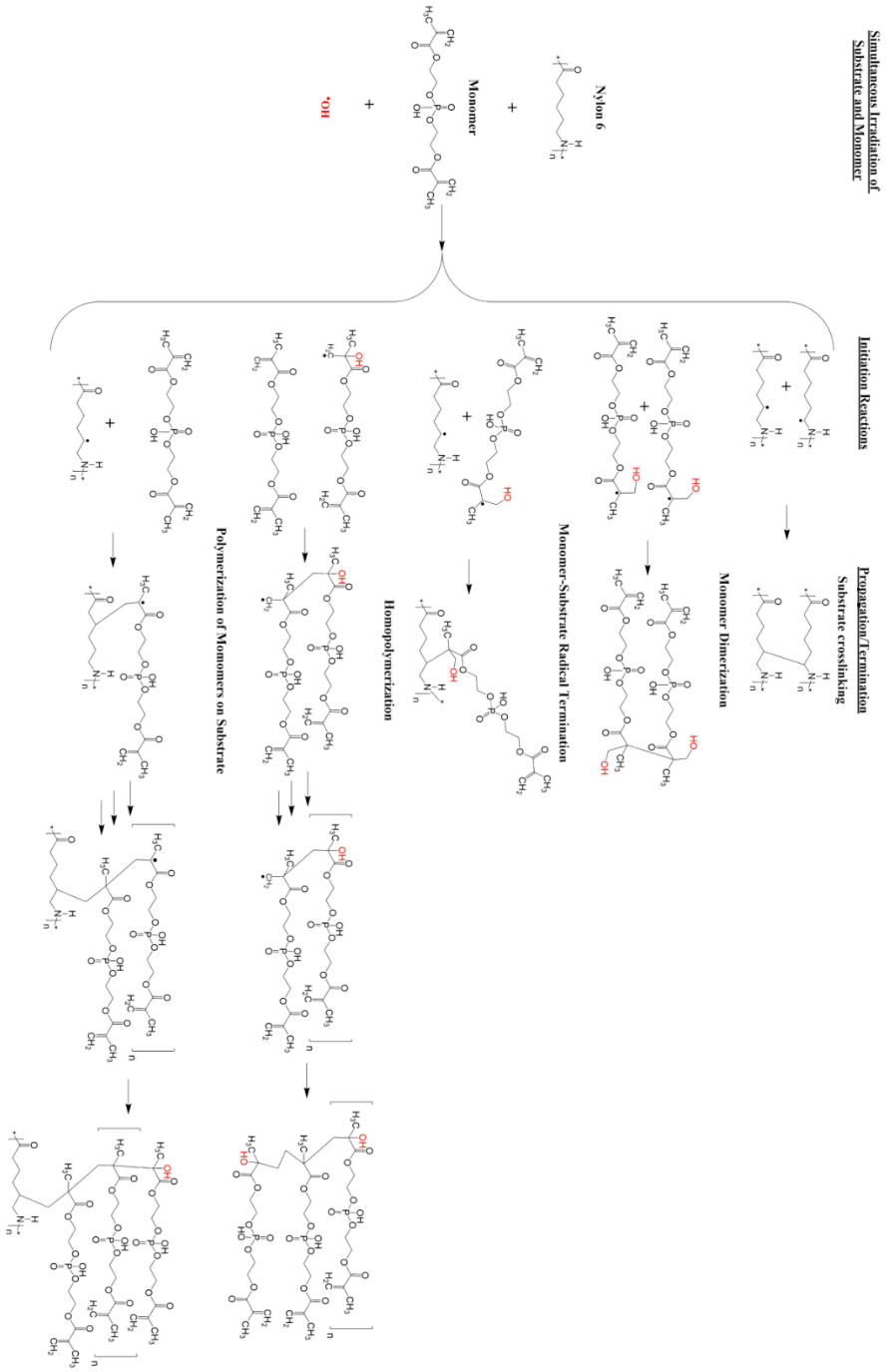

Figure 4.7 – The different radical reactions that would occur during the irradiation of nylon 6 fabric exposed to a solution of B2MP.

The propagation reaction kinetics were monitored by integrating the areas of the 1635, 1697, and 1728 cm^{-1} bands, and plotting them as a function of time. Figure 4.8 shows typical kinetic traces obtained from this procedure, following the pulsing of a N_2O-saturated [20 mM] B2MP D_2O solution. The very sharp-fast decrease/increase in absorption within the first ~120 s (indicated by the red dash-lined box in Figure 4.8) is caused by the 12 successive electron pulses during the irradiation period.

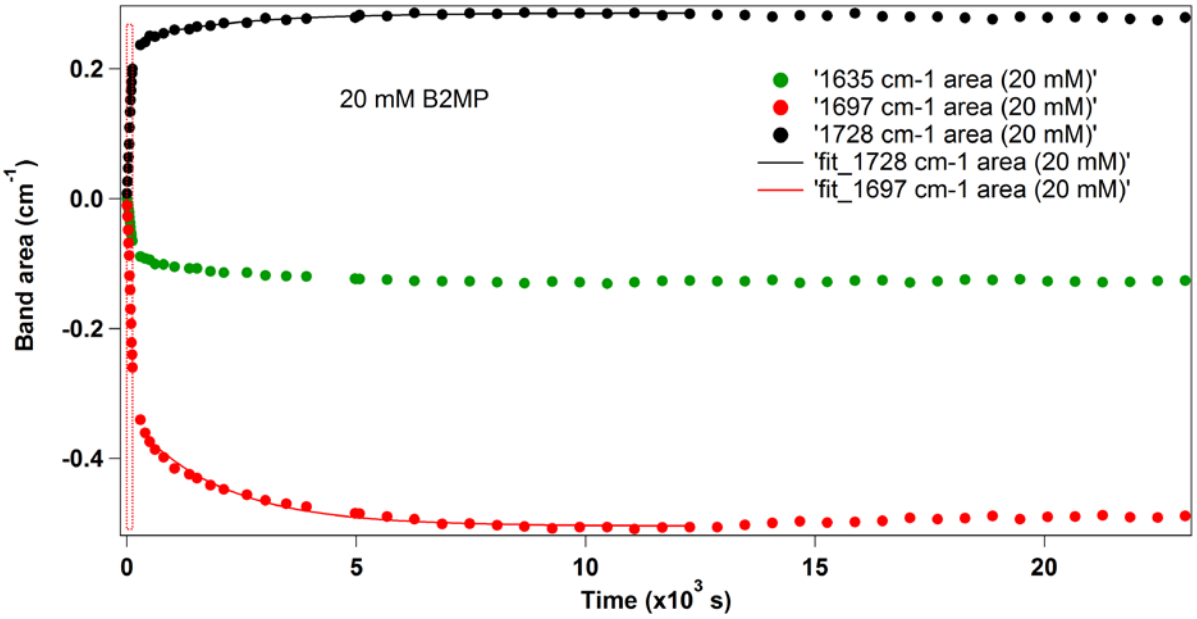

Figure 4.8 – The growth and decay of the 1635, 1697, and 1728 cm^{-1} peaks in the FTIR spectra of a 20 mM B2MP solution in D_2O.

The reaction rate constant of the decay at 1697 cm^{-1} was measured as a function of [B2MP] concentration. Since the data did not fit well to a single exponential function at the higher concentrations of B2MP, double exponential fitting of the kinetic traces was performed, always starting from the first time point immediately after the last electron

pulse. Of the two rate constants obtained from the double exponential fits, only the higher rate constant showed a significant dependence on [B2MP]. Therefore, a pseudo-first-order plot of these rate constants as a function of [B2MP] was prepared (Figure 4.9). These results represent the kinetics of the propagation reactions, where the propagating C-centered radicals add to the double bonds of the B2MP, equations 4.5-4.7:

$$\text{OD-B2MP}^{\bullet} + \text{B2MP} \rightarrow \text{OD-B2MP-B2MP}^{\bullet} \quad (4.5)$$

$$\text{DB2MP}^{\bullet} + \text{B2MP} \rightarrow \text{DB2MP-B2MP}^{\bullet} \quad (4.6)$$

$$\text{B2MP}^{\bullet}(\text{-H}) + \text{B2MP} \rightarrow \text{B2MP-B2MP}^{\bullet}(\text{-H}) \quad (4.7)$$

The second-order reaction rate constant of the propagation reaction is the slope in Fig. 4.9, which was found to be $0.2 \pm 0.04\ M^{-1}s^{-1}$.

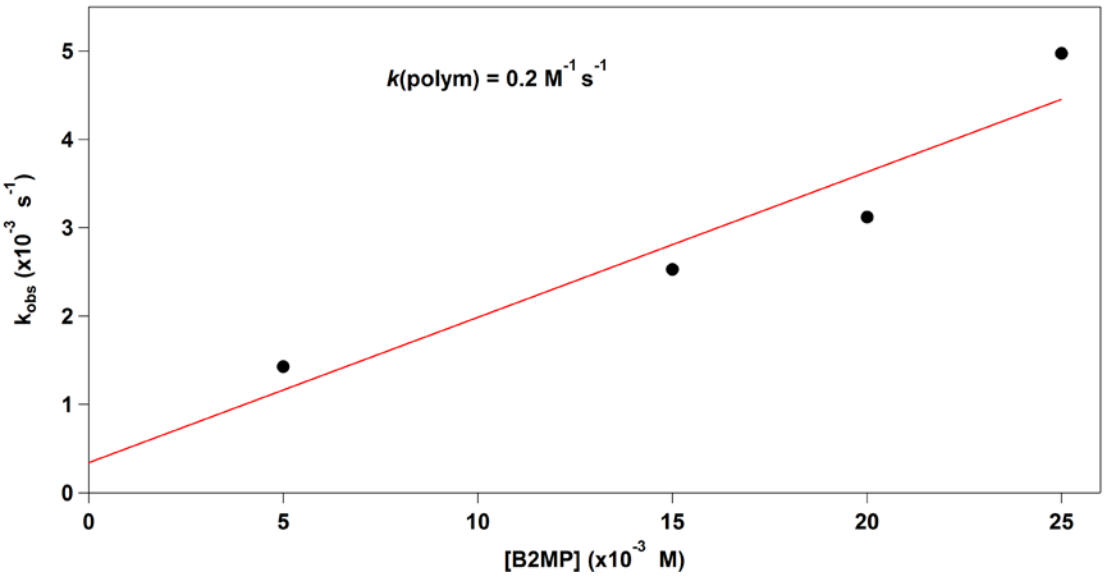

Figure 4.9 – The linear regression of the trend in rate constant versus the concentration of B2MP in solution to obtain the actual second order rate constant of this propagation reaction.

As for the second-order buildup of the 1728 cm^{-1} absorption band, this can be explained by the fact that under these pulse radiolysis conditions, where the dose per pulse is relatively high, one expects that the second-order dimerization reaction of the B2MP radicals competes with the propagation reaction. Figure 4.10 shows the buildup of the 1728 cm^{-1} absorption band at various [B2MP] concentrations.

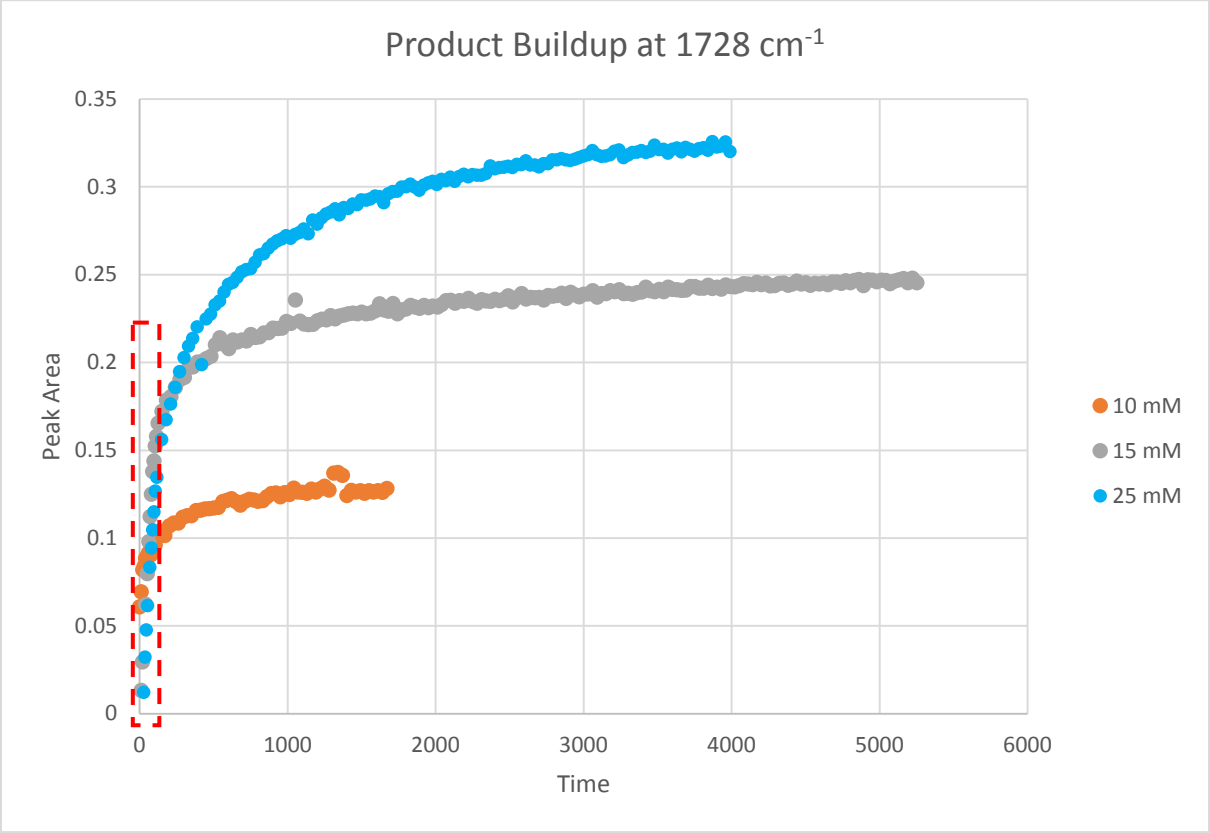

Figure 4.10 – The buildup of the product shown by the increase in absorbance of the B2MP solutions at 1728 cm^{-1}. The red box surrounds data points taken during the irradiation of the solution, which are ignore in the kinetics calculations.

The following kinetics equation, eq. 4.8, as derived in section 3.6.4, can be used to determine the reaction constant, k, from the results shown in Fig. 4.10,

$$\frac{\mathbf{1}}{\boldsymbol{D_\infty - D_t}} = \frac{\mathbf{4kt}}{\boldsymbol{\varepsilon_{1728\ cm^{-1}}\, l}} + \frac{\mathbf{1}}{\boldsymbol{D_\infty}} \tag{4.8}$$

where D_t is the optical absorbance at time, t, D_∞ is the final absorbance, k is the second-order rate constant of dimerization, ε is the molar extinction coefficient of the absorbing chemical (in this case the B2MP dimer), and l is the optical path length of the IR cell.

Figure 4.11 depicts the plot of $\frac{1}{D_\infty - D_t}$ vs. t. Hence the second-order rate constant, k, is calculated via the following equations, equations 4.9 and 4.10:

$$Slope = \frac{4k}{\varepsilon_{1728\ cm^{-1}}\, l} \tag{4.9}$$

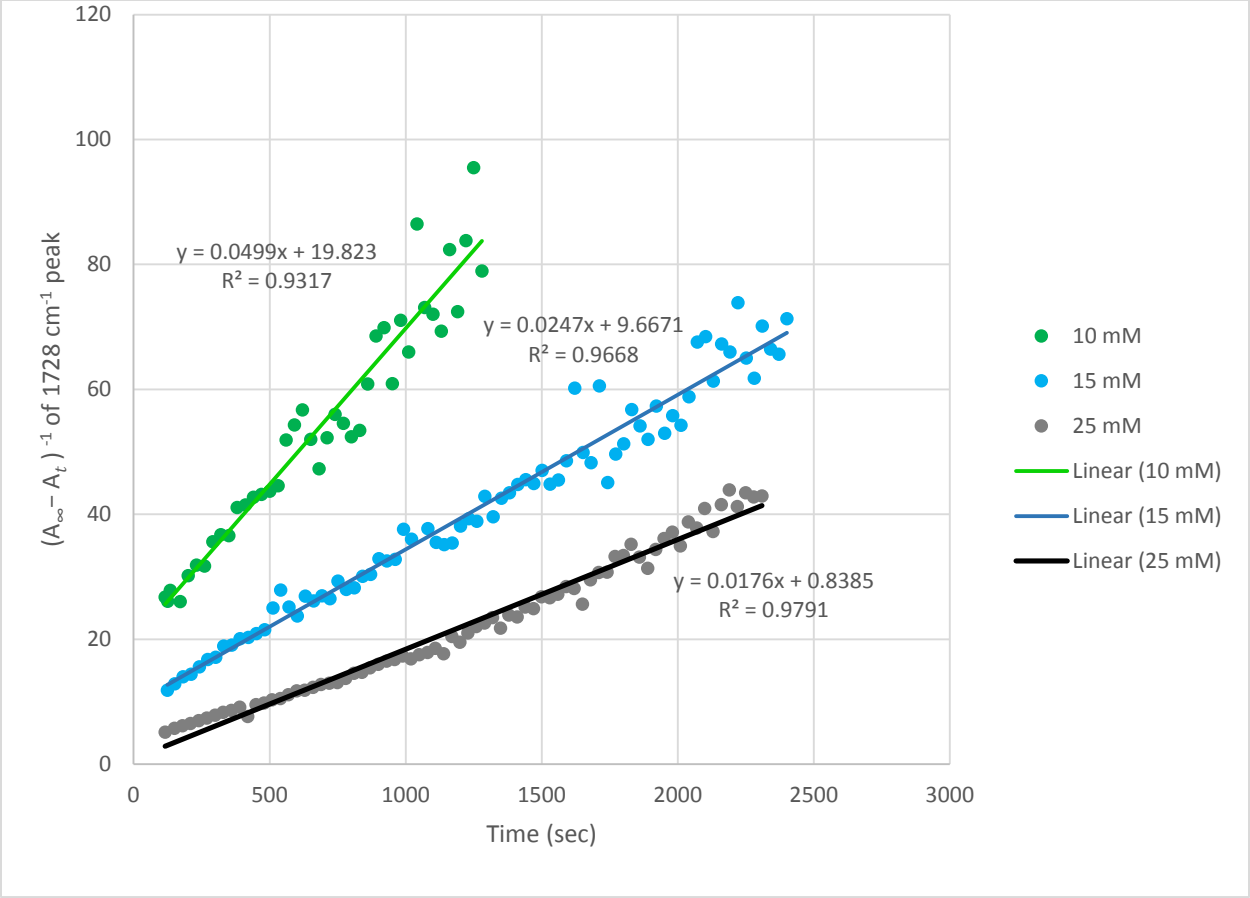

Figure 4.11 –The various fits of the increase in absorbance at 1728 cm^{-1} for different concentration of B2MP in solution.

$$k\ (M^{-1}s^{-1}) = \varepsilon^{1728}\ (M^{-1}cm^{-1}) \bullet \text{slope}\ (s^{-1}) \bullet \ell\ (cm)\ /\ 4 \qquad (4.10)$$

Since we do not know the value of ε_{1728}, it is not possible to determine the actual second-order rate constant, *k*, for the dimerization reaction. However, the slopes in Figure 4.11 are proportional to *k*. As in the case of any free radial polymerization reaction, the free radical dimerization reactions are independent of the initial monomer concentration, [B2MP]. They are only dependent on the dose per pulse and pulse repetition. However, as

shown in Figure 4.12, which plots the slopes of the Figure 4.11 graphs versus [B2MP], the dimerization (termination) reaction rate constant of the B2MP$^{\bullet}$ radical decreases as the initial [B2MP] concentration increases. This decease may be related to the increase in the viscosity of the B2MP polymer chain in solution. As the initial [B2MP] concentration increases, the chain polymerization reaction enhances, which leads to an increase in the viscosity.

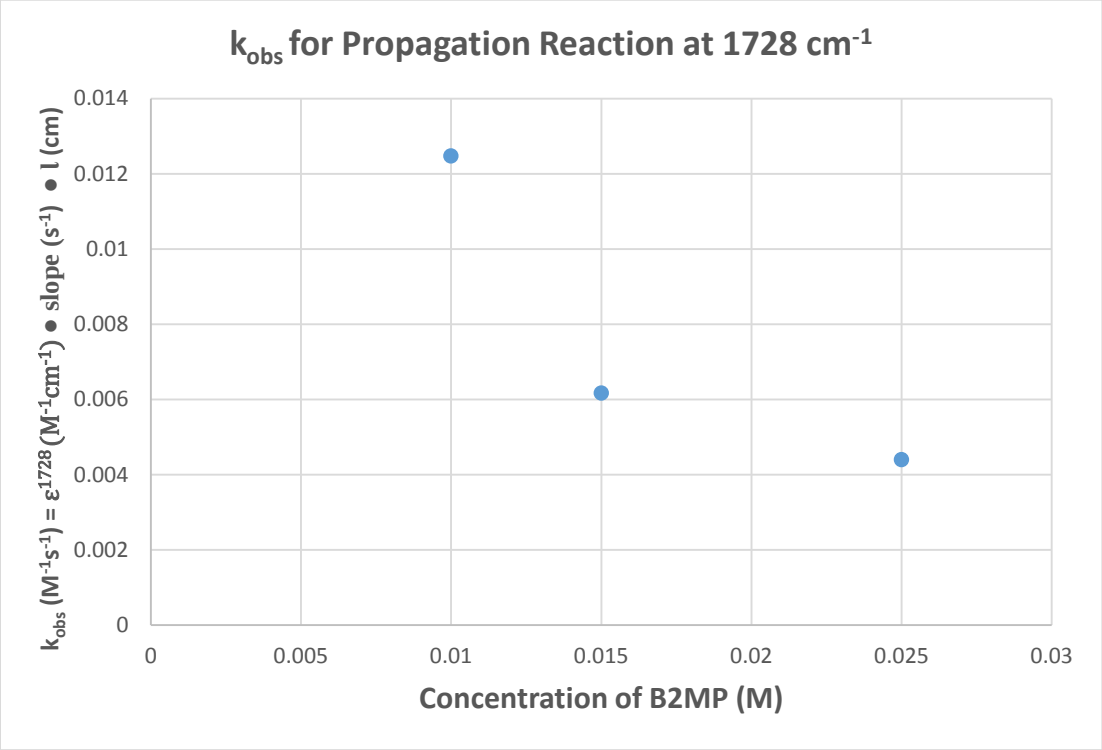

Figure 4.12 – The trend in rate constants of the propagation reaction occurring at 1728 cm^{-1} with concentration of B2MP.

4.2.3 Characterization

The attachment of B2MP to the surface of the winged nylon 6 fabric was evaluated through the use of FTIR-ATR. Fig. 4.13 illustrates a comparison between the clean winged nylon 6 and a B2MP-grafted winged nylon 6 sample. Of particular importance are the strong peaks emergent in the B2MP spectrum associated with the attachment of the phosphate group. The peak at ~979 cm^{-1} is most likely the P-O-C stretching vibration while the peak at ~1030 cm^{-1} is most likely the P=O stretching vibration[143,144].

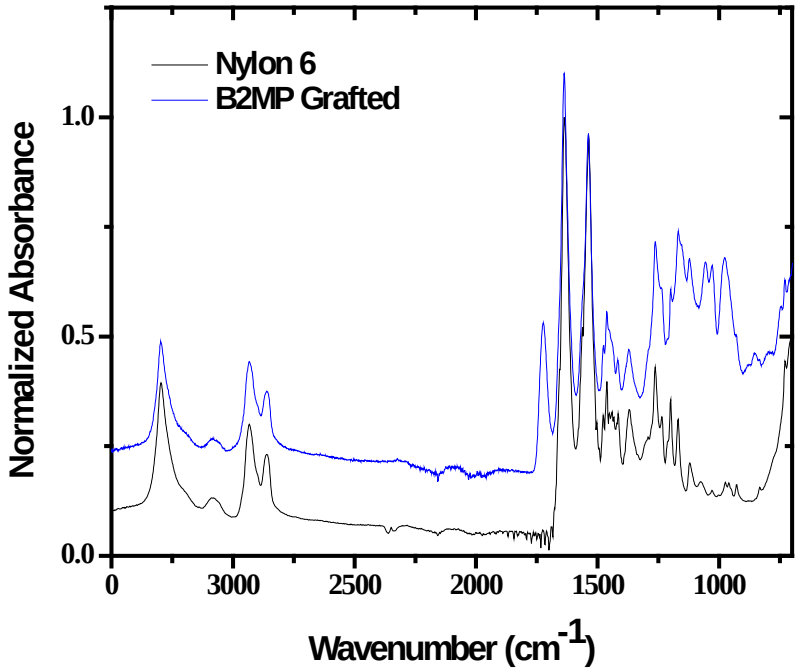

Figure 4.13 – The FTIR spectra of both a clean, ungrafted winged nylon 6 sample and a B2MP-grafted winged nylon 6 sample.

4.2.4 Extraction Testing

In order to fabricate the grafted samples, squares of winged nylon-6 fabric weighing about 30-40 mg were placed inside septum-capped vials with concentrations of B2MP of about 60 mg/L in water. The vial was then purged with nitrogen to limit the amount of dissolved oxygen in the system and sealed with paraffin film.

Using 40 kGy of Co-60 irradiation (with an activity of $1.78 * 10^{15}$ Bq) at a 10 kGy/hr dose rate, the B2MP monomer was grafted to the surface of fabric. After irradiation, the fabric and solution contained homopolymer which could detract from the ability of the fabric to adsorb uranium and could introduce error into the mass values for the fabric. To remove the homopolymer, the fabric was washed and sonicated in deionized water twice. Finally, the fabric was dried to a constant weight using an oven. The total grafting density of the fabric sample varied from about 80-140%, but grafting densities on the order of 120% were found to have the greatest extraction capability.

The grafted fabric was subsequently cut into smaller sections and each section was exposed to a different volume of 20 ± 1 mg/L U in seawater for 24 hours in an EPA approved rotator operating at 30 revolutions per minute. The rotator was designed to constantly agitate the sample to ensure movement of the water and more accurately simulate the dynamic conditions of seawater. After a seawater exposure of 24 hours, the uranium loading capacity of each sample was determined by measuring the remaining concentration of uranium in the respective solution through the use of an ICP-AES, and comparing it to the initial 20 mg/L solution. The final capacity was shown to be above 20 mg U/g adsorbent for the majority of samples where the initial volume of 20 mg/L U in

seawater exceeded 50 mL. Table 4.2 and Fig. 4.14 exhibit the specific data associated with this result.

Table 4.2 - Uranium Loading Capacity raw data

Sample Name	U conc. Before extraction, mg/L	U conc. after extraction, mg/L	Volume of Seawater, mL	U (sorbed), mg/g
B2MPct 224#1	19.05	5.917	10	9.586
B2MPct225#1	19.255	6.264	10	8.778
B2MPct224#2	20.617	10.253	20	15.585
B2MPct225#2	20.619	11.886	20	13.646
B2MPct224#3	20.613	13.202	50	24.704
B2MPct225#3	20.51	12.942	50	23.949
B2MPct224#4	19.944	13.3	100	44.293

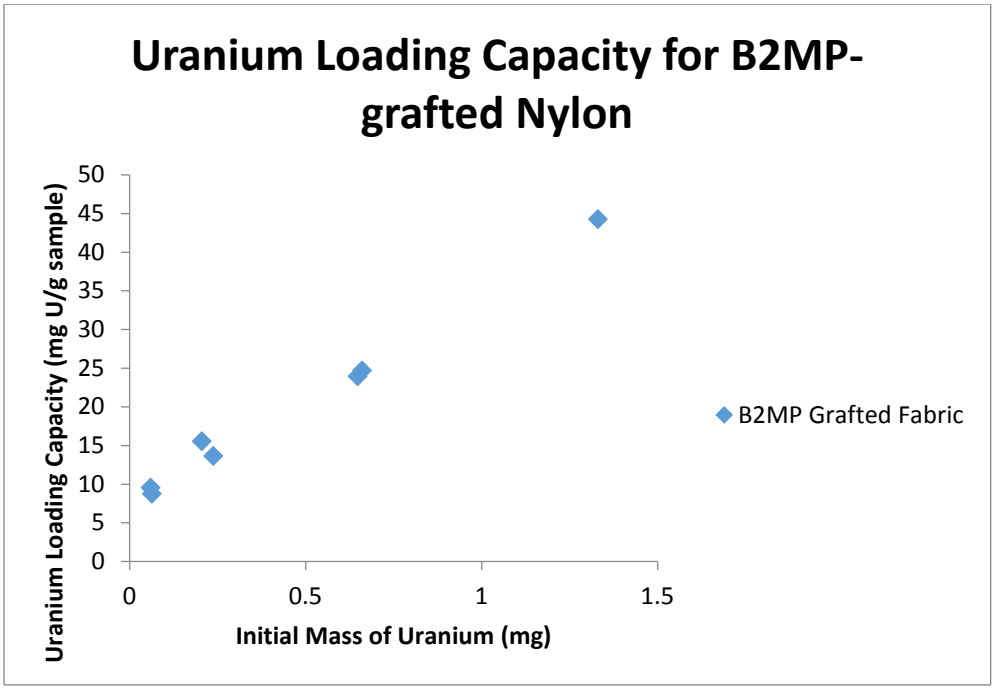

Figure 4.14 – Loading of uranium on adsorbent with increasing mass of uranium in solution for B2MP grafted onto winged nylon-6 using Co-60 irradiation up to 40 kGy total dose at 10 kGy/hr after 24 hour exposure to solutions of 20 mg/L U in seawater.

In order to fabricate the grafted samples, squares of winged nylon 6 fabric weighing about 30-40 mg were placed inside septum-capped vials with 0.093 M concentrations of B2MP. The vial was then purged with nitrogen to limit the amount of dissolved oxygen in the system and sealed with paraffin film.

Using 60 kGy of Co-60 irradiation (with an activity of $1.78 * 10^{15}$ Bq) at a 5 kGy/hr dose rate, the B2MP monomer was grafted to the surface of fabric. After irradiation, the fabric and solution contained homopolymer which could detract from the ability of the fabric to adsorb uranium and could introduce error into the mass values for the fabric. To remove the homopolymer, the fabric was washed and sonicated in deionized water twice. Finally, the fabric was dried to a constant weight using an oven.

The grafted fabric was subsequently exposed to a volume of 10 ± 1 mg/L U in seawater for 50 hours in the EPA approved rotator. Subsequently, the uranium loading capacity of each sample was determined by measuring the remaining concentration of uranium in the respective solution through the use of an ICP-AES, and comparing it to the initial 10 mg/L solution. Subsequently, any remaining uranyl ions or other ions remaining on the fabric were eluted by washing the fabric with ammonium oxalate. This exposure of the fabric to the solution of 10 mg/L uranium in seawater for 50 hours was then repeated 20 times. Figure 4.15 exhibits the specific data associated with achieving this result.

The extraction capacity of the fabric is thus shown to maintain its stability up through 20 regeneration cycles to within 20% of the initial value when ammonium oxalate was used as the eluent for uranium from the surface of the B2MP-grafted fabric.

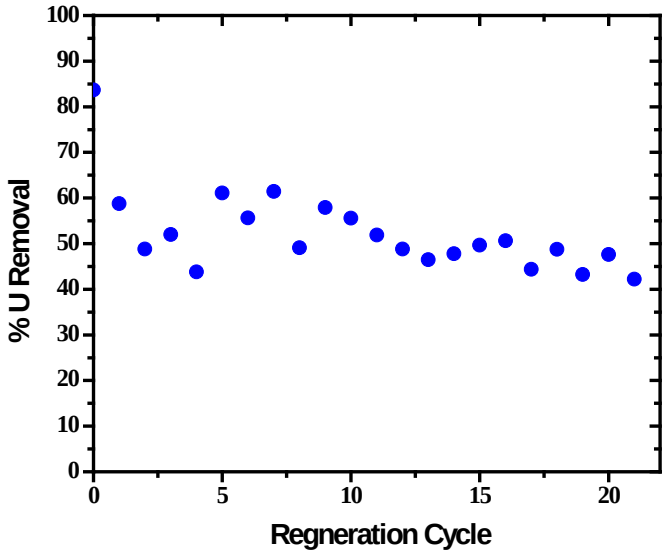

Figure 4.15 – Uranium removal % of B2MP-grafted Nylon-6 fabric after each regeneration.

The loss in loading capacity of this fabric over the course of many regeneration cycles could have a number of possible causes. The initial significant drop in % uranium removal could be due to an initial conformational change in the grafted co-polymer that limits the ability to extract as much uranium as the virgin fabric even after the elution of the uranium. The slow loss of uranium capacity over the subsequent cycles could be due to the loss of phosphate groups or fabric mass due to physical and chemical processing of the fabric with each regeneration cycle, i.e. the rotation of the fabric in a bottle or the use of ammonium oxalate to strip the fabric of uranium.

4.3 Oxalate Compound

4.3.1 Grafting

Initial DAOx grafting experiments were performed with aqueous solutions. DAOx was initially attempted to be dissolved in water through 30 minutes of sonication, however this did not allow for sufficient time for the DAOx to be completely dissolved. Irradiations proceeded using 5.54 kGy/hr Co-60 irradiations to 10, 20, 30, and 40 kGy. These samples only achieved a maximum of 8% DoG. Due to the fact that the DAOx samples were sonicated for only about an hour, it was assumed that the DAOx was not completely dissolved in solution upon irradiation. After irradiation, the water in the DAOx was cloudy most likely indicating homopolymerization. On the samples that had been exposed to higher doses, there were small hair-like extensions coming off the surface of the fibers. While these hair-like structures could not be verified as oligomers of DAOx, it was proposed that decreasing the monomer concentration and increasing the dose rate through the use of electron beam irradiation would increase the DoG of the fabric.

Initial experiments with the electron beam used the same 56 mM concentration of DAOx as in the prior Co-60 experiment, but used doses from 60-120 kGy and a dose rate of roughly 160 kGy/hr. This irradiation resulted in negligible degrees of grafting, however this is most likely due to the lack of proper dissolution of the monomer in solution along with a lack of the use of purging to make the atmosphere in the sample vials inert.

Following these experiments, sonication was limited in its use towards dissolving the monomer in solution due to its ability to degrade the polymer substrate[145].

In order to improve DAOx dissolution in the monomer solution, a co-solvent of methanol was used. These samples were irradiated using Co-60 with a dose rate of 1.1 kGy/hr. While this co-solvent did improve the ability of the monomer to dissolve in solution, it resulted in even lower degrees of grafting. The initial presumption was that the lower doses of this experiment resulted in the lower DoGs.

The following experiment once again used methanol as a co-solvent for the DAOx monomer, but it used a N_2O atmosphere in the vials and used higher dose rates. For these DAOx samples, the same dose of 30 kGy was achieved, but 1.04 kGy/hr and 5.3 kGy/hr dose rates were used. There was very little difference between the DoGs of these two dose rates. It was following this experiment that it was suggested to try using as high concentrations as possible using a co-monomer or surfactant in order to obtain a high enough DoG to begin to optimize experimental parameters.

It was believed that homopolymerization was having a significant effect on the total DoG exhibited by the fabrics and as such an alternate method to irradiation condition control was attempted to reduce it. Mohr's Salt, ammonium iron (II) sulfate, had been shown previously to limit homopolymerization. Ethanol was used in this case as well as a co-solvent in place of methanol to see if it allowed for higher DoGs. Significant DoGs were believed to have been generated through the use of Mohr's salt, but this was later attributed to the crystallization of the remaining salt on the surface of the fabric. Experiments with DAOx in pure ethanol generated DoGs of about 10%, not significantly higher than the DoGs obtained in previous experiments. Direct radiation grafting of DAOx onto nylon 6 was performed in the absence of oxygen in neat (where neat refers to a system that contains no solvent) liquid DAOx and also in aqueous solutions in the presence of a surfactant.

The following experiments were able to use pure aqueous solutions of DAOx at 56 mM without a co-solvent as long as the solution was stirred overnight. This led to the complete dissolution of the monomer. Solutions were examined and no visible agglomeration of DAOx was seen following the stopping of mixing. Complete dissolution was further promoted with heating of the monomer solution to 65°C. Mohr's salt was continued in its use, however multiple cleaning regimens were tested in an attempt to remove any excess material that was not grafted to the surface of the fabric. These washing steps, including sonication in water (to remove excess salts) and in methanol or ethanol, still resulted in fabrics that had DoGs of over 100%. This was further shown when experiments were performed with increasing quantities of Mohr's salt. The DoG of fabric samples grafted with the help of Mohr's salt reached a maximum at about 2%. If the Mohr's salt was mainly resulting in an increase of final fabric mass due to a mechanism by which it was precipitating on the surface of the fibers then the average DoG of the fabrics should reach a plateau or continue to increase after a certain increase in the Mohr's salt concentration. To the contrary, the DoG of the fabrics began to decrease again after roughly 2 wt. % Mohr's salt. Based on published mechanisms of how Mohr's salt is supposed to inhibit homopolymerization, this can be attributed to the Mohr's salt beginning to inhibit not only the homopolymerization reaction, but also the grafting reaction as well[142].

Further investigation was carried out to examine the mechanism of Mohr's salt in affecting the DoG of the fabric following DAOx grafting. Two different iron salts separate from Mohr's salt were used in an attempt to elucidate one component of the mechanism of the Mohr's salt during the grafting steps. Ferric chloride and ferrous sulfate were used along with control solutions with no iron salt or Mohr's salt. The ferric and no iron salt

solutions expressed little to no grafting, whereas the ferrous salts showed degrees of grafting on roughly the same order of magnitude with Mohr's salt still generating the highest DoGs.

Winged nylon 6 fabric was also grafted using pure monomer solution. Compared to the B2MP solutions, which saw complete solidification of the monomer in a polymer matrix within 20 kGy, the DAOx did not experience any amount of solidification and merely increased in apparent viscosity. However, this was coupled with DoGs between 3 and 22%, indicating that grafting with pure monomer would be a possible pathway towards higher DoGs with the optimization of the grafting process.

In response to the lower DoGs seen with alternate monomer-solvent systems of B2MP, methanol was used as a partial solvent. Different amounts of methanol were added to 1 mL of B2MP in contact with fabric in order to slow down the process of homopolymerization that led to the solidification of the monomer by itself during irradiation. These samples also completely solidified upon irradiation even at doses as low as 10 kGy.

Pure DAOx and a solution of DAOx and Mohr's salt in aqueous solution were used to graft the monomer to the surface of winged nylon 6 fabric. The monomer only samples achieved grafting densities as high as 19.6% whereas the fabrics grafted with Mohr's salt and DAOx solution achieved DoGs of over 100% in some cases. These experiments were repeats of previous experimental parameters and yielded similar results indicating consistency with the experimental procedure. An attempt was made to perform indirect grafting using the same solutions, however both of these solutions only yielded DoGs less than 10%. It was believed that the method for indirect grafting had to be improved as the monomer solution injections were carried out in air and the fabrics were irradiated at room

temperature. This most likely led to an introduction of oxygen to the sensitive radical system and a rapid decrease in radical concentration in the fabric following the irradiation, respectively.

Higher doses at high dose rates similar to those of previous experiments led to higher DoGs. The observation that neat DAOx liquid formed a white precipitate upon addition of ethanol could suggest that the viscosity of the DAOx monomer traps radicals and the longer irradiations give more time for these radicals to diffuse through the monomer all the while the radical concentration in the neat monomer has either plateaued or increases continuously throughout the irradiation. This theory would have to be tested as the addition of ethanol could merely be causing already present DAOx polymer chains to swell, although this could be readily tested through the use of EPR to measure the radical signal in the solution. Also, as expected, the use of surfactant concentration that led to a more stable solution resulted in higher degrees of grafting, though not by a significant amount. The large amount of homopolymerization present in these solutions after irradiation suggests that by altering the dose rate, temperature, and other factors of the irradiation conditions this homopolymerization can be reduced and higher degrees of grafting can be obtained. The size of the homopolymerization might also lend itself to adjusting the surfactant concentration even further to obtain micelles of sizes that promote higher DoGs. Based on experiments with neat DAOx as the monomer solution during irradiation, DAOx grafted samples with high DoGs can be consistently obtained through the use of neat monomer grafting. Use of the TWEEN-20 surfactant can now be used as a viable grafting method if a stable monomer-surfactant solution can be obtained. Heat treating grafted samples also had a noticeable beneficial effect on the final DoGs. This is slightly surprising

since the grafting reaction is an exothermic process so any additional heat energy should slow down the grafting reaction. However, it is possible that slowing the grafting reaction down allowed more time for radicals to diffuse into the material to graft.

In order to ensure that the surfactant TWEEN-20 was not being grafted to the surface of the winged nylon 6, grafting experiments were performed consisting solely of solutions containing TWEEN-20 in water. The low DoGs (<5%) obtained by TWEEN-20 support the notion that any amount of TWEEN-20 grafting that may have occurred is statistically insignificant especially in comparison to the grafting accomplished with DAOx-TWEEN-20 mixtures. There was a viable color change with a couple of the fabrics exposed to this compound while under irradiation; the origin of this change is unknown.

The reaction rate constant of the hydrated electron e_{aq}^- with DAOx, under anaerobic conditions, was determined by monitoring the decay of e_{aq}^- as it reacted with DAOx. Under our experimental conditions, radiolysis of water will yield the following oxidizing, reducing, and stable species, with their radiation-chemical yields given in μmole per joule[27]:

$$G(^{\bullet}OH) = 0.29$$

$$G(e_{aq}^-) = 0.29$$

$$G(H) = 0.06$$

$$G(H_2) = 0.\ 04$$

$$G(H_2O_2) = 0.08$$

Prior to the pulse radiolysis experiments, DAOx aqueous solutions were purged with Ar to remove the dissolved oxygen. This is a very important step to prevent the scavenging of e_{aq}^- by oxygen according to the following very fast reaction, eq. 4.11,

$$e_{aq}^- + O_2 \rightarrow O_2^{\bullet -} \qquad (4.11)$$

which has a reaction rate constant of 2×10^{10} $M^{-1}s^{-1}$.

In the radiation chemistry of aqueous solutions, t-butanol can be used routinely to scavenge □OH radicals in order to permit measurement of the reactions of e_{aq}^- with other solutes.

Hence, in all of these experiments, 0.2 M t-butanol was added to the DAOx aqueous solutions in order to scavenge the $^{\bullet}OH$ radicals, eq. 4.12,

$$^{\bullet}OH + (CH_3)_3COH \rightarrow H_2O + {}^{\bullet}CH_2(CH_3)_2OH \qquad (4.12)$$

with a reaction rate constant of 6×10^8 $M^{-1}s^{-1}$. $^{\bullet}CH_2(CH_3)_2OH$ is very unreactive, and does not interfere with the radiation chemistry of the other solutes. Another advantage of $^{\bullet}CH_2(CH_3)_2OH$ is that it does not interfere with the absorption of other species in the pulse radiolysis experiments, since it has a very low molar extinction coefficient in the ultraviolet region.

Figure 4.16 shows the prompt formation of e_{aq}^- following pulse radiolysis and its decay, monitored at a wavelength of 480 nm, in Ar-saturated aqueous solutions of various concentrations of DAOx with 0.2 M t-butanol. While the observed buildup of the e_{aq}^- signal is limited by the response function of the FND-100 silicon photodiode detector, the decay represents the pseudo-first order reaction of e_{aq}^- with DAOx. It should be mentioned that e_{aq}^- signal would be larger if it was monitored at 720 nm, since e_{aq}^- has its maximum

absorption there. However, 480 nm was used in these experiments in an attempt to observe the absorption spectrum of the $(DAOx)^{\bullet-}$ anion, eq. 4.13:

$$e_{aq}^{-} + DAOx \rightarrow (DAOx)^{\bullet-+} \qquad (4.13)$$

It should be noted that Figure 4.16 shows that the decay after the pulses at a monitoring wavelength of 480 nm does not reach a zero value, suggesting that the $(DAOx)^{\bullet-}$ anion has a weak absorption around this wavelength region. More investigation needs to be done on the pulse radiolysis transient spectroscopy of this system.

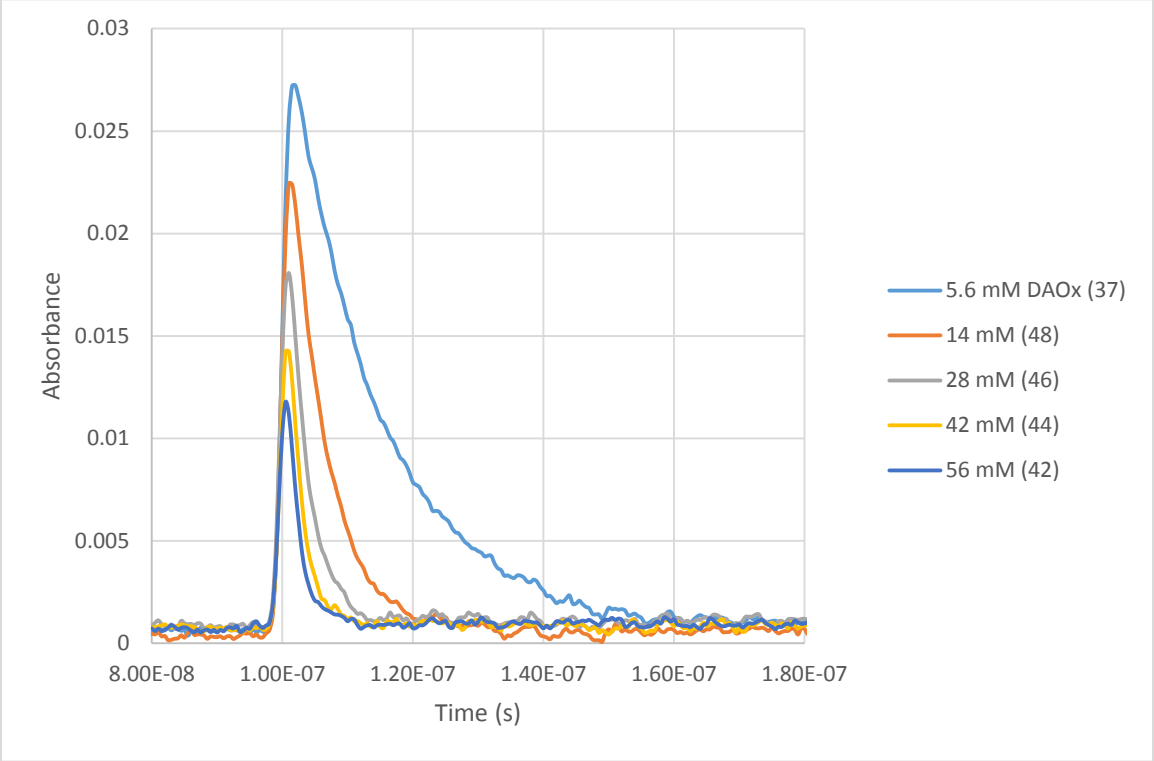

Figure 4.16 – The decay behavior of the absorbance of the aqueous electron at 480 nm with varying concentrations of DAOx.

Figure 4.17 shows the observed pseudo-first-order rate constants for the pseudo-first order reaction of e_{aq}^- with DAOx as a function of DAOx concentration. The slope of the linear fit to the fitted line data represents the second-order rate constant for the reaction of e_{aq}^- with DAOx, with a value of 9 x $10^9 \pm 9 \times 10^8$ $M^{-1}s^{-1}$.

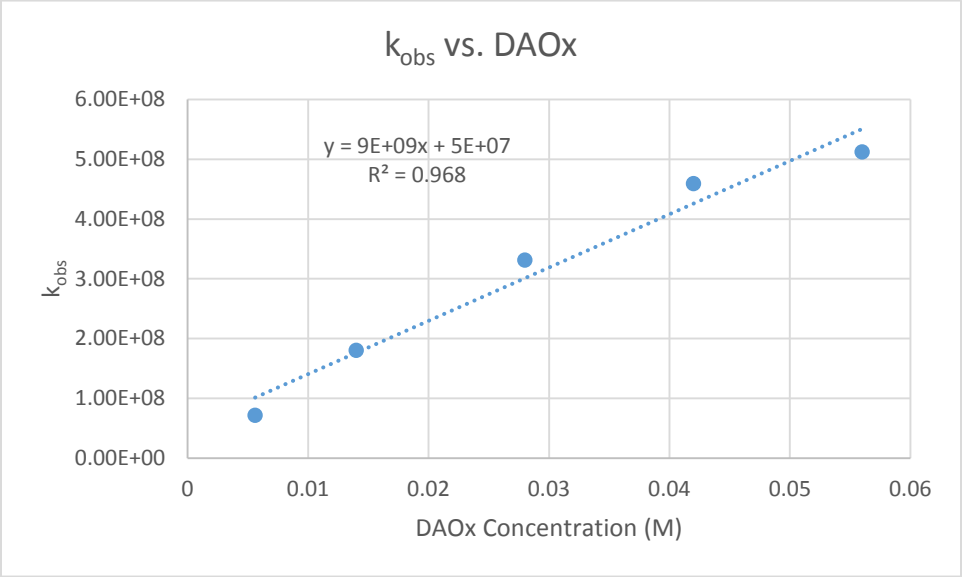

Figure 4.17 – The observed pseudo-first order rate constants for varying concentrations of DAOx. The derived second order rate constant from the linear regression of this graph gives a value of 9 $\times 10^9 \pm 9 \times 10^8$ $M^{-1}s^{-1}$.

As with any anion, the produced $(DAOx)^{\bullet -}$ anion undergoes a very rapid solvolysis reaction producing carbon-centered radicals, eq. 4.14:

$$(DAOx)^{\bullet -} + H_2O \rightarrow (H\text{-}DAOx)^{\bullet} + OH^- \qquad (4.14)$$

The $(H\text{-}DAOx)^{\bullet}$ carbon-centered radical initiates the polymerization reaction of the DAOx.

Lower doses of about 150 kGy were used for subsequent neat DAOx grafting experiments in order to reduce the DoG to about 100%, which is more on the order of the expected best uranium extraction performance. Heating of the DAOx samples during direct grafting resulted in improved DoGs although the extent to which direct heating improved grafting was unexpected. This high DoG could be the result of excess homopolymerization due to the increased diffusion as a result of the higher temperature. Lower temperatures and doses should result in more ideal grafting.

The dissolution of DAOx homopolymer using DCM was important for future cleaning of DAOx and other monomer grafted fabrics. By determining which solvent can effectively dissolve homopolymer, more thorough cleanings can be performed and more accurate measurements of final mass can be made.

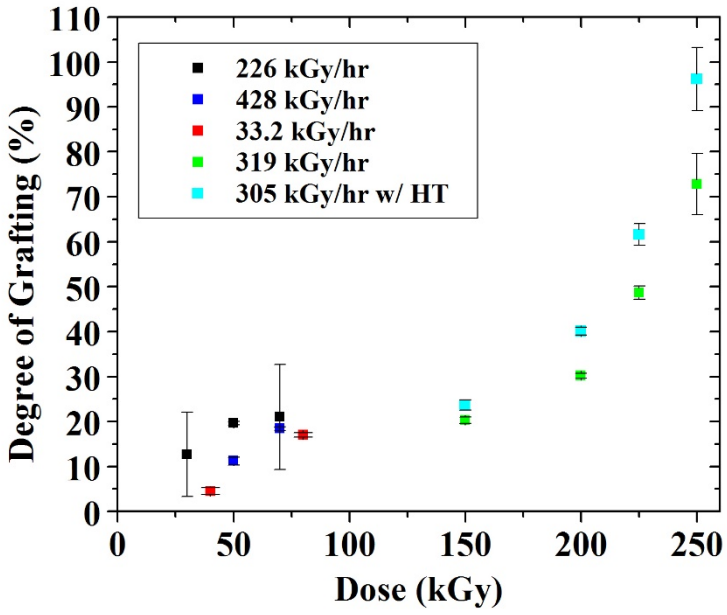

Figure 4.18 - Grafting density of pure DAOx on nylon 6 as a function of dose at various dose rates in the absence of oxygen. HT = heat treatment following irradiation.

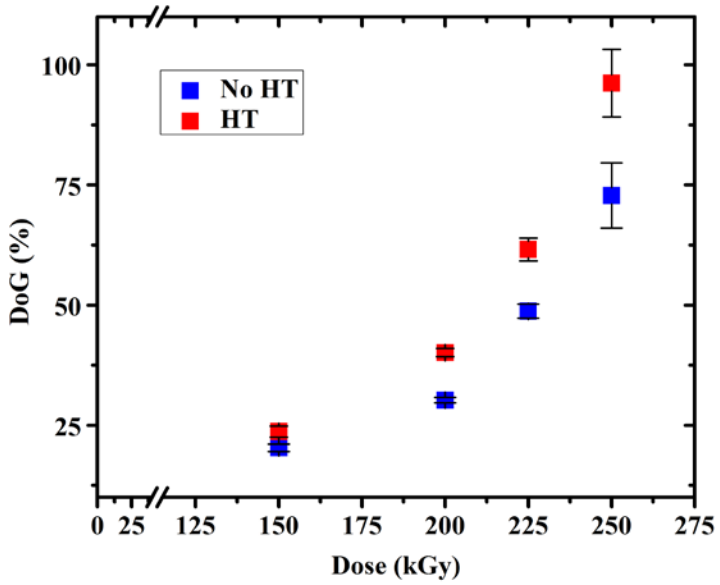

Figure 4.19 – By exposing irradiated sample vials to higher temperatures (60 ºC) after irradiation for at least 12 hours, the final DoG of the sample can be increased.

In these experiments, the oxygen-free mixtures contain only DAOx and nylon 6. Figure 4.18 shows that as the dose increases, the DoG increases. Figure 4.19 illustrates that following an irradiation with a heat treatment involving the exposure of the sample to temperatures of 60°C increases DoG. The irradiation was carried out at room temperature at varying dose rates. As shown in Figure 4.20, radiation induces the formation of the C-centered free radicals of nylon$^{\bullet}$ and DAOx$^{\bullet}$. These free radicals undergo various desired reactions (grafting through the formation of C-C bonds between DAOx and the nylon 6), as well as undesired reactions, consisting of DAOx homopolymerization and the crosslinking reactions of nylon$^{\bullet}$.

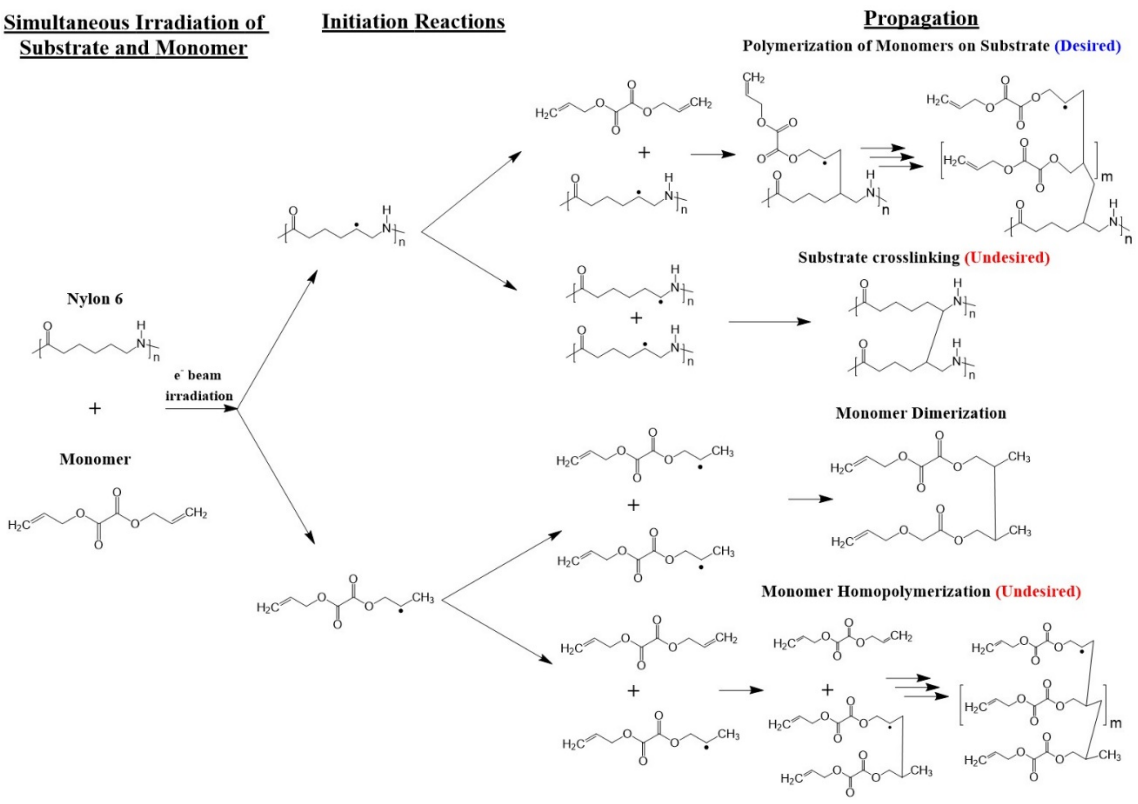

Figure 4.20 - Reaction of the graft polymerization reactions of neat monomer on the nylon 6 fabric in the absence of oxygen and solvent.

Therefore, under our experimental conditions, the decay rates of the DAOx• and nylon• can be expressed as follows, equations 4.15 and 4.16:

$$\frac{-d[DAOx^{\cdot}]}{dt} = k_1[nylon^{\cdot}][DAOx^{\cdot}] + 2k_2[DAOx^{\cdot}]^2 + k_3[DAOx^{\cdot}][DAOx] + k_4[nylon-(DAOx)n-DAOx^{\cdot}][DAOx^{\cdot}] \quad (4.15)$$

$$\frac{-d[nylon^{\cdot}]}{dt} = k_1[nylon^{\cdot}][DAOx^{\cdot}] + k_5[nylon^{\cdot}][DAOx] + 2k_6[nylon^{\cdot}]^2 \quad (4.16)$$

where k_1, k_2, k_3, k_4, k_5, k_6 are the rate constants of the desired grafting reaction, the undesired termination reaction of the DAOx• radicals, the undesired homopolymerization reaction of the DAOx, the termination reaction of the growing grafted DAOx• radicals, the

desired grafting-addition reaction of the DAOx on nylon, and the undesired crosslinking reaction of the nylon, respectively.

Figure 4.18 also shows that after receiving a dose of more than approximately 175 kGy, the grafting density increases much more sharply as a function of dose. This can be explained by the fact that as the viscosity of the medium increases with increasing dose, the diffusion of the DAOx$^{\bullet}$ radicals is slowed down, thus hindering the homopolymerization reactions and enhancing the grafting on the nylon surface.

In conclusion, my results demonstrate that radiation grafting polymerization of DAOx on nylon 6 through a solvent-free, single-step-direct process can be accomplished in the absence of oxygen. The desired reaction between the radiolytically produced nylon$^{\bullet}$ and DAOx$^{\bullet}$ C-centered radicals to form the grafting C-C bonds occurs despite the strong competition from the DAOx homo-polymerization reaction. These results also show that at radiation doses up to around 175 kGy, the undesirable homo-polymerization is the predominant reaction. However, as the viscosity increases due to the homo-polymerization reaction, the diffusion of the DAOx$^{\bullet}$ C-centered radicals is slowed down. This hinders the homo-polymerization reaction and enhances the local grafting reaction, and this allows reaching a grafting density of 140% at a dose level of 250 kGy.

Radiation grafting in aqueous solutions and in the presence of a surfactant:

Degrees of grafting as high as 25 % have been reached in the aqueous, N_2O-saturated mixtures containing 0.11 M DAOx and 4.5 x 10^{-3} M TWEEN 20. Under these experimental conditions, water absorbed most of the electrons from the electron accelerator resulting in

the formation of the following active species with their radiation chemical yields in micromole per joule:

$G(^{\bullet}OH) = G(e_{aq}^{-}) = G(H_3O^{+}) = 0.28$, $G(^{\bullet}H) = 0.062$, $G(H_2) = 0.042$, $G(H_2O_2) = 0.082$

Hydroxyl radicals ($^{\bullet}OH$) constitute a powerful oxidant, and they are highly reactive (through addition, abstraction or electron transfer). The $^{\bullet}OH$ radicals are responsible for initiating the grafting polymerization and other reactions in this system through the production of DAOx$^{\bullet}$ and nylon$^{\bullet}$ radicals upon reacting with nylon and DAOx. On the other hand, hydrated electrons (e_{aq}^{-}) are very strong reducing radicals and can be converted to $^{\bullet}OH$ radicals through the following reactions, eq. 4.17:

$$N_2O + e_{aq}^{-} + H_2O \rightarrow {}^{\bullet}OH + N_2 + OH^{-} \qquad (4.17)$$

The above reaction is very fast, having a reaction rate constant of $k = 8 \times 10^9\ M^{-1}s^{-1}$ [146]. Hence, saturating the system with N_2O prior to irradiation, would double the $^{\bullet}OH$ yield to $G(^{\bullet}OH) = 0.56$ micromole per joules. In addition to $^{\bullet}OH$, H-atoms ($^{\bullet}H$) with $G(^{\bullet}H) = 0.062$ micromole per joule, also react with nylon and DAOx to produce DAOx$^{\bullet}$ and nylon$^{\bullet}$. Under these irradiation conditions and in the absence of oxygen, the radiolytically produced $^{\bullet}OH$ radicals and H-atoms add to the unsaturation site of DAOx and abstract H-atom from the backbone of the polymer substrate (nylon) producing OH—DAOx$^{\bullet}$, and H-DAOx$^{\bullet}$ radicals, and $^{\bullet}$nylon (-H) radicals, respectively. It should be mentioned that $^{\bullet}OH$ and $^{\bullet}H$ are also scavenged by the TWEEN surfactant, since the mixture contains, 4.2×10^{-3} M TWEEN, leading to a decrease in the concentrations of OH—DAOx$^{\bullet}$, H-DAOx$^{\bullet}$, and $^{\bullet}$nylon (-H) radicals. This also leads to the possibility of TWEEN being grafted on nylon 6. This can dramatically decrease the number of sites available for uranium adsorption.

Initial indirect grafting experiments with neat DAOx solutions yielded poor DoGs, even with the use of dry ice in an environmentally controlled chamber during the irradiations to maintain the winged nylon 6 samples cold enough to preserve the radicals generated during the irradiations. On the other hand, direct grafting of DAOx to winged nylon 6 at elevated temperatures yielded extremely high DoGs (>400% in some cases).

These experiments showed that a DoG 25% can be achieved at dose of 250 kGy. This relatively low grafting density may be explained by the fact that the surfactant TWEEN also scavenges the •OH radicals, causing a decrease in the radiolytic yields of nylon• and DAOx• C-centered radicals, and thus its presence causes a decrease in the grafting density.

4.3.2 Characterization

Surface characterization using XPS and Zeta Potential

XPS of clean winged nylon and at grafted DAOx sample that had been grafted through the use of Mohr's salt were obtained. The fabric sample used for this experiment was initially a bright yellow, which was a by-product of the use of Mohr's salt during the grafting process. Upon placing the DAOx sample under vacuum for the XPS measurements, the bright yellow color of the fabric from the grafting or precipitate faded. This was possibly due to the evaporation of ammonia trapped in the fabric from the Mohr's salt, although this theory does have the flaw of not considering the idea that washing with methanol and water should have removed this substance. The XPS results revealed some chemical groups, such as the ester group, that should not exist in pure nylon 6. The presence of these compounds is most likely due to handling with bare skin or dirt from tweezers or surfaces. Another pure nylon 6 sample will have to be run, but the nylon must be washed

first with acetone. The ratio of carbon to nitrogen atoms was observed to decrease in the material from pure to grafted nylon 6. This was unexpected as the grafting of a substance of mostly carbon and no nitrogen to the nylon should have resulted in an increase of the ratio of carbon to nitrogen atoms in the sample. It is possible that the different regions of the fabric along with any remaining ammonia groups from the Mohr's salt on the surface of the fabric would have resulted in this carbon to nitrogen ratio discrepancy. These initial XPS results did not show any sulfur peaks, indicating that the Mohr's salt was not present on the fabrics in its original form. The oxygen peaks in the grafted sample show an O^{2-} peak, which could be correlated to some kind of conjugated oxygen system with the ferrous ion present.

XPS was carried out on again on DAOx grafted fabrics. Samples of both nylon 6 exposed to Mohr's salt and grafted DAOx fabric that had used Mohr's salt as a homopolymerization inhibitor were tested. While at first glance the two spectra looked similar, the fine details of the spectra reveal differences between the two. Compared to the pure nylon 6, the Mohr's salt exposed nylon 6 shows a much higher level of oxygen. The nitrogen and carbon at. % of this sample are understandably decreased as well. The higher presences of oxygen in the sample could be due to a number of reasons. The presences of sulfate groups on the fabric could partially explain the increase in oxygen in the second sample, but the low sulfur content of only 0.54 at.% would suggest only an increase in the oxygens by about four times that percentage (sulfate, SO_4^{2-}). Another possibility is the oxidation of the material due to the long time that the sample was in its aqueous environment (although it should be noted that the effect of the aqueous environment would be outweighed heavily by the time factor). Examining the oxygen peak, we see a hump

around 528.5 eV that is suggestive of O^{2-} which could be present in the fabric as both oxidation of the nylon 6 as well as, and more importantly, as iron (III) oxide, Fe_2O_3. The presence of iron remaining in this fabric in the ferrous state, as indicated by the iron peaks in the spectrum. Oxidation of the fabric itself might be suggested by the presence of an ester peak in the second sample although this could also be due to contamination. The sulfur peaks only indicate sulfates present in the material. The apparent failure of washing step to remove the remaining Mohr's salt from the fabric could be due either to a gradual diffusion of the salt into the nylon fibers such that they became lodged or due to chemical additions of the components of Mohr's salt to the nylon 6 backbone. For the DAOx grafted sample washed with acetone, the results are similar to the previously tested DAOx grafted sample, but unfortunately the acetone wash did not seem to mitigate the remaining presence of iron in the fabric (although this was not wholly expected). To start, there was no trace of a sulfate peak, which lends support to the notion that time may have been the cause of the second sample's sulfur content. The oxygen peak also does not exhibit an oxide O^{2-} hump which also lends to this idea. One of the most important features of the spectra is the large ester peak in the carbon portion of the spectra that would only indicate DAOx grafting since while there was an ester peak in the second sample, it was not nearly as large. In fact, oddly enough, this ester peak is even higher than the one seen for the previously tested DAOx grafted sample. This could be due possibly to the region analyzed by the XPS for both samples just having different local degrees of grafting.

Figure 4.21 shows the XPS spectra of the ungrafted nylon and of the nylon radiation-grafted with DAOx. The XPS results demonstrate the presence of C-C/CH, oxalate, amide, C-N, and ester groups.

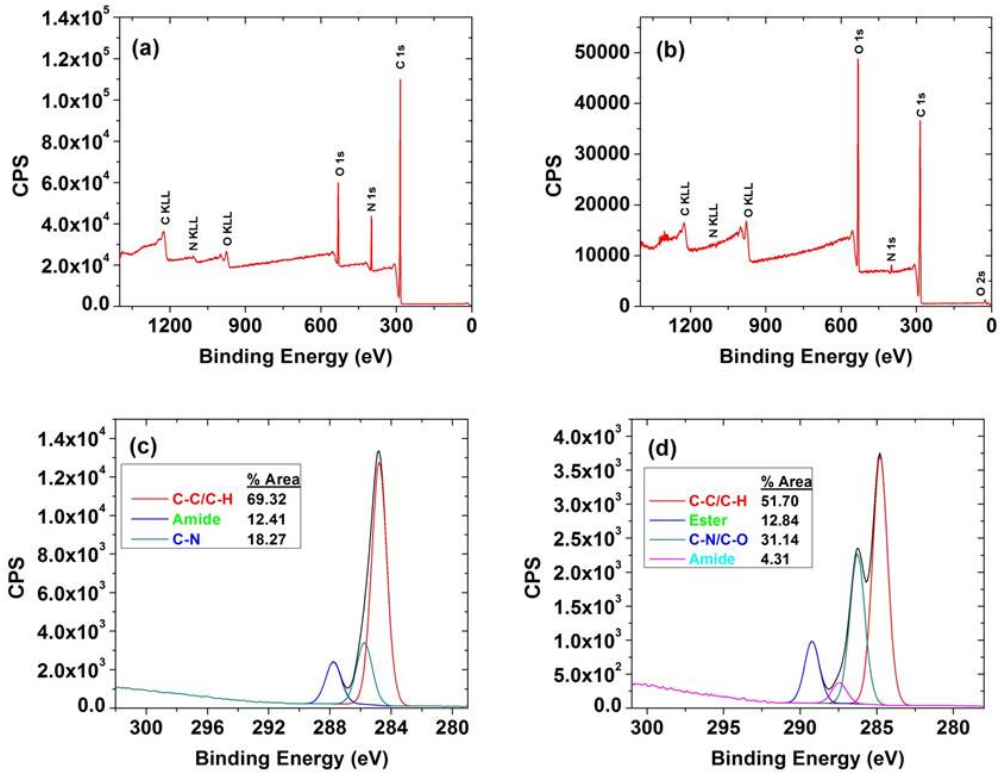

Figure 4.21 - Comparison between the XPS spectra of ungrafted nylon 6 (a,c) and DAOx grafted nylon 6 (b,d). The presence of the ester peak in the grafted nylon 6 can be attributed to the grafting of the oxalate group.

In order to reinforce the hypothesis that the uranyl ion is binding to the negative oxalate group attached to the nylon 6 fabric, zeta potential measurements were performed on grafted and un-grafted nylon 6 fabric that had been chemically transformed into microparticles. An image of the solution of the microparticles can be seen in Fig. 4.22. The zeta potentials for both the grafted and ungrafted nylon 6 fabric were measured and the results are summarized in Table 4.3. These results show that at a pH of about 8 the surface

of the oxalate-grafted fabric is negatively charged and thus suitable for extraction of UO_2^{2+} from the seawater.

Figure 4.22 - Nylon 6 particles suspended in solution.

Table 4.3 - The average sizes and zeta potentials of the grafted and non-grafted nylon 6 microparticles.

	Particles from grafted nylon 6	**Particles from non-grafted nylon 6**
Average Size	5.6 ± 1.6 μm	1.5 ± 0.12 μm
Zeta Potential in acidified deionized water (pH ~ 3)	26.4 ± 0.5 mV	40.1 ± 3.1 mV
Zeta Potential in acidified seawater (pH ~ 4.5)	-3.9 ± 0.3 mV	-3.9 ± 0.4 mV
Zeta Potential in Seawater with pH adjusted to ~8.3	-6.1 ± 0.9 mV	-4.6 ± 0.5 mV

4.3.3 Extraction Testing

Uranium Removal from Spiked Seawater

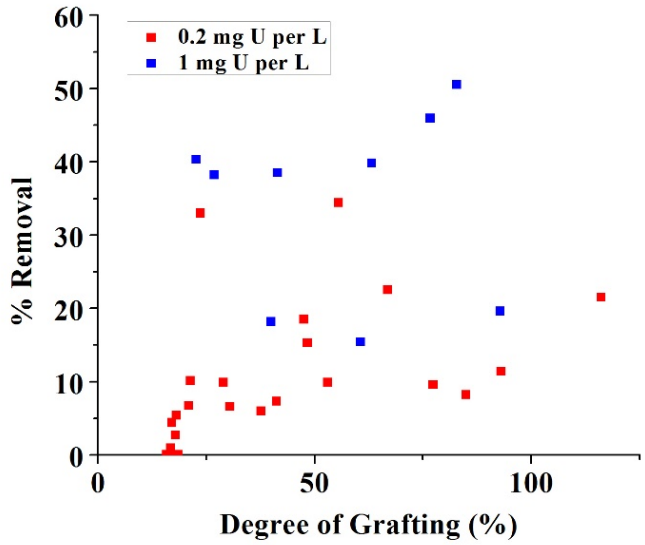

Figure 4.23 - The percent uranium removal of the fabrics from uranyl acetate and seawater solutions doped to the respective levels.

The results obtained for the removal of uranium from spiked seawater by means of nylon 6 fabrics grafted with neat DAOx are shown in Figure 4.23. The level of spiking was either 1.0 mg/L or 0.2 mg/L U (introduced as uranyl acetate). In each test, a sample weighing approximately 30 mg was rotated with 10 mL of the spiked seawater at 30 rpm for 7 days. The results show that significant removal of uranium from these solutions (>5%) took place when the DoG exceeded approximately 18%, and, in general, the percent removal of uranium from both the 1.0-mg/L and 0.2-mg/L U solutions increased with increasing DoG. The large scatter in the data can be ascribed to the non-uniform

distribution of the grafted material on the nylon 6 fibers as observed by SEM (see below). Another reason for the scatter is associated with the fact that some of the adsorbent samples were subjected, following the radiation induced grafting, to heat treatment at 50°C for 7 days. The percent removal of uranium from the test solutions observed with these samples was generally higher than the corresponding percent removal observed with samples which did not undergo heat treatment. It should also be noted that the amounts of uranium in the test solutions were very small (0.01 or 0.002 mg, respectively) so that the results in Figure 4.23 cannot provide a realistic estimate of the maximum amount of uranium that can be removed by the fabric from large volumes of seawater.

As expected, Figure shows that as the grafting density increases, the extraction of uranyl from spiked seawater increase. The scattering of the results of the percentage extraction can be related to the non-uniformity of the grafting within the samples. This non-uniformity in the grafting is the principal disadvantage of the solvent-free grafting. Notwithstanding this disadvantage, removal of as much as 50% of the uranium from the test solution was achieved using adsorbent fabrics produced using this method. In general, it was observed that the measured extent of uranium uptake from the seawater, whether spiked with 1 mg/L or 0.2 mg/L of uranium, increased with the DoG of oxalate on the polymeric fabric.

On the other hand, the extent of extraction of uranyl ion from seawater by means of fibers grafted with DAOx in an aqueous environment in the presence of TWEEN was very low (<5%). This may be due to the grafting of TWEEN onto nylon, which hinders the grafting of DAOx onto nylon, since a large fraction of the $^{\bullet}OH$ radicals may react with TWEEN, producing TWEEN$^{\bullet}$ radicals.

SEM/EDS Results

The SEM observations showed a non-uniform distribution of the grafted material on the fibers, with some sections of the fibers coated with significant amounts of grafted material and other sections free of such coating. However, the EDS results (see Table 4.4) obtained for the fabrics following contact with the uranium-spiked seawater were remarkably similar for different regions of the fabrics, showing that the relative affinities of the adsorbent for the various ionic solutes in the seawater were consistent across the entire structure of the fabric.

Table 4.4 - Comparison of different DAOx grafted nylon 6 samples in terms of their selectivity for uranium versus sodium as measured by EDS. † - % U Removal from 1 mg $U*L^{-1}$

Sample	Degree of Grafting	% U Removal (from 0.2 mg $U*L^{-1}$)	Atomic % U on Surface	Atomic % Na on Surface
DA310	**20.96%**	**6.7**	**32.8**	**51.2**
DA318	**47.60%**	**18.5**	**26.7**	**58.9**
DA321	**77.39%**	**9.6**	**26.3**	**59.2**
DA324	**76.69%**	**45.9†**	**28.4**	**55.0**

4.4 Azo Compounds

4.4.1 Selection

Following the implementation of the spectrophotometric method for the determination of the amount of uranium removed from seawater, it was hypothesized that chemicals with

similar functional groups to the one used in the spectrophotometric method would be able to extract uranium very efficiently. The monomer repertoire tested includes a number of pyridylazo compounds, such as those shown in Fig. 4.24.

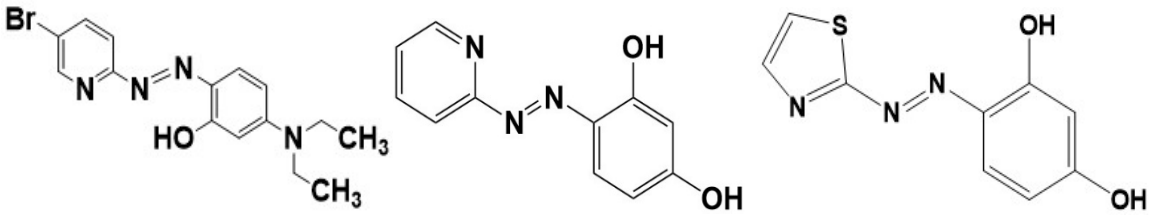

Figure 4.24 – The compounds shown are B2MP, left, PAR, middle, and TAR, right.

Unfortunately, as delivered the compounds were not readily graftable as they contained no allyl or vinyl functional groups. However, TAR and PAR can be chemically altered to include an allyl group without affecting the functional groups that are believed to contribute to the binding of uranyl (the azo group, the nearest hydroxyl group, and the nitrogen in the thiazole ring). Through the reactions mechanism outlined in Fig. 4.25, two different allyl-functionalized compounds were created.

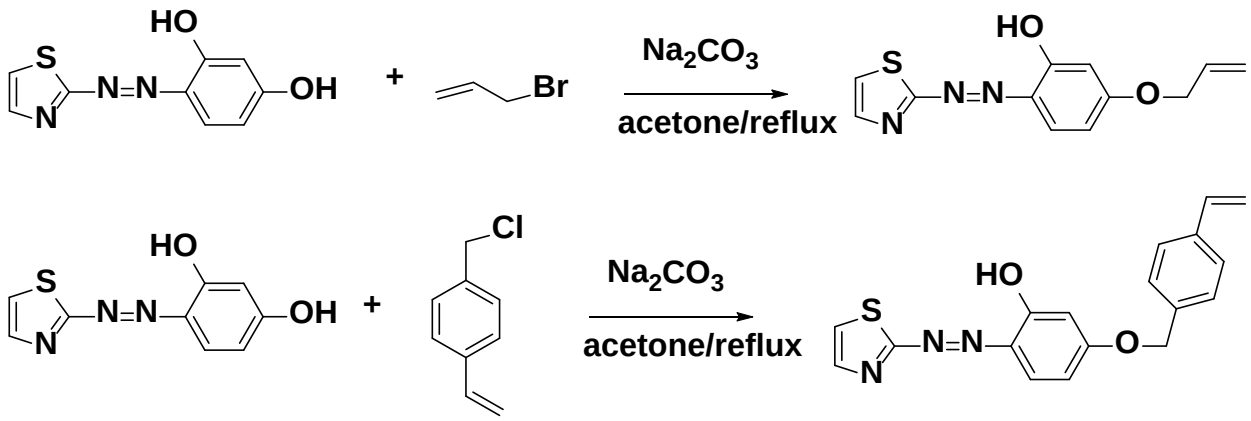

Figure 4.25 – The synthesis mechanisms for the allyl-functionalized TAR: allyl-TAR is on top and vinylbenzyl-TAR (VB-TAR) is on the bottom.

4.4.2 Grafting

The allyl-TAR compound did not show significant degrees of grafting in ethanol when irradiated to 200 kGy by electron beam, however the fact that a mass increase was seen indicates that grafting is possible.

Attempting to graft allyl-TAR in DMSO under similar conditions to experiments with ethanol (electron beam, 200-250 kGy), did not yield significant DoGs.

2-(5-Bromo-2-pyridylazo)-5-(diethylamino)phenol (Br-PADAP), allyl-TAR, and vinylbenzyl-TAR were all used as monomers in a basic solution in an attempt to directly graft the azo moiety to the surface of winged nylon 6. Using electron beam, samples were irradiated using direct grafting conditions at elevated temperature. Even with the concurrent heating and sample irradiations, higher DoGs were not seen. In fact, negative DoGs were seen across all compounds. First of all, this could indicate degradation of the nylon-6 fabric as a result of either the temperature, the irradiation, or both combined. This

also has implications for previous experiments and the DoGs wherein the % DoG would not be a good representation of the actual amount of monomer grafting. The discoloration present on the surface of the vinylbenzyl-TAR and allyl-TAR samples and the lack of color in the post-irradiated solution are strong indications that some amount of grafting of the compounds to the surface has occurred with these samples While DoG measurements did not reveal grafting, uranium extraction experiments might indicate grafting of the monomer if uranium is successfully extracted. The degradation of the fabric substrate and/or the monomer in solution could also be due to the high amount of hydroxyl radicals that might have been present in solution at the time of irradiation. These hydroxyl radicals at 250 kGy dose, in a 10 mL solution of water, with a G-value of ~0.62 μmol/J (for N_2O samples) were at a concentration of ~0.155 M, which is about two orders of magnitude higher than the monomer concentration (at best, considering monomer concentrations were not explicit and could be best case scenarios). This could possibly result in the complete degradation and/or oxidation of the allyl groups. As such, hydroxyl radical yield calculations should be applied for future experiments of this type in order to ensure appropriate radical yields. Overall, the use of a basic solution as a vehicle for azo compound grafting is promising. The nylon 6 did not show any significant degradation in the pH 10 solution at higher temperatures so higher pH solutions might be able to be used in future experiments to increase the quantity of dissolved monomer.

Indirect grafting was attempted with solutions of allyl- and vinylbenzyl-TAR in methanol. The mass loss as a results of the indirect grafting process is within the same range of the previous attempt to graft the two TAR compounds using direct methods and a basic solution most likely indicating no grafting of the monomer. This result is confusing

as the conditions for indirect grafting appeared optimal, such as the fabric temperature during irradiation was kept below its glass transition temperature, the subsequent exposure to hot monomer solution and the use of an appropriate organic solvent to limit monomer solvent-interactions. From the experiment, there are a few possible parameters that might have caused the low DoGs. One possibility might be the introduction of oxygen into the fabric vial during the monomer solution injection process. However, the quantity of oxygen possibly injected, and the amount of time before the sample was covered in an oxygen purged solution seems unlikely. It might also be possible that the irradiation and temperature conditions are not conducive to grafting. This could be tested through the use of a monomer that has been shown to be significantly more prone to polymerizing, such as styrene or B2MP. This experiment did allow for the rough estimate of the maximum concentration of the TAR compound in methanol and it showed that irradiation chamber temperatures could be lowered to below freezing using dry ice placed near the air intake in the temperature control box.

The grafting of allyl-TAR to the surface of nylon 6 was further expanded upon. In an attempt to reduce the quantity of initial material required for grafting, an indirect method was used. Unfortunately this indirect method did not result in any amount of DoG.

Direct grafting of VBC was carried out in solutions of ethanol and methanol. In both cases, significant grafting was obtained. In methanol, a DoG of 56.6% was obtained and in ethanol DoGs of over 100% were obtained.

The low grafting density of directly grafted VBC monomer in ethanol on winged nylon 6 was due to a much lower concentration of the monomer and a lower dose. In order to

return to higher degrees of grafting, the concentration of the monomers should be increased and the dose should be manipulated in order to decrease homopolymerization.

An attempt at indirectly grafting both VBC and allyl-bromide as chemical precursors to azo attachment were unsuccessful, though the initial failure was unexpected as the injections of monomer solution appeared to be successful. While it is highly likely that a small amount of oxygen may have penetrated into the vial during injection, it was not expected to completely quench the radicals present on the nylon fabric. Further indirect experiments should attempt to utilize higher concentrations of monomer, different fabric/substrate materials, different solvents, and the use of a glove bag in order to significantly reduce the penetration of oxygen during monomer injection.

The use of DCM was extremely effective in removing any VBC homopolymer from the surface of the fabric. The caveat to this was that for samples with higher doses, it appears the monomer had polymerized to the point where the DCM could no longer dissolve it effectively even after sonication. Future grafting experiments should avoid this level of polymerization. The allyl-bromide grafting was mostly unsuccessful. Gases from the allyl-bromide effused off the solution and caused significant pressure build-up in the sample vials. This was most likely due to electrons preferentially kicking off the bromine rather than radicalizing the C-C double bond for grafting. As such, the allyl-bromide samples did not achieve grafting densities above 2%, which is experimentally negligible. It should be noted that at higher allyl-bromide concentrations the DoG did show an increase compared to lower DoGs. The grafting of VBC was very successful. Even with the error during irradiation of leaving the turntable off during the 25 kGy irradiation, the resulting DoGs showed a clear trend versus both VBC concentration and dose. All of these samples

will be used as substrates for azo-attachment. The reproducibility of the DoGs within sets of samples with the same dose indicates that the procedure of radiation and washing are consistent and should be used in future grafting experiments. Based off TAR-attached fabric performance, the optimum DoG can be obtained for VBC that results in the highest uranium extraction.

While a number of experimental errors associated with the irradiations of the fabrics resulted in high error values for the total dose received for some fabric sets, there was a clear trend between concentrations of VBC and doses which followed the trend previously seen with earlier experiments. For the 24 wt. % VBC samples, the trend of DoG vs. dose shows a large widening in DoG deviation at higher doses most likely due to a large buildup of homopolymerization. At lower doses for the 24 wt. % VBC solution, the deviation between DoGs was much smaller. The attempt at indirect grafting of VBC proved fruitful as the indirect DoG reached values as high as 38%, and with an average around 10% for all samples. The main differences between this experiment and previous indirect grafting experiments are the higher concentration of monomer in solution and the fact that all samples were irradiated in a constant dose rate environment, i.e. the turntable was not on for a portion of the initial irradiation and the turntable was not used at all during the second irradiation. Assuming concentration is the minor cause of the indirect grafting, we can examine why the lack of turntable rotation might have impacted the amount of indirect grafting. Without rotation, all samples would receive a constant dose rate and will reach a plateau of radical concentration. In a variable dose rate environment, it is probably that the maximum radical concentration will be based on a time average dose rate across all points in the rotation. As such, it may be necessary to restrict the rotation for indirect irradiation

and to re-do dosimetry measurements for future indirect experiments. At higher doses, the homopolymerization in directly grafted VBC solutions was extensive enough to the point where multiple washings including sonication would not remove the excess material. After drying the fabric, the homopolymer was still flaking off the fabric and it is unclear why this material would not have been removed during washing. TAR attachment onto grafted fibers appeared to be successful as TAR attachment was confirmed by both a color change on the fabric surface and a significant mass change. The mass change due to TAR grafting was actually the highest amongst all previous experiments most likely due to an increase in reaction temperature. One odd effect noticed was that the irradiated, but non-grafted control fabric had a small color change, which was unexpected as the TAR should not have reacted with anything on the surface of the nylon 6. Further analysis of the fabric was required to determine which chemical process would have resulted in the color change. One possibility based on previous observations of non-irradiated fabric non changing color is that the oxidation of the surface of the fabric due to the surface radical exposure to oxygen allowed TAR to react with the surface and bind to it through an unknown and unexpected chemical reaction. Due to the increased reaction temperature however, this theory cannot be verified. This experiment further validated the need for a more consistent baseline grafting procedure for the VBC attachment in order to elucidate more subtle variables that would have an impact on final uranium extraction, such as the TAR attachment reflux temperature.

While the DoGs of the fabric samples were high enough to be distinguished from possible error, such that there was a small amount of grafting, the DoGs were far from the values expected. As such, it appears the use of the glove bag, while important is not the

only factor preventing high degrees of grafting. Other parameters that can be altered to improve DoG include the monomer concentration, the solvent, dose, and the temperature and time of post irradiation heat treatment.

While numerous grafting techniques and parameters were attempted in an effort to graft these compounds, they were all mostly unsuccessful and the time and cost of synthesizing and purifying these two compounds made sample processing difficult. In order to improve on the economics and DoG of the thiazolylazo compound on the surface of the polymer fabric, a new order was devised for processing samples. Instead of performing the chemical attachment of the allyl group to the TAR compound first, the vinylbenzyl chloride (VBC) precursor was grafted to the surface of nylon fabric first. Degrees of grafting of 150% and higher were achieved. The relationship between DoG and dose for this compound is shown in Fig. 4.26.

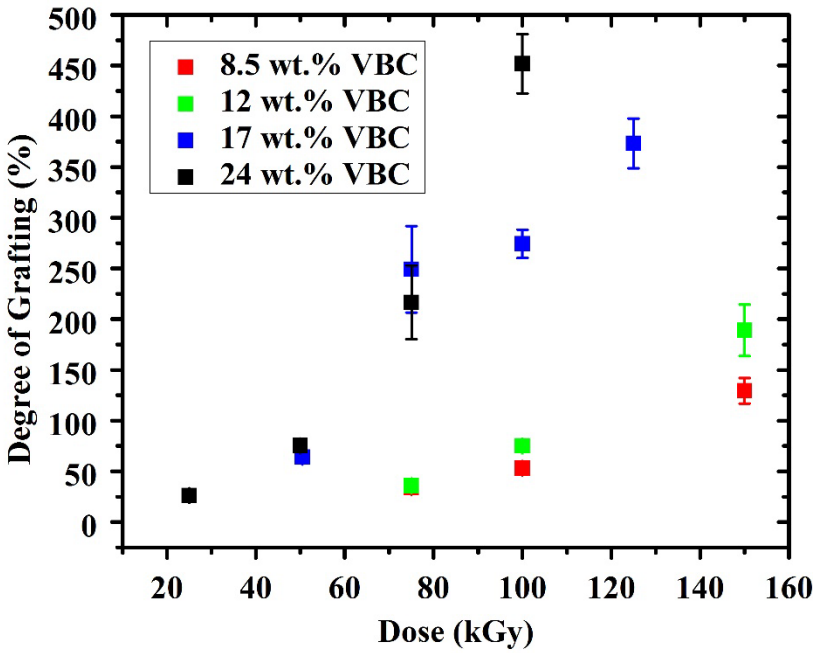

Figure 4.26 – The relationship between dose and DoG of VBC on nylon 6 under electron beam irradiation at a dose rate of 250 kGy/hr with two different concentrations of VBC in ethanol.

After the grafting step of the chemical precursor to the surface of the nylon fabric, the now chlorine functionalized fabric can have the TAR or PAR compound chemically attached to its surface. A scheme for this method of attaching PAR to the surface of the fabric is shown in Fig. 4.27. This method has several procedural improvements over the previous method. For example, the fabric grafting can be optimized prior to chemical attachment of the PAR or TAR groups, thereby reducing the amount of the more expensive azo compound necessary to optimize the system. This method will also serve to improve the exposure of the azo compounds to the seawater environment, as the chemically attached

PAR or TAR will only be attached at the surface of any homopolymer, versus being trapped inside homopolymer if the allyl-functionalized azo compound had been grafted instead.

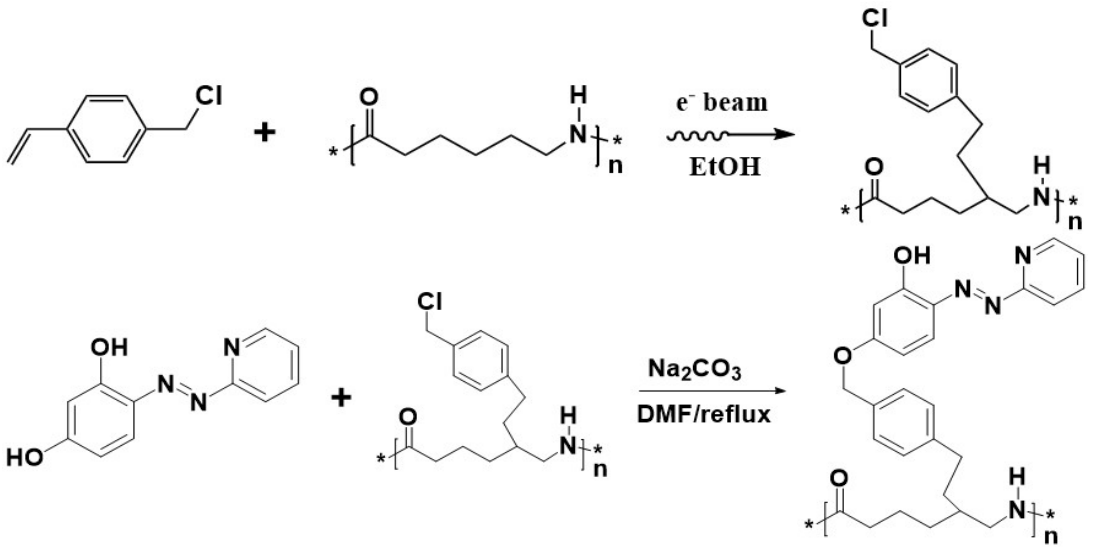

Figure 4.27 – The grafting and reaction mechanism for first attaching VBC to the surface of the nylon 6 using electron beam irradiation and then chemically attaching TAR to the grafted VBC.

The incorporation of MAA into the grafting procedure was begun in an attempt to improve the hydrophilicity of the surface of the fabrics. Indirect grafting was successfully achieved and while the DoGs achieved were not as high as those published in literature, they were nonetheless higher than any previous indirect grafting results and hold promise for improving DoGs in future experiments. A scheme for the different radical mechanisms that occur during the radiation grafting of VBC and MAA to the surface of nylon 6 is shown in Fig. 4.28.

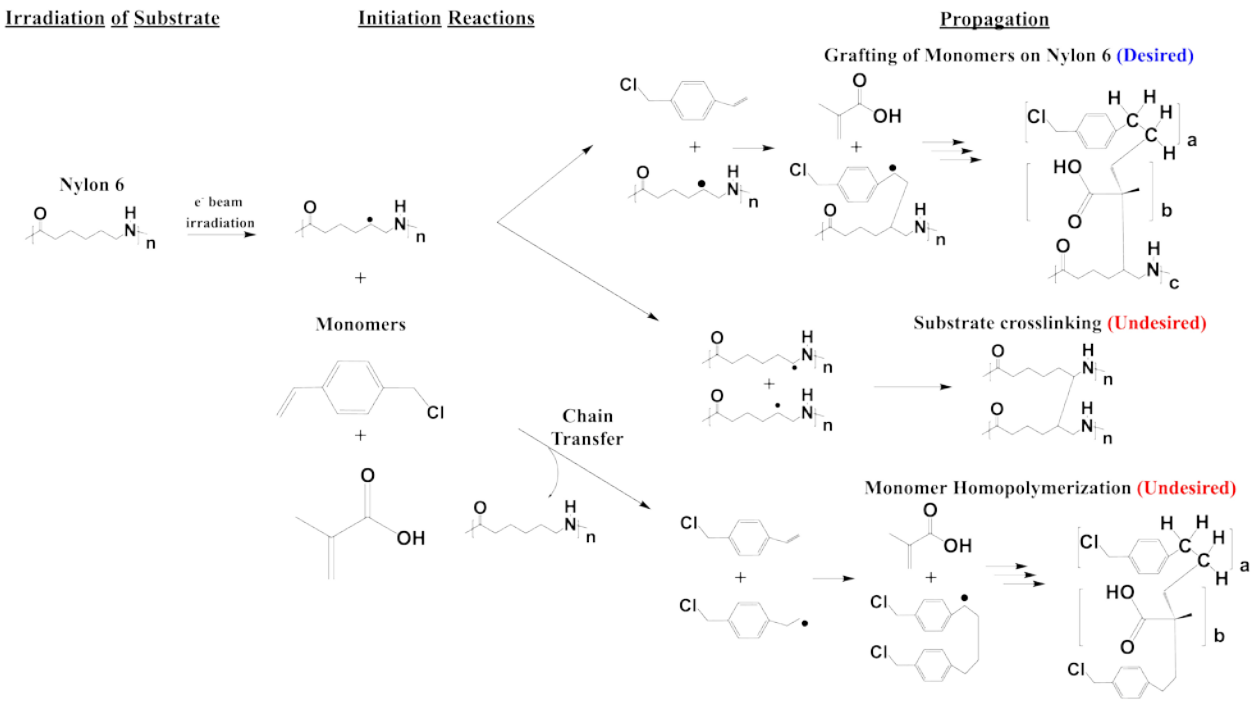

Figure 4.28 – Upon irradiation, the radicals on the backbone of the nylon 6 polymer are able to proceed through a number of different reactions either with the selected monomers, VBC and MAA, or with itself. Grafting of the monomers onto the nylon 6 is the preferred reaction, whereas crosslinking and homopolymerization following chain transfer are not desired.

Between the VBC and VBC/MAA samples of winged nylon-6, there did not appear to be a clear difference in DoGs which might indicate that the total wt. % of monomer in the solution plays a more important role than the concentration of each monomer individually in this case, though more experiments involving different monomers and concentrations will be required to prove this. The 3M nylon 6 (non-winged) exhibited lower DoGs as compared to its winged nylon 6 counterpart, but not significantly lower, as seen in Fig. 4.29. This might have been caused by the higher surface area of the winged fabric. The

winged PET fabric should negative degrees of grafting. This might have been due to a loss of material during the initial washing of the fabric in acetone prior to irradiation. The dose used on the fabric might also have been too high for effective grafting to occur on this material.

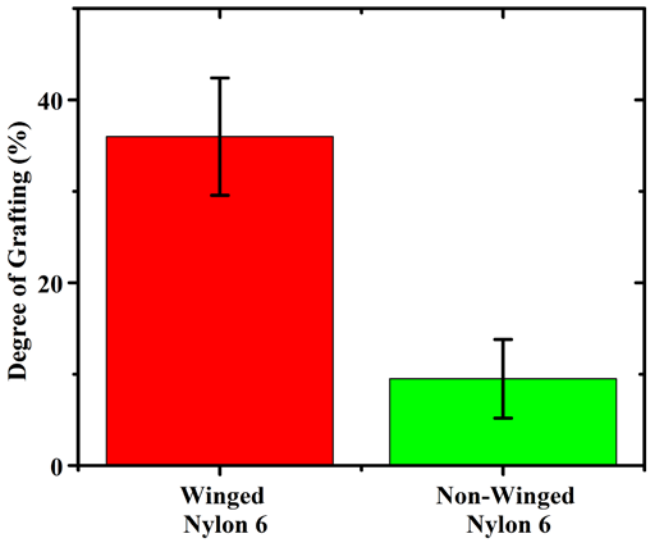

Figure 4.29 – A significant difference in DoG for indirectly grafted nylon was seen between the winged and non-winged varieties of the polymer.

Different wt. % of VBC and MAA dissolved in DMSO provided DoGs on the same order of magnitude as seen in Fig. 4.30. The grafting of these solutions as a follow-up to previous indirect grafting experiments showed that the procedure could allow for relative consistency of DoGs.

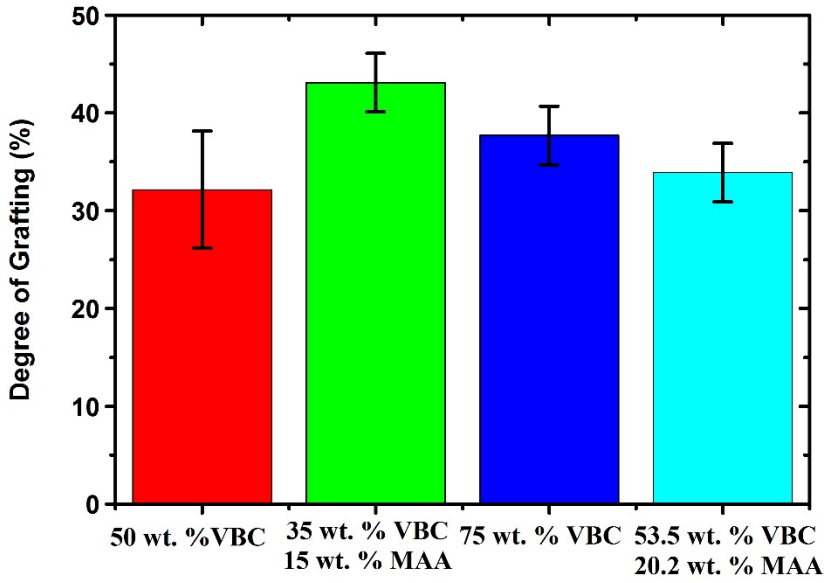

Figure 4.30 – Even at different monomer ratios, the total DoG of the indirectly grafted winged nylon 6 fabric irradiated under the same conditions was relatively consistent. This provides the opportunity to tune the VBC:MAA ratio without worrying about a decrease in DoG for these monomer concentrations.

Unfortunately the majority of the fabrics irradiated through the use of the 2 MeV Van de Graaff accelerator at NIST and doused in monomer solution did not result in DoGs that would be significant enough to proceed with PAR attachment and uranium extraction experiments. Most DoGs were below 10% particularly for VBC grafted fabrics. The notable exceptions to this were two samples of 75 wt. % MAA with DoGs over 25% and most of the 75 wt. % B2MP samples. The B2MP samples reference actually polymerized significantly in the vials such that a gel-like material was produced. The high degrees of grafting for the 75 wt. % B2MP samples might be due mostly to stuck-on homopolymer,

through these samples should still be tested for their ability to extraction uranium from seawater. From my hypothesis regarding these 2 MeV grafting experiments. It was unclear if the HDPE fibers produced higher DoGs as the DoGs were too low to obtain any reliable comparison. I posit that the lower energy of the Van de Graaff resulted in a reduced concentration of radicals throughout the samples which led to the reduced DoGs. The long time that it took to take the samples from the Van de Graaff room to the glove bag may have also contributed to the reduced DoGs as this would allow for a longer radical decay time. The fact that I did not use dry ice temperatures during the irradiations also reduced radical lifetimes. To elaborate, the lower electron energy of the Van de Graaff would result in decreased depth of penetration of the electrons into the samples as compared to the 10.4 MeV electrons from the MIRF facility.

4.4.3 Characterization

Four different azo compounds, Br-PADAP, PAR, 1-(2-Pyridylazo)-2-naphthol (PAN), and 2-(2-Pyridylazo)-1-naphthol (ISOPAN), were independently mixed with uranyl acetate in methanol in 1:1 molar ratios as this was the expected molar ratio between azo and uranyl that would form in an aqueous environment. The azo compound and the uranyl acetate were dissolved in methanol separately then mixed together and stirred. The methanol was allowed to evaporate and the four azo-uranyl mixtures were collected for XPS analysis. Based on the XPS analysis results, the creation of a uranyl-chelated pyridylazo compound outside of solution appeared to be a success. Both physical characteristics and XPS data of the chelated compounds suggested this. The uniformity of the crystals and the presence of uranium in the XPS data were the main supporting

observations respectively for this conclusion. From the XPS data, the most informative characteristic that suggested a 1:1 binding motif for uranium to the pyridylazo group/compound was the similar atomic percentage between the bromine and uranium atoms in the U-chelated Br-PADAP compound as shown in Fig. 4.31. The slightly higher U concentration could be due to the overlapping of the N_{1s} peak at ~400 eV with the U_{4f} peak.

Unfortunately, due to the lack of an atom of similar atomic percentage to U in PAR, PAN, and ISOPAN, this evaluation is not possible. However, the atomic % of U in PAR is on the correct order of magnitude in comparison to the three nitrogens present per pyridylazo group, as shown in Fig. 4.32.

Again, the overlap of the U_{4f} and N_{1s} peaks could explain any discrepancies. One important caveat to these conclusions is that in this experiment, the uranyl acetate and chelating monomer were mixed in 1:1 molar concentrations, which would result in the atomic percentages seen in the XPS results. Therefore, in order to more fully determine whether or not the uranium was actually bound to the monomer, the uranium bound monomer must be examined. Unfortunately again, the nitrogen functional groups that bind to uranium have overlapping peaks with the uranium which means their energy shift cannot be evaluated. This leaves the energy shift of the hydroxyl group. In both Br-PADAP and PAR, the unchelated compound shows a O_{1s} peak around 532.5 eV. When these compounds are chelated to uranium however, the peaks shift to lower energies by about 1 eV. This weakening of the binding energy would suggest that the oxygen is sharing its electron density through a chelation to the uranyl ion.

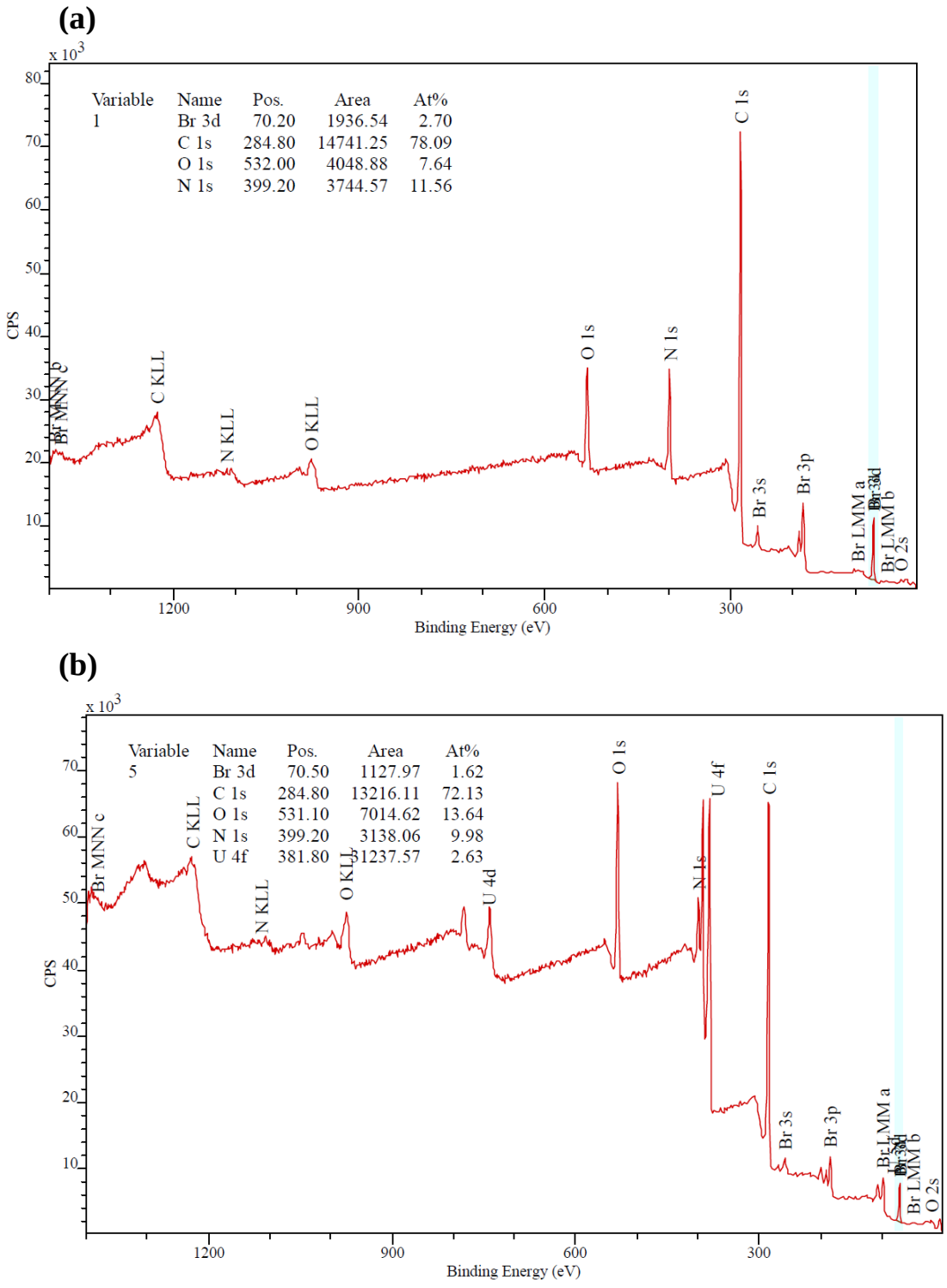

Figure 4.31 – (a) XPS spectra of Br-PADAP, (b) XPS spectra of Br-PADAP chelated to uranyl acetate.

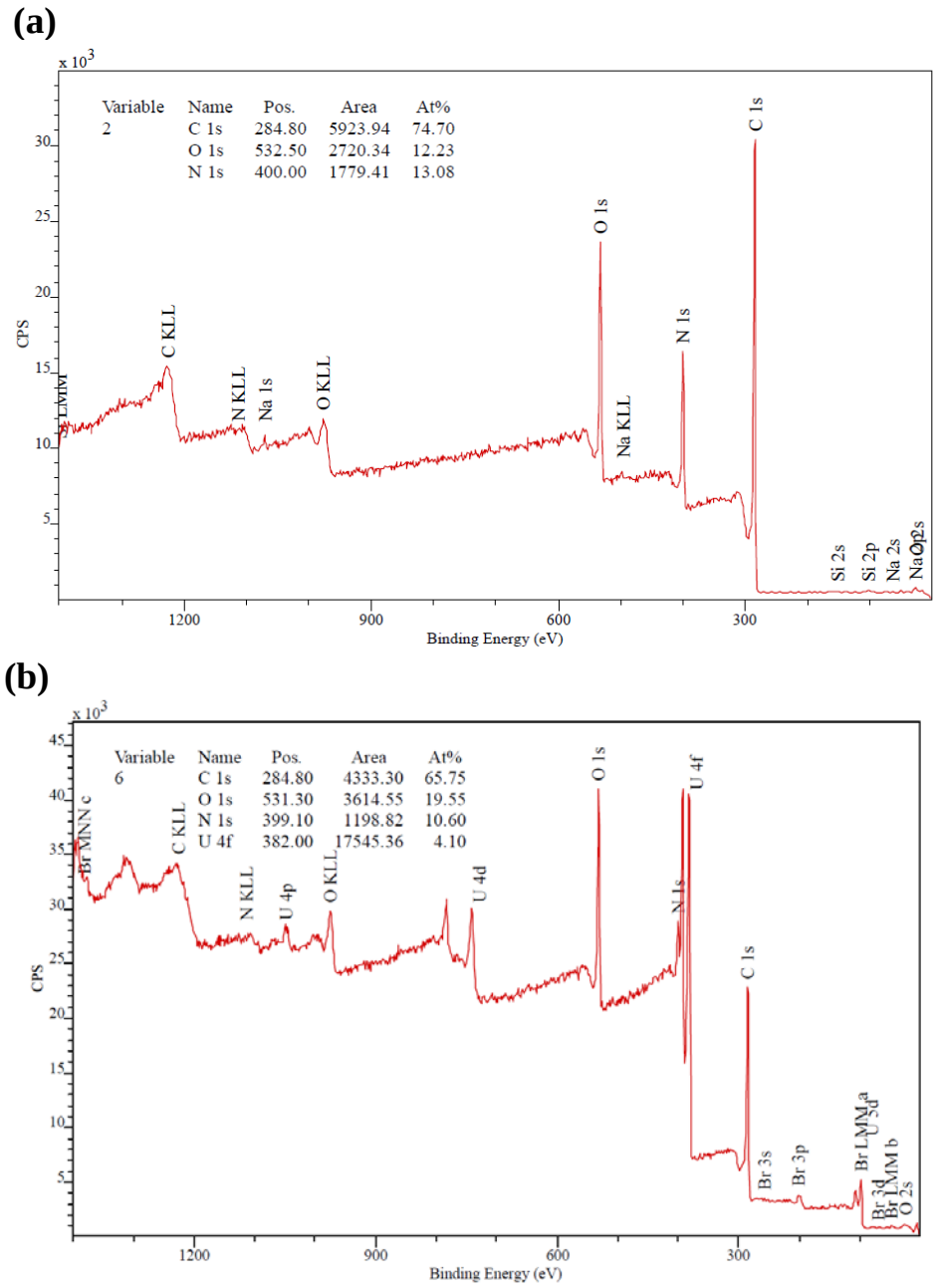

Figure 4.32 – (a) XPS spectra of PAR, (b) XPS spectra of PAR chelated to uranyl acetate.

The attachment of the azo compound to the surface of the grafted polymer was confirmed through the use of FTIR-ATR and SEM-EDS. Both techniques were able to observe an initial increase in C-Cl bonds or the atomic percent of chlorine on the surface

of the fabric, resepectively. Examples of the FTIR-ATR and the SEM-EDS data are shown in Figs. 4.33 and 4.34 respectively. Table 4.5 includes the EDS data from Fig. 4.34. Fig. 4.35 and Table 4.6 illustrate the effect of PAR attachment to a VBC grafted fabric. Following PAR attachment, as expected the chlorine content of the fabric decreases indicating a successful attachment.

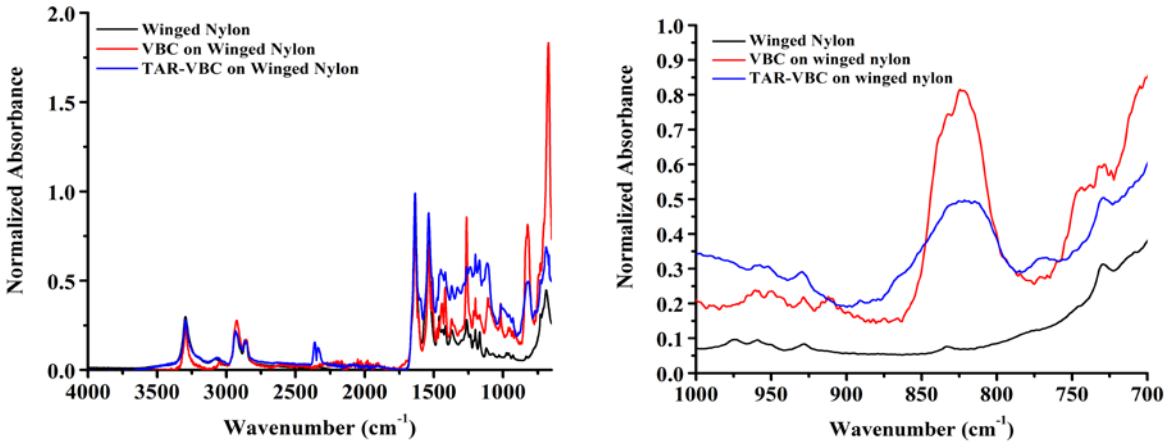

Figure 4.33 – FTIR-ATR scans of clean winged nylon, winged nylon grafted with VBC, and VBC-grafted winged nylon that has been chemically functionalized with the TAR monomer. The full spectrum is on the left and the right spectrum shows the peak associated with the C-Cl stretching vibration.

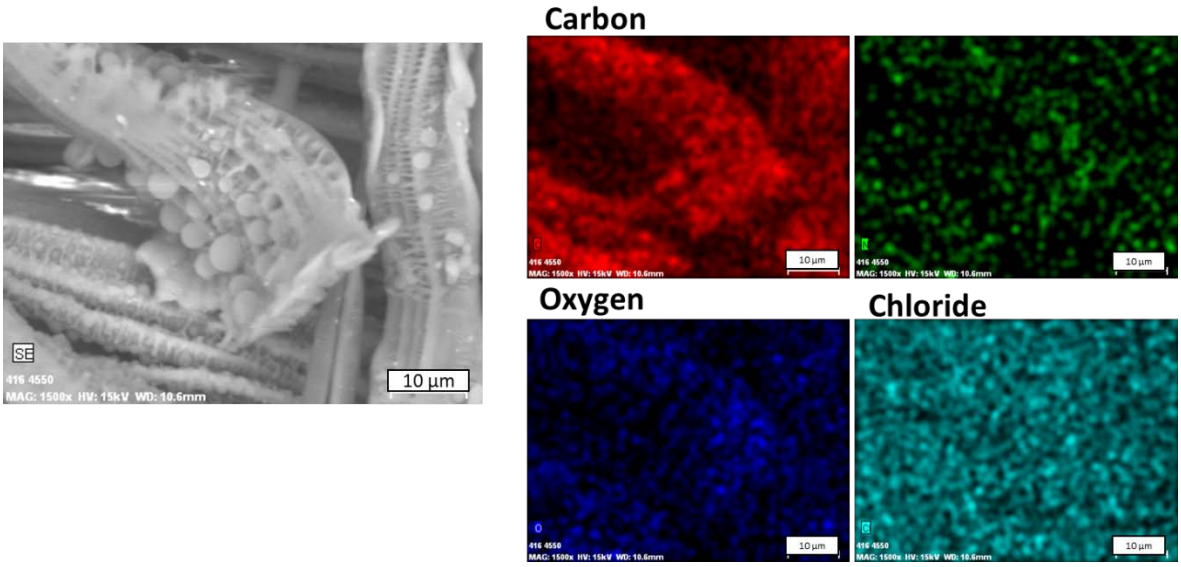

Figure 4.34 - SEM-EDS of directly grafted winged nylon 6 with VBC.

Table 4.5 Tabulated EDS results from the fabric in Fig. 4.34.

Element	Unn. C [wt. %]	Norm. C [wt. %]	Atom. C [at. %]	Error (1 σ) [wt. %]
Carbon	78.39	78.39	83.38	10.15
Nitrogen	8.74	8.74	7.97	2.61
Oxygen	9.16	9.16	7.31	1.95
Chloride	3.71	3.71	1.34	0.17
Total	*100.0*	*100.0*	*100.0*	

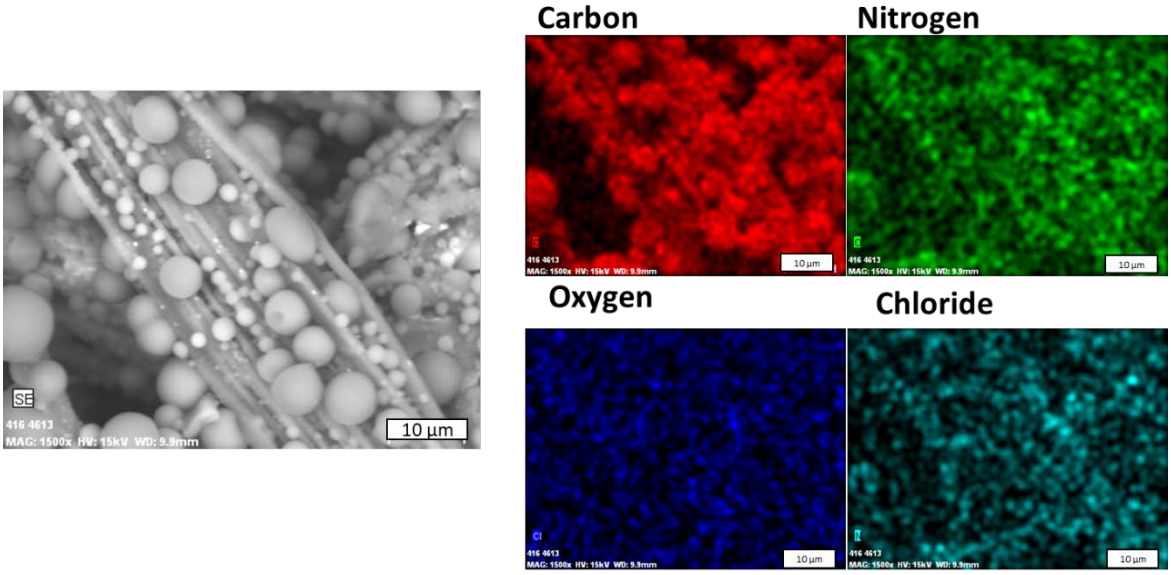

Figure 4.35 SEM-EDS of the same fabric as previous figure post-PAR attachment.

Table 4.6 Tabulated EDS results from the fabric in Fig. 4.35.

Element	Unn. C [wt. %]	Norm. C [wt. %]	Atom. C [at. %]	Error (1 σ) [wt. %]
Carbon	**77.35**	**77.35**	**80.99**	**8.75**
Nitrogen	**11.90**	**11.90**	**10.68**	**2.22**
Oxygen	**10.44**	**10.44**	**8.20**	**1.62**
Chloride	**0.24**	**0.24**	**0.08**	**0.04**
Total	***100.0***	***100.0***	***100.0***	

The loss in chlorine as seen in SEM-EDS for directly grafted VBC samples upon conversion to PAR-grafted samples is also seen for indirectly grafted fabrics, see Fig. 4.36.

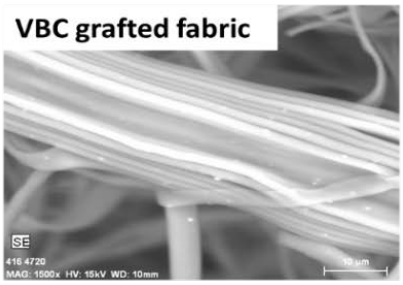

Element	Norm. C [wt. %]	Atom. C [at. %]	Error (1 σ) [wt. %]
Carbon	73.01	78.89	9.32
Nitrogen	10.82	10.01	2.71
Oxygen	11.91	9.65	2.20
Chlorine	4.26	1.56	0.18

Element	Norm. C [wt. %]	Atom. C [at. %]	Error (1 σ) [wt. %]
Carbon	71.33	75.87	8.74
Nitrogen	12.63	11.52	2.92
Oxygen	15.26	12.19	2.63
Chlorine	0.05	0.02	0.03

Figure 4.36 – SEM-EDS analysis of both the VBC grafted (top) and PAR functionalized fabric (bottom).

4.4.4 Extraction Testing and Performance

The preliminary results of the grafted PAR fabric are promising, as shown in Fig. 4.37. However the amount of uranium removal seen for 0.2 ppm U in 10 mL seawater is still far below what was expected based on the charcoal tests. It is believed that the potential seen in the charcoal tests can be obtained by improving the DoG of the monomer and by increasing the surface area of the grafted polymer chains, which would in turn allow for a higher amount of PAR to be attached at their surface.

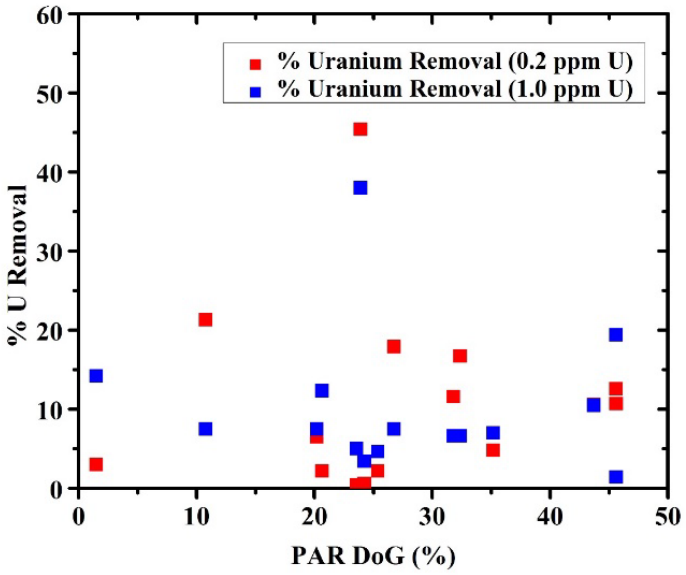

Figure 4.37 – A selection of samples produced by the irradiation grafting of VBC and then the chemical attachment of PAR with their % uranium removal from 10 mL of 0.2 ppm and 1.0 ppm U in seawater solution.

Unfortunately, these results were inconsistent with the ICP-MS based analysis of the fabrics after the fabrics were dissolved in 2% nitric acid as the amount of uranium on the surface of each fabric sample differed between the spectrophotometric and ICP-MS methods. This discrepancy is illustrated in Fig. 4.38. One reason for this difference could be that the incomplete dissolution of the nylon 6 fabric could have left some uranium trapped in the fabric. Due to the fact that acid and low pH solutions have been used to elute uranium off of fabrics in other research, this explanation is less likely and can be refuted with the implementation of perchloric dissolution. A more likely possibility is that the indirect nature of the spectrophotometric method resulted in an incorrect determination of

the total uranium adsorbed by the fabrics, however refinement of the ICP-MS analysis for this particular system is required before this can be established.

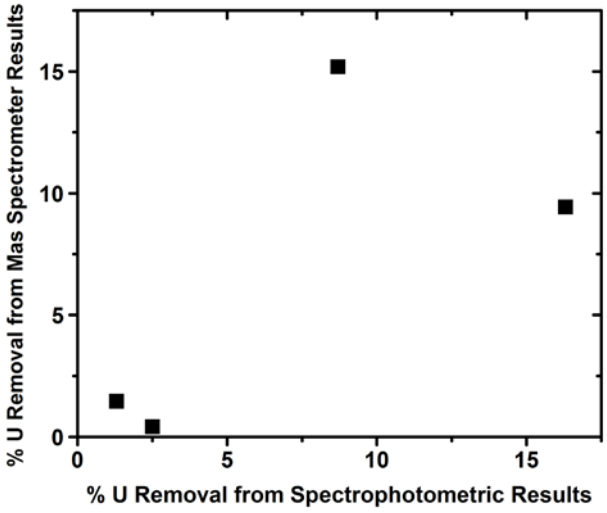

Figure 4.38 – The calculated % U removal by the spectrophotometric method did not correlate linearly with the ICP-MS method exhibited by the lack of linearity (the linear fit has an R^2 value of 0.19) in the distribution of the various samples.

To test if the azo grafted nylon 6 fabrics would be capable of extracting uranium from natural seawater, grafted fabric samples were placed in the seawater flow loop for seven days while being exposed to a flow rate of about 1.4 liters per minute, which is within the same range of flow rates used by Pacific Northwest National Laboratory in their flow-through column exposures[136]. Through the use of laser ablation ICP-MS, these fabrics were tested for the concentration of uranium on their surface.

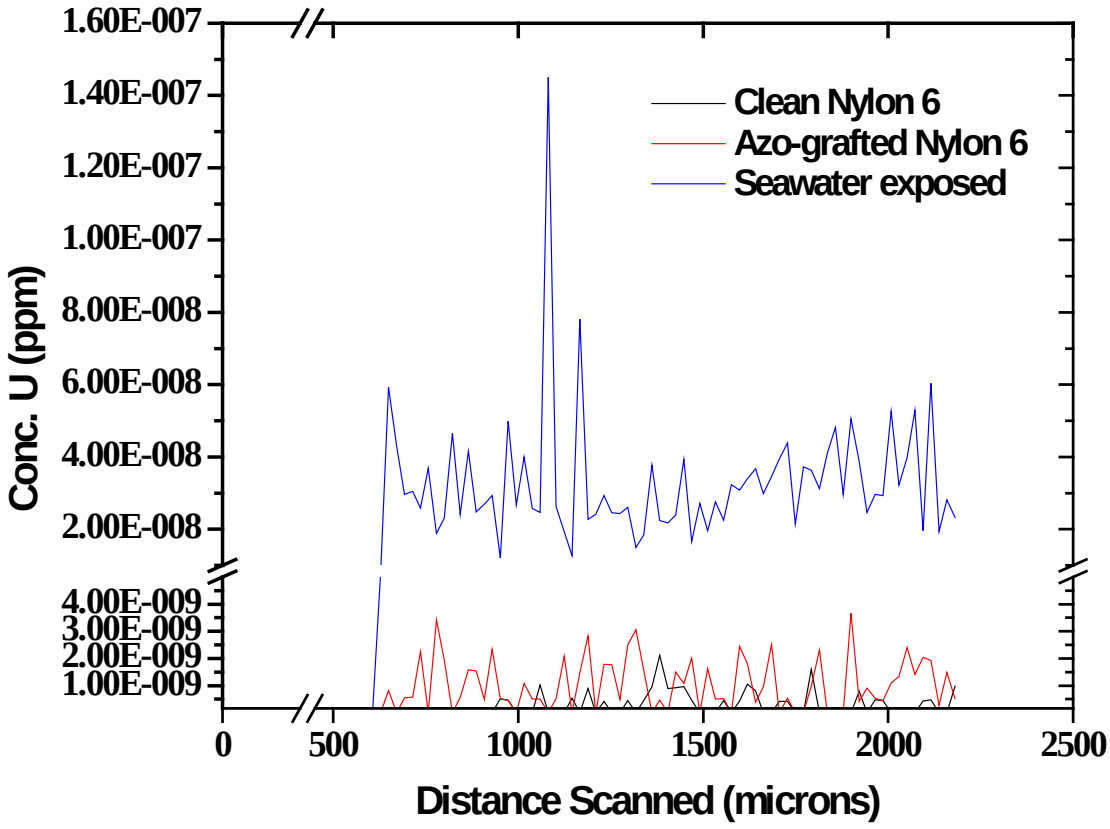

Figure 4.39 – Concentration of uranium on the surface of clean nylon 6, azo-grafted nylon 6, and seawater exposed nylon 6. The exposed nylon 6 sample was placed in the flow loop for one week, which contained natural concentrations of seawater.

The results of line scans of the laser over a distance of about 2 mm on the fabric, as shown in Fig. 4.39, show that the azo fabric was able to remove uranium from the seawater. The concentration of uranium however was extremely small and therefore it is difficult to ascertain if this uranium is merely residual uranium salts present on the surface of the fabric following the exposure that are not actually bound to the azo groups.

By using the laser ablation apparatus to drill a hole into the exposed fabric at two different locations and for different time periods, as shown in figure 4.40, it is clearly shown that the concentration of uranium on the fabric is limited mainly to the surface of the fabric.

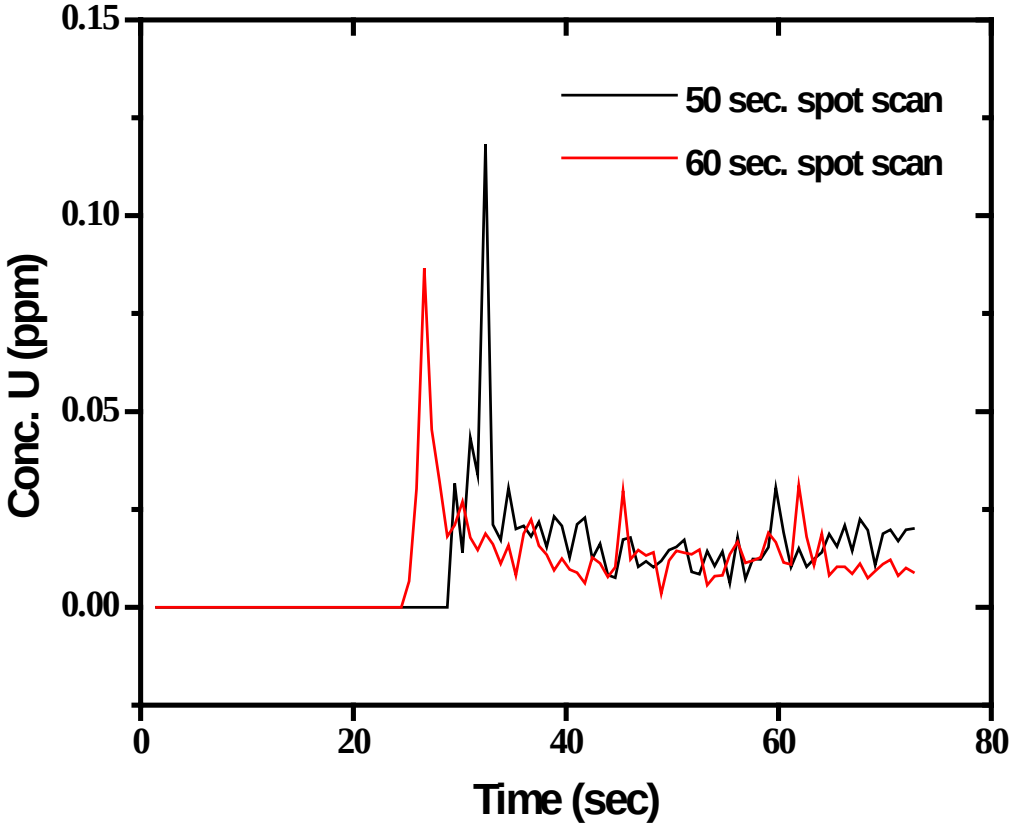

Figure 4.40 – Laser ablation of the seawater exposed, azo grafted fabric in a single location with an 80 µm beam diameter. The 0 ppm concentration shown in the first 20-25 seconds was performed to obtain a background as the laser was not on in this time frame.

4.3 Challenges and Possible Solutions to Improving Extraction

4.3.1 Grafting of ligands and suppression of homopolymerization

To comply with this dissertation's goal of reducing the use of organic solvents, water or a water-surfactant solution may be used instead. Water is a highly desirable solvent for grafting applications where simplicity, low cost and environmental compatibility are required. In such aqueous systems where solubility of the monomer is poor, radiation grafting is often performed on an emulsion or dispersion, which greatly increases the rate of homopolymer formation. If these homopolymers cannot be effectively removed they may result in a significant decrease in adsorptive capacity. Furthermore, incomplete solubility of the monomer in water makes it difficult to obtain a consistent product. The rate of homopolymer formation may be minimized through control over certain grafting variables (such as dose rate, irradiation temperature and the use of stirring/agitation) which may be challenging in high-radiation areas where devices for stirring or heating would be rapidly destroyed. To limit the undesirable effects of homopolymerization during water-based grafting, the use of alternative grafting methods and, if necessary, the use of chemical stabilizers, homopolymerization inhibitors or alternative solvents will be investigated. If stirring and heating during the grafting process are found to be impractical or ineffective, the use of surfactants or phase-merging agents (non-reactive towards hydroxyl radicals, which are important to the grafting process and are produced upon the irradiation of water) will be attempted. In addition, a search for more water-soluble molecules that can be used to adsorb uranium will continue, and molecules likely to combine high affinity for uranyl and high solubility in water will be synthesized as necessary.

Many of the monomers currently used exist at room temperature as a liquid. Utilizing techniques for reducing homopolymerization such as indirect grafting along with using a monomer solution containing no solvent (neat grafting) could also serve to improve the grafting of selected monomers.

Grafting of ligands could also be improved through the use of heavy ion irradiation, which could increase the quantity of radicals on the surface of and in the interior of the polymer substrate.

4.3.2 Low Loading Capacities

All current grafted fabric samples to date have only achieved loading capacities orders of magnitude lower than the amidoxime fabrics currently being developed and tested by other groups. This must be taken within the context of our current uranium extraction testing apparatus. For test volumes of 10 mL containing 1 ppm U, and for a fabric mass of 15 mg, the maximum loading capacity that can be achieved is only about 0.67 mg U/g of fabric, which is much lower than the capabilities of current state of the art fabrics and experimental techniques. Improvement of the loading capacity of fabrics could also be achieved through the incorporation of other monomers onto the fabric substrate. Chemicals containing the phosphate functional group that had been previously screened for their uranium extracting ability could be used as copolymers to possibly improve the uranium loading capacity of fabrics.

4.3.3 Extraction Testing Utilizing Natural Uranium Concentrations

To date, uranium extraction testing of grafted fabrics have been undertaken using spike uranium solutions in order to accommodate the uranium detection limits of our current experimental techniques. These measurements however are indirectly determining the concentration of uranium adsorbed by the fabric and are not providing an accurate determination of the kinetics of uranium adsorption. A new protocol is being developed utilizing the much more sensitive inductively coupled plasma mass spectrometer (ICP-MS). This will permit extraction testing to be run with non-spiked ($\leq$10 μg/L U) seawater. As well, the quantity of uranium adsorbed by the fabric will be able to be measured directly since the ICP-MS will be determining uranium concentration from acid-digested fabric samples. Future testing will be conducted in this medium and supplemented by the spectrophotometric method, since extrapolation from results obtained with higher concentrations of uranyl is complicated by the fact that at such high concentrations the ratio of uranyl levels to those of competing ions is much higher than it is in actual seawater.

5. Conclusions and Future Work

5.1 Conclusions

The dissertation highlights the development of new polymer adsorbents through the use of new, highly efficient ligands such as DAOx, PAR, and B2MP, attached to novel, advanced polymeric substrates with very high surface area, the winged polymers. These efficient adsorbents can also provide support to the separation of uranium from streams contaminated with this element as a result of mining operations or discharge of low-level uranium-containing wastes.

Due to ever-increasing global demand and limited terrestrial resources, uranium that can be economically utilized by conventional mining should be supplemented by a new technique to ensure and promote the future of nuclear power. In recent decades, extensive research has been performed on developing adsorbents that can be used to recover uranium from seawater, where it is present at a low concentration (about 3 ppb) but, given the volume of the oceans, exists in very large amounts[14]. However, existing adsorbents, based mainly on polymers to which amidoxime groups have been attached, still leave much room for improvement. Without significant improvements in adsorbent technology, the extraction of uranium from seawater is likely to remain uneconomical.

However, as described, the objective of this dissertation is the development of a high-performance adsorbent for uranium based on the radiation-induced grafting of novel functional groups onto durable, ultra-high surface area winged fabrics. Based on the promising goals regarding the improved capacity of these novel adsorbents for uranium, an

improved durability and regenerability, as well as the feasibility of a “green chemistry” route to the fabrication of the novel adsorbents, the objective of this work was met.

In the process of developing sorbers of uranium through radiation grafting, a number of different conclusions can also be made regarding the use of radiation to produce grafted materials with similar components and methods as described in this dissertation. For the different materials a grafting procedure was established and, in the case of DAOx and VBC, was optimized for the production of grafted materials by tuning dose, dose rate, irradiation temperature, post-irradiation heat treatment temperature, monomer concentration, and choice of solvent. The selected radiation and experimental conditions developed for each monomer will be explored in section 5.2.

5.2 Contributions to Science

This dissertation establishes the science of and methods for the production of substrates grafted with novel monomers for the extraction of uranium from seawater. The importance of the exploration of new uranium extraction systems utilizing radiation grafting of novel monomers is magnified by the focus of other, similar uranium extraction research on the amidoxime monomer. By expanding the amount of monomer systems known to extract uranium from seawater and by establishing the science behind the fabrication of these systems, future efforts to expand the use of this technology will have a greater number of pathways and resources for doing so.

5.2.1 Fabrication of a Phosphate-based Uranium Extracting Material

Based the natural prevalence of uranium in phosphate deposits, the attachment of phosphate groups and related compounds to a nylon 6 substrate has been accomplished. In particular, the B2MP monomer has been found to readily polymerize while even under low doses of radiation most likely due to the presence of two MAA groups per molecule. As a result, B2MP was capable of grafting to the surface of nylon 6 with the use of an aqueous solvent. While the concentration of B2MP in this solution was quite low, different co-solvents were added to the solution to improve solubility without significantly impacting the mechanism by which radiolytically produced hydroxyl radicals would interact with the substrate and monomer to produce free radicals that would lead to grafting.

5.2.2 Fabrication of an Oxalate-based Uranium Extracting Material

While the functional group had only previously been utilized in one of its salts to strip U(VI) from resins and other media[85], an organic oxalate possessing carbon-carbon double bonds has been grafted to a polymer substrate and used to extract uranium from seawater.

The development of an optimal procedure for the attachment of DAOx to the surface of nylon 6 has found that increased temperatures and high dose rates provide higher degrees of grafting for this monomer. Due to its low solubility in aqueous systems, a neat solution of the monomer has been used to generate suitable degrees of grafting without the generation of significant homopolymer in solution that had been produced in solutions of other neat monomer solutions following irradiation. By irradiating a neat solution of DAOx with nylon 6 under inert atmosphere and at elevated temperatures, significant amounts of grafting can be achieved without significant production of homopolymer on the surface

that might interfere with the extraction of uranium. The use of a neat solution allows for a significant increase in the viability of this technology as it reduces the amount of initial materials needed to fabricate a uranium adsorbent along with reducing materials waste.

5.2.3 Fabrication of an Azo-based Uranium Extracting Material

While azo compounds have been used to chelate to the uranyl ion since the 1950s[114], their use in extracting uranium from seawater had not been explored due to the lack of exploration into attaching the compound to a stable substrate. This dissertation has evaluated and established a successful method for the covalent attachment of various azo compounds to a polymer substrate through a grafted intermediate compound. In particular, the high rate of polymerization while under direct grafting was shown to lead to a significant buildup of homopolymer in the VBC samples. The indirect grafting method was used instead, where it was learned that high doses and dose rates were more suitable than low doses and dose rates. At low does and dose rates, the time required for the irradiation would lend itself more to crosslinking, and thus the population of radicals at the end of the irradiation would not be sufficient to produce highly grafted fabrics while making the fabric more brittle due to the increase in the crosslinking density. The high populations and lifetimes of the radicals generated with these radiation conditions exceeded the time needed to add the monomer solution into the vials such that a significant amount of grafting could occur. Especially important for this grafting procedure was that it led to undetectable amounts of homopolymerization.

5.2.4 Elucidation of Radical Kinetics in Both the Aqueous and Solid State Systems

Through the use of EPR and pulse radiolysis, the behavior of radicals during and following irradiation were elucidated to better evaluate the radiation conditions used for grafting. The determination of the radical lifetimes for winged nylon 6 radicals established the viability of the indirect grafting method for winged nylon 6. Due to the time lapse between the end of the irradiation period and the introduction of monomers into the irradiated fabric sample vials, it was imperative that the population of radicals on the surface of the winged nylon 6 fabric be sufficient to produce reasonable degrees of grafting.

Through the use of pulse radiolysis, the reaction rate constants of major polymerization pathways for both B2MP and DAOx were determined. The establishment of these constants as well as the development of a reaction model to describe the polymerization reaction occurring in these systems allows for a greater understanding of the grafting mechanism and can be used in future work to more accurately model the material system.

5.2.5 Establishment of the Use of Radiolytically Produced Hydroxyl Radicals for Material Synthesis

This dissertation has established the use of hydroxyl radicals in the production of grafted polymer materials. For both B2MP and DAOx, aqueous monomer solutions were used to produce grafted nylon 6 fabrics which could be used for the extraction of uranium from seawater. While the concentration of the monomer in solution severely hampered the maximum DoG obtainable by the system, the synthesis and use of more readily soluble monomers utilizing the phosphate, azo, or oxalate functional groups could lead to improved

DoGs and greater uranium extraction efficiencies while maintaining the principles of green chemistry.

5.3 Future Work

There are a number of different avenues that can be explored to further improve not only the final goal of extracting uranium from seawater, but also grafting the sorber compounds onto a substrate surface.

The primary goal of this dissertation is the development of novel materials for the extraction of uranium from seawater. Future work to improve the fulfillment of this goal will focus on improving the attachment of uranium chelating monomers to the surface of substrate fabrics as well as testing out other similar monomers. By further optimizing the radiation grafting conditions and exploring the use of other hydrophilic co-monomers, the extraction capacities of the fabricated materials can be improved. Through the use of contact angle experiments on fabrics grafted with different hydrophilic monomers, the optimal hydrophilicity can be determined when these values are compared with uranium extraction performance. Also, the indirect grafting method for the various monomer systems can be improved to further increase the DoG of the material without any noticeable increase in homopolymerization. Irradiating fabrics at lower temperatures while reducing the amount of time between the end of the irradiation and the injection of monomer solution into the sample vials could greatly increase the population of free radicals available on the surface of the substrate for grafting.

The development of new compounds based on the initial phosphate, azo, and oxalate compounds and the methods by which they can be attached to a suitable substrate is another

avenue of future scientific exploration. As an example, compounds like the azo analogue compound shown in Fig. 5.1 could further improve uranium extraction due the presence of two available binding sites on the same molecule as well as the increase in the quantity of hydroxyl groups available for uranyl binding in a similar fashion to the glutarimidedioxime complex of the amidoxime functional group.

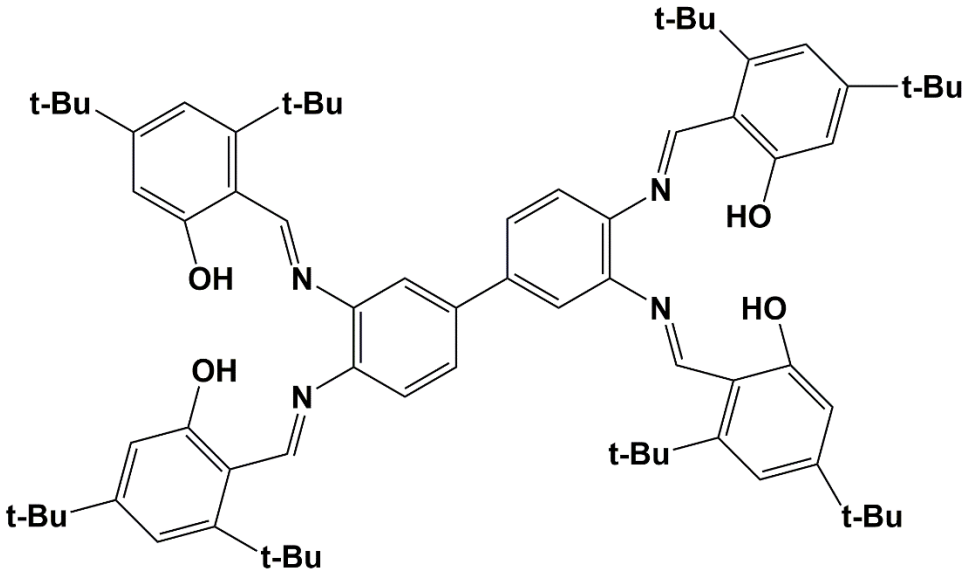

Figure 5.1 - Synthesized compound containing two theoretical uranyl binding centers of similar configuration to those possessed by the azo class of compounds.

Compounds could also be improved to increase their ability to graft to a polymer substrate. The chemical improvements could be carried out through an increase in the amount of carbon-carbon double bonds in their structure or through an improvement in the distance of the carbon-carbon double bonds from the uranium binding center. By improving the amount of monomer grafted to the surface of a substrate and decreasing the amount of homopolymer formed on the surface of the substrate, more sites can be made available for binding to uranium and therefore the ultimate loading capacity of the fabrics

can be improved. The polymer substrate could be altered as well. In particular, the use of high surface area polyethylene could lead to higher degrees of grafting due to the greater reactivity of its carbon-centered radical. Polyethylene has been a substrate of choice for many other groups working on extracting uranium from seawater and so returning to the use of this material while utilizing the uranium extraction monomers from this dissertation could improve the performance of the uranium extraction technology[52,68,121,122].

Numerous computational studies have been performed on the extraction of uranium from seawater using the amidoxime compounds and their derivatives[67,69,70,77]. These studies have provided extremely valuable information to the uranium extraction community in regards to the chemistry of uranyl binding exhibited by these molecules as well as contributing to ultimate feasibility studies of this technology. Specifically, if the binding modes of uranyl to the different compounds explored in this work can be determined computationally with support from experimental data from techniques like X-ray diffraction, then the compounds can be evaluated for their ability to extract uranium without having to be grafted to the substrate.

Studies of the thermodynamics of the uranyl-bound phosphate, azo, and oxalate systems will also provide added support for the requirements of these material to extract uranium from seawater and allow these systems to be compared more directly with alternative systems. Evaluation of the thermodynamics of the system can be performed using a stop-flow machine, microcalorimetry, and potentiometry.

As a supplement to the current work, future experiments can be performed using the techniques described already. Further pulse radiolysis studies can be performed on different monomer systems. Current pulse radiolysis work has only examined aqueous

based systems, however the organic based monomer systems also need to be examined. These studies will be significantly different as the major radical species will not be generated through the hydroxyl radical from the irradiation of water, but will be produced in the monomer (due to its much higher concentration) and in the organic solvent (in many cases DMSO).

Pulse radiolysis studies of radical interactions with monomer solution will be supplemented by further EPR studies of nylon 6 and other substrates such as polyethylene and polypropylene especially as they relate to indirect grafting of monomer. The EPR spectra obtained from these studies will be able to provide clues as to the distribution of binding cites within the molecular backbone of these molecules for the uranium extracting monomer. The decay rate of the radicals within the substrates will provide information regarding the optimal irradiation parameters and the experimental parameters, specifically as they relate to the amount of time allowed before the monomer solution would need to be introduced into the irradiated system. If the radicals are shown to decay at a significantly faster rate than what is allowed for while transferring the irradiated vials to an inert atmosphere working space, the temperature under which samples are irradiated will have to be lowered to decrease the rate.

List of References

(1) *Annual Energy Outlook 2016 with Projections to 2040*; DOE/EIA-0383(2016); U.S. Energy Information Administration: Washington, DC, 2016; p 256.

(2) *Uranium 2014: Resources, Production and Demand*; 7209; OECD Nuclear Energy Agency, 2014; pp 1–508.

(3) Uranium Supplies: Supply of Uranium - World Nuclear Association http://www.world-nuclear.org/information-library/nuclear-fuel-cycle/uranium-resources/supply-of-uranium.aspx (accessed Oct 18, 2016).

(4) Mudd, G. M. Critical Review of Acid in Situ Leach Uranium Mining: 1. USA and Australia. *Environ. Geol. 41* (3–4), 390–403.

(5) Abdelouas, A. Uranium Mill Tailings: Geochemistry, Mineralogy, and Environmental Impact. *Elements* **2006**, *2* (6), 335–341.

(6) Fernandes, H. M.; Franklin, M. R.; Veiga, L. H. S.; Freitas, P.; Gomiero, L. A. Management of Uranium Mill Tailing: Geochemical Processes and Radiological Risk Assessment. *J. Environ. Radioact.* **1996**, *30* (1), 69–95.

(7) Prakash, O. *Cultural History of India*; New Age International, 2005.

(8) Periodic Table of Elements in the Ocean http://www.mbari.org/science/upper-ocean-systems/chemical-sensor-group/periodic-table-of-elements-in-the-ocean/ (accessed Oct 19, 2017).

(9) CHARETTE, M. A.; SMITH, W. H. F. The Volume of Earth's Ocean. *Oceanography* **2010**, *23* (2), 112–114.

(10) Shahmansouri, A.; Min, J.; Jin, L.; Bellona, C. Feasibility of Extracting Valuable Minerals from Desalination Concentrate: A Comprehensive Literature Review. *J. Clean. Prod.* **2015**, *100*, 4–16.

(11) Wang, L.; Meng, C.; Ma, W. Preparation of Lithium Ion-Sieve and Utilizing in Recovery of Lithium from Seawater. *Front. Chem. Eng. China* **2009**, *3* (1), 65–67.

(12) Ooi, K.; Miyai, Y.; Katoh, S. Recovery of Lithium from Seawater by Manganese Oxide Adsorbent. *Sep. Sci. Technol.* **1986**, *21* (8), 755–766.

(13) Umeno, A.; Miyai, Y.; Takagi, N.; Chitrakar, R.; Sakane, K.; Ooi, K. Preparation and Adsorptive Properties of Membrane-Type Adsorbents for Lithium Recovery from Seawater. *Ind. Eng. Chem. Res.* **2002**, *41* (17), 4281–4287.

(14) Bardi, U. Extracting Minerals from Seawater: An Energy Analysis. *Sustainability* **2010**, *2* (4), 980–992.

(15) Sodaye, H.; Nisan, S.; Poletiko, C.; Prabhakar, S.; Tewari, P. K. Extraction of Uranium from the Concentrated Brine Rejected by Integrated Nuclear Desalination Plants. *Desalination* **2009**, *235* (1–3), 9–32.

(16) Rao, L. Recent International R&D Activities in the Extraction of Uranium from Seawater. *Lawrence Berkeley Natl. Lab.* **2011**.

(17) Park, J.; Gill, G. A.; Strivens, J. E.; Kuo, L.-J.; Jeters, R. T.; Avila, A.; Wood, J. R.; Schlafer, N. J.; Janke, C. J.; Miller, E. A.; et al. Effect of Biofouling on the Performance of Amidoxime-Based Polymeric Uranium Adsorbents. *Ind. Eng. Chem. Res.* **2016**, *55* (15), 4328–4338.

(18) Schenk, H. J.; Astheimer, L.; Witte, E. G.; Schwochau, K. Development of Sorbers for the Recovery of Uranium from Seawater. 1. Assessment of Key Parameters and Screening Studies of Sorber Materials. *Sep. Sci. Technol.* **1982**, *17* (11), 1293–1308.

(19) Tamada, M. Current Status of Technology for Collection of Uranium from Seawater. *Jpn. At. Energy Agency* **2009**.

(20) Suzuki, T.; Saito, K.; Sugo, T.; Ogura, H.; Oguma, K. Fractional Elution and Determination of Uranium and Vanadium Adsorbed on Amidoxime Fiber from Seawater. *Anal. Sci.* **2000**, *16* (4), 429–432.

(21) Wu, W.; Priest, C.; Zhou, J.; Peng, C.; Liu, H.; Jiang, D. Solvation of the $Ca_2UO_2(CO_3)_3$ Complex in Seawater from Classical Molecular Dynamics. *J. Phys. Chem. B* **2016**, *120* (29), 7227–7233.

(22) Endrizzi, F.; Leggett, C. J.; Rao, L. Scientific Basis for Efficient Extraction of Uranium from Seawater. I: Understanding the Chemical Speciation of Uranium under Seawater Conditions. *Ind. Eng. Chem. Res.* **2016**, *55* (15), 4249–4256.

(23) Dunk, R. M.; Mills, R. A.; Jenkins, W. J. A Reevaluation of the Oceanic Uranium Budget for the Holocene. *Chem. Geol.* **2002**, *190* (1), 45–67.

(24) Andersen, M. B.; Vance, D.; Morford, J. L.; Bura-Nakić, E.; Breitenbach, S. F. M.; Och, L. Closing in on the Marine 238U/235U Budget. *Chem. Geol.* **2016**, *420*, 11–22.

(25) Conca, J. Uranium Seawater Extraction Makes Nuclear Power Completely Renewable. *Forbes*. July 1, 2016.

(26) Clough, R. L. High-Energy Radiation and Polymers: A Review of Commercial Processes and Emerging Applications. *Nucl. Instrum. Methods Phys. Res. Sect. B Beam Interact. Mater. At.* **2001**, *185* (1), 8–33.

(27) Spinks, J. W. T.; Woods, R. J. *An Introduction to Radiation Chemistry*; Wiley: New York, 1964.

(28) Hawker, C. J.; Bosman, A. W.; Harth, E. New Polymer Synthesis by Nitroxide Mediated Living Radical Polymerizations. *Chem. Rev.* **2001**, *101* (12), 3661–3688.

(29) Wilson, J. E. *Radiation Chemistry of Monomers, Polymers, and Plastics*; M. Dekker: New York, 1974.

(30) El-Sawy, N. M.; Hegazy, E.-S. A.; Rabie, A. M.; Hamed, A.; Miligy, G. A. Radiation-Initiated Graft Copolymerization of Acrylic Acid and Vinyl Acetate onto LDPE Films in Two Individual Steps. *Polym. Int.* **1993**, *32* (2), 131–135.

(31) Kabanov, V. Y. Radiation Induced Graft Polymerization in the USSR. *Int. J. Radiat. Appl. Instrum. Part C Radiat. Phys. Chem.* **1989**, *33* (1), 51–60.

(32) Alkan Gürsel, S.; Gubler, L.; Gupta, B.; Scherer, G. G. Radiation Grafted Membranes. In *Fuel Cells I*; Scherer, G. G., Ed.; Springer Berlin Heidelberg: Berlin, Heidelberg, 2008; pp 157–217.

(33) Smith, S. D.; Alexandratos, S. D. ION-SELECTIVE POLYMER-SUPPORTED REAGENTS. *Solvent Extr. Ion Exch.* **2000**, *18* (4), 779–807.

(34) Sahakian, G. S.; Khachatryan, H. F. Pulsar Gamma-Ray Emission. *Astrophysics* **1999**, *42* (4), 477–483.

(35) Fishman, G. J.; Bhat, P. N.; Mallozzi, R.; Horack, J. M.; Koshut, T.; Kouveliotou, C.; Pendleton, G. N.; Meegan, C. A.; Wilson, R. B.; Paciesas, W. S. Discovery of Intense Gamma-Ray Flashes of Atmospheric Origin. *Sci.-AAAS-Wkly. Pap. Ed.-Guide Sci. Inf.* **1994**, *264* (5163), 1313–1316.

(36) Dwyer, J. R.; Smith, D. M. Deadly Rays from Clouds. *Sci. Am.* **2012**, *307* (2), 54–59.

(37) Farhataziz; Rodgers, M. A. J. *Radiation Chemistry: Principles and Applications*; VCH Publishers: New York, N.Y., 1987.

(38) Appleby, A.; Schwarz, H. A. Radical and Molecular Yields in Water Irradiated by .gamma.-Rays and Heavy Ions. *J. Phys. Chem.* **1969**, *73* (6), 1937–1941.

(39) Choi, S. U.; Lichtin, N. N. The Radiolysis of Methanol and Methanolic Solutions. III. The Effect of Oxygen on the Radiolysis of Liquid Methanol by 60Co γ-Rays and by 10B (N, α) 7Li Recoils. *J. Am. Chem. Soc.* **1964**, *86* (19), 3948–3953.

(40) Seki, H.; Imamura, M. Isotopic Compositions of the Hydrogen Produced from Liquid Methanol-d1 by Irradiation of 60Co γ Rays and of the 10B(n, α)7Li Recoil Particles. *J. Chem. Phys.* **1968**, *48* (4), 1866–1867.

(41) Baxendale, J. H.; Busi, F. *The Study of Fast Processes and Transient Species by Electron Pulse Radiolysis: Proceedings of the NATO Advanced Study Institute Held Ay Capri, Italy, 7–18 September, 1981*; Springer Science & Business Media, 1981.

(42) Kumar, M.; Neta, P. Radiolytic Reductions and Oxidations in Dimethyl Sulfoxide Solutions: Solvent Effects on Reactivity of Halogen Atom Complexes. *J. Phys. Chem.* **1992**, *96* (8), 3350–3354.

(43) Bensasson, R.; Land, E. J. Transient Species in the Pulse Radiolysis of Dimethyl Sulphoxide. *Chem. Phys. Lett.* **1972**, *15* (2), 195–198.

(44) Stannett, V. T. Radiation Grafting — State-of-the-Art. *Int. J. Radiat. Appl. Instrum. Part C Radiat. Phys. Chem.* **1990**, *35* (1), 82–87.

(45) Bhattacharya, A.; Misra, B. N. Grafting: A Versatile Means to Modify Polymers: Techniques, Factors and Applications. *Prog. Polym. Sci.* **2004**, *29* (8), 767–814.

(46) Davies, R. V.; Kennedy, J.; McILROY, R. W.; Spence, R.; Hill, K. M. Extraction of Uranium from Sea Water. *Nature* **1964**, *203* (4950), 1110–1115.

(47) Tularam, G. A.; Ilahee, M. Environmental Concerns of Desalinating Seawater Using Reverse Osmosis. *J. Environ. Monit.* **2007**, *9* (8), 805.

(48) KANNO, M. Present Status of Study on Extraction of Uranium from Sea Water. *J. Nucl. Sci. Technol.* **1984**, *21* (1), 1–9.

(49) van Reis, R.; Zydney, A. Bioprocess Membrane Technology. *J. Membr. Sci.* **2007**, *297* (1–2), 16–50.

(50) Tamada, M.; Seko, N.; Yoshii, F. Application of Radiation-Graft Material for Metal Adsorbent and Crosslinked Natural Polymer for Healthcare Product. *Radiat. Phys. Chem.* **2004**, *71* (1–2), 223–227.

(51) Seko, N.; Katakai, A.; Hasegawa, S.; Tamada, M.; Kasai, N.; Takeda, H.; Sugo, T.; Saito, K. Aquaculture of Uranium in Seawater by a Fabric-Adsorbent Submerged System. *Nucl. Technol.* **2003**, *144* (2), 274–278.

(52) Oyola, Y.; Janke, C. J.; Dai, S. Synthesis, Development, and Testing of High-Surface-Area Polymer-Based Adsorbents for the Selective Recovery of Uranium from Seawater. *Ind. Eng. Chem. Res.* **2016**, *55* (15), 4149–4160.

(53) Nobukawa, H.; Tamehiro, M. DEVELOPMENT OF FLOATING TYPE-EXTRACTION SYSTEM OF URANIUM FROM SEA WATER USING SEA WATER CURRENT AND WAVE POWER. **1989**.

(54) Nobukawa, H.; Kitamura, M.; Kobayashi, M.; Nakagawa, H.; Takagi, N.; Tamehiro, M. Development of Floating Type-Extraction System of Uranium from Seawater Using Sea Current and Wave Power (Rep. 3). *J. Soc. Nav. Archit. Jpn.* **1992**, *1992* (172), 519–528.

(55) Egawa, H.; Kabay, N.; Shuto, T.; Jyo, A. Recovery of Uranium from Seawater. 13. Long-Term Stability Tests for High-Performance Chelating Resins Containing Amidoxime Groups and Evaluation of Elution Process. *Ind. Eng. Chem. Res.* **1993**, *32* (3), 540–547.

(56) *2015 Uranium Marketing Annual Report*; U.S. Energy Information Administration: Washington, DC, 2016.

(57) Seko, N.; Katakai, A.; Tamada, M.; Sugo, T.; Yoshii, F. Fine Fibrous Amidoxime Adsorbent Synthesized by Grafting and Uranium Adsorption–Elution Cyclic Test with Seawater. *Sep. Sci. Technol.* **2004**, *39* (16), 3753–3767.

(58) Pan, H.-B.; Wai, C. M.; Kuo, L.-J.; Gill, G.; Tian, G.; Rao, L.; Das, S.; Mayes, R. T.; Janke, C. J. Bicarbonate Elution of Uranium from Amidoxime-Based Polymer Adsorbents for Sequestering Uranium from Seawater. *Chem. Sel.* **2017**, *2* (13), 3769–3774.

(59) Yue, Y.; Zhang, C.; Tang, Q.; Mayes, R. T.; Liao, W.-P.; Liao, C.; Tsouris, C.; Stankovich, J. J.; Chen, J.; Hensley, D. K.; et al. A Poly(acrylonitrile)-Functionalized Porous Aromatic Framework Synthesized by Atom-Transfer

Radical Polymerization for the Extraction of Uranium from Seawater. *Ind. Eng. Chem. Res.* **2016**, *55* (15), 4125–4129.

(60) Pan, H.-B.; Kuo, L.-J.; Wai, C. M.; Miyamoto, N.; Joshi, R.; Wood, J. R.; Strivens, J. E.; Janke, C. J.; Oyola, Y.; Das, S.; et al. Elution of Uranium and Transition Metals from Amidoxime-Based Polymer Adsorbents for Sequestering Uranium from Seawater. *Ind. Eng. Chem. Res.* **2016**, *55* (15), 4313–4320.

(61) Oyola, Y.; Dai, S. High Surface-Area Amidoxime-Based Polymer Fibers Co-Grafted with Various Acid Monomers Yielding Increased Adsorption Capacity for the Extraction of Uranium from Seawater. *Dalton Trans* **2016**, *45* (21), 8824–8834.

(62) Ladshaw, A. P.; Das, S.; Liao, W.-P.; Yiacoumi, S.; Janke, C. J.; Mayes, R. T.; Dai, S.; Tsouris, C. Experiments and Modeling of Uranium Uptake by Amidoxime-Based Adsorbent in the Presence of Other Ions in Simulated Seawater. *Ind. Eng. Chem. Res.* **2016**, *55* (15), 4241–4248.

(63) Brown, S.; Yue, Y.; Kuo, L.-J.; Mehio, N.; Li, M.; Gill, G.; Tsouris, C.; Mayes, R. T.; Saito, T.; Dai, S. Uranium Adsorbent Fibers Prepared by Atom-Transfer Radical Polymerization (ATRP) from Poly(vinyl Chloride)- *Co* -Chlorinated Poly(vinyl Chloride) (PVC- *Co* -CPVC) Fiber. *Ind. Eng. Chem. Res.* **2016**, *55* (15), 4139–4148.

(64) Brown, S.; Chatterjee, S.; Li, M.; Yue, Y.; Tsouris, C.; Janke, C. J.; Saito, T.; Dai, S. Uranium Adsorbent Fibers Prepared by Atom-Transfer Radical Polymerization from Chlorinated Polypropylene and Polyethylene Trunk Fibers. *Ind. Eng. Chem. Res.* **2016**, *55* (15), 4130–4138.

(65) Das, S.; Oyola, Y.; Mayes, R. T.; Janke, C. J.; Kuo, L.-J.; Gill, G.; Wood, J. R.; Dai, S. Extracting Uranium from Seawater: Promising AF Series Adsorbents. *Ind. Eng. Chem. Res.* **2016**, *55* (15), 4110–4117.

(66) Das, S.; Oyola, Y.; Mayes, R. T.; Janke, C. J.; Kuo, L.-J.; Gill, G.; Wood, J. R.; Dai, S. Extracting Uranium from Seawater: Promising AI Series Adsorbents. *Ind. Eng. Chem. Res.* **2016**, *55* (15), 4103–4109.

(67) Endrizzi, F.; Melchior, A.; Tolazzi, M.; Rao, L. Complexation of uranium(VI) with Glutarimidoxioxime: Thermodynamic and Computational Studies. *Dalton Trans* **2015**, *44* (31), 13835–13844.

(68) Das, S.; Brown, S.; Mayes, R. T.; Janke, C. J.; Tsouris, C.; Kuo, L.-J.; Gill, G.; Dai, S. Novel Poly(imide Dioxime) Sorbents: Development and Testing for Enhanced Extraction of Uranium from Natural Seawater. *Chem. Eng. J.* **2016**, *298*, 125–135.

(69) Ivanov, A. S.; Bryantsev, V. S. Assessing Ligand Selectivity for Uranium over Vanadium Ions to Aid in the Discovery of Superior Adsorbents for Extraction of UO_2^{2+} from Seawater. *Dalton Trans* **2016**, *45* (26), 10744–10751.

(70) Abney, C. W.; Mayes, R. T.; Piechowicz, M.; Lin, Z.; Bryantsev, V. S.; Veith, G. M.; Dai, S.; Lin, W. XAFS Investigation of Polyamidoxime-Bound Uranyl Contests the Paradigm from Small Molecule Studies. *Energy Environ. Sci.* **2016**, *9* (2), 448–453.

(71) Endrizzi, F.; Rao, L. Chemical Speciation of Uranium(VI) in Marine Environments: Complexation of Calcium and Magnesium Ions with

[(UO2)(CO3)3]4− and the Effect on the Extraction of Uranium from Seawater. *Chem. – Eur. J.* **2014**, *20* (44), 14499–14506.

(72) Kuo, L.-J.; Gill, G. A.; Strivens, J. E.; Wood, J. R.; Schlafer, N. J.; Wai, C. M.; Pan, H. B. *Investigations into the Reusability of Amidoxime-Based Polymeric Uranium Adsorbents*; PNNL--25874; Pacific Northwest National Lab. (PNNL), Richland, WA (United States), 2016.

(73) Rahman, M. L.; Sarkar, S. M.; Yusoff, M. M.; Abdullah, M. H. Efficient Removal of Transition Metal Ions Using Poly(amidoxime) Ligand from Polymer Grafted Kenaf Cellulose. *RSC Adv.* **2015**, *6* (1), 745–757.

(74) Wang, H.; Gurau, G.; Rogers, R. D. Ionic Liquid Processing of Cellulose. *Chem. Soc. Rev.* **2012**, *41* (4), 1519.

(75) Qin, Y.; Lu, X.; Sun, N.; Rogers, R. D. Dissolution or Extraction of Crustacean Shells Using Ionic Liquids to Obtain High Molecular Weight Purified Chitin and Direct Production of Chitin Films and Fibers. *Green Chem.* **2010**, *12* (6), 968.

(76) Shen, X.; Shamshina, J. L.; Berton, P.; Gurau, G.; Rogers, R. D. Hydrogels Based on Cellulose and Chitin: Fabrication, Properties, and Applications. *Green Chem* **2016**, *18* (1), 53–75.

(77) Piechowicz, M.; Abney, C. W.; Zhou, X.; Thacker, N. C.; Li, Z.; Lin, W. Design, Synthesis, and Characterization of a Bifunctional Chelator with Ultrahigh Capacity for Uranium Uptake from Seawater Simulant. *Ind. Eng. Chem. Res.* **2016**, *55* (15), 4170–4178.

(78) Parker, B. F.; Knight, A. S.; Vukovic, S.; Arnold, J.; Francis, M. B. A Peptoid-Based Combinatorial and Computational Approach to Developing Ligands for

Uranyl Sequestration from Seawater. *Ind. Eng. Chem. Res.* **2016**, *55* (15), 4187–4194.

(79) Dietz, T. C.; Tomaszewski, C. E.; Tsinas, Z.; Poster, D.; Barkatt, A.; Adel-Hadadi, M.; Bateman, F. B.; Cumberland, L. T.; Schneider, E.; Gaskell, K.; et al. Uranium Removal from Seawater by Means of Polyamide 6 Fibers Directly Grafted with Diallyl Oxalate through a Single-Step, Solvent-Free Irradiation Process. *Ind. Eng. Chem. Res.* **2016**, *55* (15), 4179–4186.

(80) Sugasaka, K.; Katoh, S.; Takai, N.; Takahashi, H.; Umezawa, Y. Recovery of Uranium from Seawater. *Sep. Sci. Technol.* **1981**, *16* (9), 971–985.

(81) Saito, T.; Brown, S.; Chatterjee, S.; Kim, J.; Tsouris, C.; Mayes, R. T.; Kuo, L.-J.; Gill, G.; Oyola, Y.; Janke, C. J.; et al. Uranium Recovery from Seawater: Development of Fiber Adsorbents Prepared via Atom-Transfer Radical Polymerization. *J. Mater. Chem. A* **2014**, *2* (35), 14674–14681.

(82) Alexandratos, S. D.; Zhu, X.; Florent, M.; Sellin, R. Polymer-Supported Bifunctional Amidoximes for the Sorption of Uranium from Seawater. *Ind. Eng. Chem. Res.* **2016**, *55* (15), 4208–4216.

(83) Basuki, F.; Seko, N.; Tamada, M.; Sugo, T.; Kume, T. Direct Synthesis of Adsorbent Having Phosphoric Acid with Radiation Induced Graftpolymerization. *J. Ion Exch.* **2003**, *14* (Supplement), 209–212.

(84) Lanham, W. B.; Runion, T. C. *Purex Process for Plutonium and Uranium Recovery*; ORNL-479(Del.); Oak Ridge National Lab., Tenn., 1949.

(85) Dietz, M. L.; Horwitz, E. P.; Sajdak, L. R.; Chiarizia, R. An Improved Extraction Chromatographic Resin for the Separation of Uranium from Acidic Nitrate Media. *Talanta* **2001**, *54* (6), 1173–1184.

(86) Unsworth, E. R.; Cook, J. M.; Hill, S. J. Determination of Uranium and Thorium in Natural Waters with a High Matrix Concentration Using Solid-Phase Extraction Inductively Coupled Plasma Mass Spectrometry. *Anal. Chim. Acta* **2001**, *442* (1), 141–146.

(87) Benkhedda, K.; Epov, V. N.; Evans, R. D. Flow-Injection Technique for Determination of Uranium and Thorium Isotopes in Urine by Inductively Coupled Plasma Mass Spectrometry. *Anal. Bioanal. Chem.* **2005**, *381* (8), 1596–1603.

(88) Johnson, D. A.; Florence, T. M. Spectrophotometric Determination of Uranium(vi) with 2-(5-Bromo-2-Pyridylazo)-5-Diethylaminophenol. *Anal. Chim. Acta* **1971**, *53* (1), 73–79.

(89) Savvin, S. B. Analytical Use of Arsenazo III. *Talanta* **1961**, *8* (9), 673–685.

(90) Savvin, S. B. Analytical Applications of Arsenazo III—III. *Talanta* **1964**, *11* (1), 7–19.

(91) Kuo, L.-J.; Janke, C. J.; Wood, J. R.; Strivens, J. E.; Das, S.; Oyola, Y.; Mayes, R. T.; Gill, G. A. Characterization and Testing of Amidoxime-Based Adsorbent Materials to Extract Uranium from Natural Seawater. *Ind. Eng. Chem. Res.* **2016**, *55* (15), 4285–4293.

(92) Flicker Byers, M.; Schneider, E. Optimization of the Passive Recovery of Uranium from Seawater. *Ind. Eng. Chem. Res.* **2016**, *55* (15), 4351–4361.

(93) Mehio, N.; Ivanov, A. S.; Ladshaw, A. P.; Dai, S.; Bryantsev, V. S. Theoretical Study of Oxovanadium(IV) Complexation with Formamidoximate: Implications for the Design of Uranyl-Selective Adsorbents. *Ind. Eng. Chem. Res.* **2016**, *55* (15), 4231–4240.

(94) MacCready, W. L.; Wethington Jr, J. A.; Hurst, F. J. Uranium Extraction from Florida Phosphates. *Nucl. Technol.* **1981**, *53* (3), 344–353.

(95) Sandino, A.; Bruno, J. The Solubility of (UO2) 3 (PO4) 2· 4H2O (S) and the Formation of U (VI) Phosphate Complexes: Their Influence in Uranium Speciation in Natural Waters. *Geochim. Cosmochim. Acta* **1992**, *56* (12), 4135–4145.

(96) Byrne, R. H.; Lee, J. H.; Bingler, L. S. Rare Earth Element Complexation by PO43− Ions in Aqueous Solution. *Geochim. Cosmochim. Acta* **1991**, *55* (10), 2729–2735.

(97) Havel, J. Spectrophotometric Study of Complex Formation of Uranyl with Oxalic Acid. *Collect. Czechoslov. Chem. Commun.* **1969**, *34* (11), 3248-.

(98) Erten, H.; Mohammed, A.; Choppin, G. Variation of Stability-Constants of Thorium and Uranium Oxalate Complexes with Ionic-Strength. *Radiochim. Acta* **1994**, *66–7*, 123–128.

(99) Grinberg, A.A.; Ptitsyn, B.V.; Tekster, E.H. Physico-Chemical Properties of Aqueous Solutions of Complex Uranyl Oxalates. *Trans. Radium Inst. Acad. Sci. USSR* **1956**, *7*, 74–86.

(100) Moskvin, A.I.; Zakharova, F.A. Study of Formation of Uranyl Complex Ions in Oxalate Solutions by the Solubility Method. *Zhurnal Neorganicheskoi Khimii* **1959**, *4*, 2151–2160.

(101) Havel, J.; Soto-Guerrero, J.; Lubal, P. Spectrophotometric Study of Uranyl–oxalate Complexation in Solution. *Polyhedron* **2002**, *21* (14–15), 1411–1420.

(102) Petit, J.; Geertsen, V.; Beaucaire, C.; Stambouli, M. Metal Complexes Stability Constant Determination by Hyphenation of Capillary Electrophoresis with Inductively Coupled Plasma Mass Spectrometry: The Case of 1:1 Metal-to-Ligand Stoichiometry. *J. Chromatogr. A* **2009**, *1216* (18), 4113–4120.

(103) Crea, F.; De Robertis, A.; De Stefano, C.; Sammartano, S. Dioxouranium(VI)–carboxylate Complexes: A Calorimetric and Potentiometric Investigation of Interaction with Oxalate at Infinite Dilution and in NaCl Aqueous Solution at I = 1.0 Mol L−1 and T = 25 °C. *Talanta* **2007**, *71* (2), 948–963.

(104) Jayadevan, N. C.; Chackraburtty. Crystal and Molecular-Structure of Uranyl Oxalate Trihydrate. *Acta Crystallogr. Sect. B-Struct. Sci.* **1972**, *B 28* (NOV15), 3178–3182.

(105) Mikhailov, Y. N.; Gorbunova, Y. E.; Shishkina, O. V.; Serezhkina, L. B.; Serezhkin, V. N. X-Ray Diffraction Study of the Crystals of (NH(4))(6)[(UO(2))(2)(C(2)O(4))(SeO(4))(4)] Center Dot 2H(2)O and Refinement of the Crystal Structure of [UO(2)C(2)O(4) Center Dot H(2)O] Center Dot 2H(2)O. *Russ. J. Inorg. Chem.* **1999**, *44* (9), 1370–1375.

(106) Artem'eva, M. Y.; Serezhkin, V. N.; Smirnov, O. P.; Plakhtii, V. P. Neutron Diffraction Study of Uranyl Oxalate [UO2(C2O4)(D2O)] · 2D2O. *Russ. J. Inorg. Chem.* **2006**, *51* (8), 1307–1310.

(107) Giesting, P. A.; Porter, N. J.; Burns, P. C. Uranyl Oxalate Hydrates: Structures and IR Spectra. *Z. Für Krist.* **2006**, *221* (4/2006), 252–259.

(108) Bühl, M.; Grenthe, I. Binding Modes of Oxalate in UO2(oxalate) in Aqueous Solution Studied with First-Principles Molecular Dynamics Simulations. Implications for the Chelate Effect. *Dalton Trans.* **2011**, *40* (42), 11192–11199.

(109) Pollard, F. H.; Hanson, P.; Geary, W. J. 4-(2-Pyridylazo)-Resorcinol as a Possible Analytical Reagent for the Colorimetric Estimation of Cobalt, Lead, and Uranium ,. *Anal. Chim. Acta* **1959**, *20*, 26–31.

(110) Florence, T. M.; Farrar, Y. Spectrophotometric Determination of Uranium with 4-(2-Pyridylazo)resorcinol. *Anal. Chem.* **1963**, *35* (11), 1613–1616.

(111) Neas, R. E.; Guyon, J. C. Indirect Spectrophotometric Determination of Oxalate Using Uranium and 4-(2-Pyridylazo) Resorcinol. *Anal. Chem.* **1972**, *44* (4), 799–805.

(112) Hovind, H. avard R. Thiazolylazo Dyes and Their Applications in Analytical Chemistry. A Review. *Analyst* **1975**, *100* (1196), 769–796.

(113) Rawat, N.; Mohapatra, P. K.; Manchanda, V. K. Kinetics of Complexation of Uranium with 2-(5-Bromo-2-Pyridylazo)-5-(Diethylamino) Phenol (Br-PADAP) in a 1:1 Water-Ethanol Medium. *J. Solut. Chem.* **2006**, *35* (6), 803–814.

(114) Fritz, J. S.; Richard, M. J.; Lane, W. J. Spectrophotometric Determination of Rare Earths. *Anal. Chem.* **1958**, *30* (11), 1776–1779.

(115) Basargin, N. N.; Ivanov, V. M.; Kuznetsov, Vv.; Mikhailova, A. V. 40 Years since the Discovery of the Arsenazo III Reagent. *J. Anal. Chem.* **2000**, *55* (3), 204–210.

(116) Savvin, S. B. Analytical Applications of Arsenazo III—II. *Talanta* **1964**, *11* (1), 1–6.

(117) Sommer, L.; Ivanov, V. M. Spectrophotometric Study of the Reaction of the Uranyl Ion with 4-(2-Thiazolylazo) Resorcinol. *Talanta* **1967**, *14* (2), 171–185.

(118) Iwamoto, T. Acid-Base Property and Metal Chelate Formation of 4-(2-Pyridylazo)-Resorcinol. *Bull. Chem. Soc. Jpn.* **1961**, *34* (5), 605–610.

(119) Ekstrom, A.; Johnson, D. A. The Kinetics and Mechanism of the Reaction of U(VI) with 4-(2-Pyridylazo) Resorcinol (PAR). *J. Inorg. Nucl. Chem.* **1974**, *36* (11), 2549–2556.

(120) Kawai, T.; Saito, K.; Sugita, K.; Kawakami, T.; Kanno, J.; Katakai, A.; Seko, N.; Sugo, T. Preparation of Hydrophilic Amidoxime Fibers by Cografting Acrylonitrile and Methacrylic Acid from an Optimized Monomer Composition. *Radiat. Phys. Chem.* **2000**, *59* (4), 405–411.

(121) Kawai, T.; Saito, K.; Sugita, K.; Katakai, A.; Seko, N.; Sugo, T.; Kanno, J.; Kawakami, T. Comparison of Amidoxime Adsorbents Prepared by Cografting Methacrylic Acid and 2-Hydroxyethyl Methacrylate with Acrylonitrile onto Polyethylene. *Ind. Eng. Chem. Res.* **2000**, *39* (8), 2910–2915.

(122) Hu, J.; Ma, H.; Xing, Z.; Liu, X.; Xu, L.; Li, R.; Lin, C.; Wang, M.; Li, J.; Wu, G. Preparation of Amidoximated Ultrahigh Molecular Weight Polyethylene Fiber by Radiation Grafting and Uranium Adsorption Test. *Ind. Eng. Chem. Res.* **2015**.

(123) Chemical Compatibility http://www.spectrumlabs.com/dialysis/Compatibility.html (accessed May 13, 2016).

(124) Chappas, W.; Pourdeyhimi, B. United States Patent: 8410006 - Composite Filter Media with High Surface Area Fibers. 8410006, April 2, 2013.

(125) image002.jpg (197×305) http://old.ilhamalqaradawi.com/gamma_cell_files/image002.jpg (accessed Sep 1, 2017).

(126) Instruction Manual Gammacell 220 Cobalt 60 Irradiation Unit. Atomic Energy of Canada Limited July 1968.

(127) Corey, P. L. Medical-Industrial Radiation Facility https://www.nist.gov/laboratories/tools-instruments/medical-industrial-radiation-facility (accessed Aug 29, 2017).

(128) Overview Alanine Dosimeter Reader EPR - Radiation dosimetry and EPR dosimetry for free radicals detection | Bruker https://www.bruker.com/products/mr/epr/e-scan/alanine-dosimeter-reader/overview.html (accessed Aug 31, 2017).

(129) Grills, D. C.; Cook, A. R.; Fujita, E.; George, M. W.; Preses, J. M.; Wishart, J. F. Application of External-Cavity Quantum Cascade Infrared Lasers to Nanosecond Time-Resolved Infrared Spectroscopy of Condensed-Phase Samples Following Pulse Radiolysis. *Appl. Spectrosc.* **2010**, *64* (6), 563–570.

(130) BNL | Chemistry | Electron- and Photo-Induced Processes Group | Accelerator Center for Energy Research

https://www.bnl.gov/chemistry/EPIP/instrumentation.php (accessed Aug 31, 2017).

(131) Baxendale, J. H.; Stott, D. A. Pulse Radiolysis of Aqueous CNS–solutions and the Rates of Hydroxyl-Radical Reactions. *Chem. Commun. Lond.* **1967**, No. 14, 699–700.

(132) Baxendale, J. H.; Bevan, P. L. T.; Stott, D. A. Pulse Radiolysis of Aqueous Thiocyanate and Iodide Solutions. *Trans. Faraday Soc.* **1968**, *64*, 2389–2397.

(133) Espenson, J. H. *Chemical Kinetics and Reaction Mechanisms*, 2nd ed.; McGraw-Hill, Inc., 1995; Vol. 102.

(134) Kasser, M. J. THE PHOTOCHEMISTRY OF POLYENYL RADICALS AND ITS APPLICATION TO UHMWPE FOR USE IN ARTIFICIAL CARTILAGE. **2009**.

(135) Instruments | Electron Paramagnetic Resonance (EPR) Facility https://epr.chem.wisc.edu/content/instruments (accessed Oct 22, 2017).

(136) Gill, G. A.; Kuo, L.-J.; Janke, C. J.; Park, J.; Jeters, R. T.; Bonheyo, G. T.; Pan, H.-B.; Wai, C.; Khangaonkar, T.; Bianucci, L.; et al. The Uranium from Seawater Program at the Pacific Northwest National Laboratory: Overview of Marine Testing, Adsorbent Characterization, Adsorbent Durability, Adsorbent Toxicity, and Deployment Studies. *Ind. Eng. Chem. Res.* **2016**, *55* (15), 4264–4277.

(137) th_PE_Plasma_400c.jpg (300×248) http://www.speciation.net/md/000/000/503/th_PE_Plasma_400c.jpg (accessed Sep 1, 2017).

(138) Takigami, S.; Matsumoto, I.; Nakamura, Y. Electron Spin Resonance Study of γ-Irradiated Nylon 6. *J. Appl. Polym. Sci.* **1981**, *26* (12), 4317–4330.

(139) Verma, G. S. P.; Peterlin, A. Electron Spin Resonance Study of Mechanically Stretched Nylon-6 Fibers. *Kolloid-Z. Z. Für Polym.* **1970**, *236* (2), 111–115.

(140) Beltrami, D.; Cote, G.; Mokhtari, H.; Courtaud, B.; Moyer, B. A.; Chagnes, A. Recovery of Uranium from Wet Phosphoric Acid by Solvent Extraction Processes. *Chem. Rev.* **2014**, *114* (24), 12002–12023.

(141) Bozzi, A.; Chapiro, A. Synthesis of Perm-Selective Membranes by Grafting Acrylic Acid into Air-Irradiated Teflon-FEP Films. *Int. J. Radiat. Appl. Instrum. Part C Radiat. Phys. Chem.* **1988**, *32* (2), 193–196.

(142) Hoon Seun Chang; Young Kun Kong; Chong Kwang Lee; Jae Ho Choi. Radiation-Induced Graft Copolymerization of Acrylic Acid onto Polyester. *J. Korean Nucl. Soceity* **1977**, *9* (2), 65.

(143) Jang, J.; Jeong, Y.-K. Synthesis and Flame-Retardancy of UV-Curable Methacryloyloxy Ethyl Phosphates. *Fibers Polym.* **2008**, *9* (6), 667–673.

(144) Wentrup-Byrne, E.; Grøndahl, L.; Suzuki, S. Methacryloxyethyl Phosphate-Grafted Expanded Polytetrafluoroethylene Membranes for Biomedical Applications. *Polym. Int.* **2005**, *54* (12), 1581–1588.

(145) Schnabel, W. *Polymer Degradation: Principles and Practical Applications*; Hanser International, 1981.

(146) Dainton, F. S.; Logan, S. R. Radiolysis of Aqueous Solutions Containing Nitrite Ions and Nitrous Oxide. *Trans. Faraday Soc.* **1965**, *61* (0), 715–722.